Bacterial Mapping for *Postmortem* Interval Calculation

Ana Cláudia Coelho Ferreira

Ana Cláudia Coelho Ferreira

Dissertação conducente ao **Grau de Mestre** em **Ciências Forenses**

Bacterial Mapping for *Postmortem* Interval Calculation

Trabalho realizado sob a Orientação de

Professora Doutora Ana Raquel Pinho Freitas

Professor Doutor Daniel José da Costa Barbosa

Professor Doutor Ricardo Jorge Dinis-Oliveira

DECLARAÇÃO DE INTEGRIDADE

Eu, acima identificado, declaro ter atuado com absoluta integridade na elaboração deste trabalho, confirmo que em todo o trabalho conducente à sua elaboração não recorri a qualquer forma de falsificação de resultados ou à prática de plágio (ato pelo qual um indivíduo, mesmo por omissão, assume a autoria do trabalho intelectual pertencente a outrem, na sua totalidade ou em partes dele). Mais declaro que todas as frases que retirei de trabalhos anteriores pertencentes a outros autores foram referenciadas ou redigidas com novas palavras, tendo neste caso colocado a citação da fonte bibliográfica.

Comunicações Científicas em Congressos:

o Ana Cláudia-Ferreira, Daniel Barbosa, Ricardo Jorge Dinis-Oliveira, Ana R. Freitas. Current perspective on the relevance of bacterial communities to estimate post-mortem intervals – how far are we? Poster #43. I Congresso Internacional da TOXRUN, V Congresso da Associação Portuguesa de Ciências Forenses, XIX Jornadas Científicas de Ciências do Instituto Universitário de Ciências da Saúde, Porto, 7 e 8 de abril de 2022.

Publicações Científicas:

o Cláudia-Ferreira A, Barbosa D, Dinis-Oliveira RJ, Freitas AR. Current perspective on the relevance of bacterial communities to estimate post-mortem intervals – how far are we? *RevSALUS-Revista Científica Internacional da Rede Académica das Ciências da Saúde da Lusofonia*, *4*(Sup), 86-87, 2022. https://doi.org/10.51126/revsalus.v4iSup.310

o Cláudia-Ferreira A, Barbosa DJ, Saegeman V, Fernández-Rodríguez A, Dinis-Oliveira RJ, Freitas AR, On Behalf Of The Escmid Study Group Of Forensic And Post-Mortem Microbiology Esgfor. The Future Is Now: Unraveling the Expanding Potential of Human (Necro)Microbiome in Forensic Investigations. Microorganisms, 11(10), 2509, 2023. https://doi.org/10.3390/microorganisms11102509

Agradecimentos

A realização desta dissertação de mestrado não teria sido concluída da mesma forma sem o apoio fundamental daqueles que estiveram sempre ao meu lado, que me motivaram e a quem estou profundamente agradecida.

Quero expressar a minha imensa gratidão para com a Professora Doutora Ana Freitas, a minha orientadora, que cumpriu a sua função de forma extraordinária, marcada por rigor científico, espírito critico e grande dedicação. Motivou-me deste o primeiro momento e incentivou-me sempre a desafiar os meus limites, mostrando-se pronta para me apoiar em tudo aquilo que eu sentisse dificuldade. Empenhou-se neste projeto por horas sem conta para que tudo fosse possível e no momento certo. O meu sincero agradecimento!

Ao Professor Doutor Daniel Barbosa e Professor Doutor Ricardo Dinis-Oliveira, os meus co-orientadores, que se mostraram sempre disponíveis para aquilo que fosse necessário e que, sem eles, também não teria sido possível a conclusão na integra deste projeto. Cada um contribuiu com o seu amplo conhecimento e dedicação, aos dois, o meu muito obrigada!

Quero agradecer também à Professora Doutora Carla Campos, do laboratório de microbiologia do Instituto Português de Oncologia do Porto, que tornou possível a identificação por MALDITOF-MS de espécies bacterianas em centenas de amostras, parte essencial deste trabalho.

Quero também agradecer à Técnica Patrícia e à D. Antónia pela ajuda preciosa que me deram ao longo do procedimento prático laboratorial para o desenvolvimento desta tese.

Aos meus pais e familiares agradeço por todo o apoio incondicional que me deram ao longo da minha vida acadêmica. Acreditaram sempre em mim e nas minhas capacidades e sem dúvida que foram o alicerce que me permitiu enfrentar os desafios e a percorrer este caminho do conhecimento. Um agradecimento especial à minha mãe, que nunca me deixou desistir, que me motivou a seguir em frente e acreditar em mim mesma. Foi com amor e apoio que me fez ser melhor a cada passo.

Quero agradecer ao Luís, que tal como a minha família, foi incansável, apoiou-me, incentivou-me e acreditou sempre em mim. Obrigada por todo o amor, preocupação, paciência e carinho que me dedicaste especialmente durante esta fase!

Gostaria também de agradecer à Diana e ao Guilherme, que têm sido verdadeiros exemplos e fontes de inspiração para mim desde o início da minha carreira universitária. A dedicação e determinação de cada um mostram-me que é possível alcançar tudo com esforço e comprometimento.

Para finalizar, mas muito importante também, gostava de agradecer a todos os meus amigos, que me apoiaram verdadeiramente, mostraram-se prontos para me ajudar, independentemente da distância que me separa de cada um deles. Quero agradecer especialmente ao Edu, à Majó, à Bia, à Mafalda, à Fi e à Mariana, obrigada do fundo do coração!

Resumo

A determinação do intervalo *postmortem* (PMI), o tempo decorrido desde a morte, é uma das questões mais complexas nas Ciência Forenses. Embora os fatores que influenciam a decomposição do corpo estejam bem estudados, o papel central das bactérias nas alterações *postmortem* só foi recentemente reconhecido. A maioria dos estudos centra-se na sequenciação extensiva de bactérias, mas os estudos de culturómica com maior resolução taxonómica continuam a ser escassos. O objetivo deste trabalho foi quantificar a carga bacteriana total e mapear três espécies chave (*Enterococcus faecalis, Staphylococcus aureus, Escherichia coli*) em diferentes órgãos e períodos *postmortem*. Ratos C57BL/6J SPF machos foram submetidos a três ensaios independentes durante 11 períodos de tempo, respeitando a regulação Europeia e Portuguesa para a colheita de órgãos e sacrifício animal a temperaturas controladas. Dez órgãos (intestino, estômago, músculo esquelético, fígado, baço, rim, bexiga, pulmões, cérebro e coração) foram colhidos, pesados e congelados instantaneamente em azoto líquido. Antes dos ensaios experimentais, foram analisadas amostras fecais, tendo-se confirmado a presença de *E. faecalis* e *E. coli*. As amostras foram homogeneizadas e ressuspensas em água peptonada tamponada, sendo inoculadas em meios de cultura enriquecidos não seletivos e seletivos (n=4). Após incubação aeróbica convencional, a quantificação da carga bacteriana total e individual foi efetuada através das Unidades Formadoras de Colónias (UFC) por grama de tecido ou por mL de amostra. As espécies foram identificadas por espetrometria de massa (MALDI-TOF) e a análise estatística efetuada no GraphPad Prism/10.0.1. Quarenta e quatro espécies bacterianas (13 famílias, 3 filos) foram identificadas, com uma consistência notável na presença de *Staphylococcus xylosus, E. faecalis* e *E. coli* nas três experiências. Foram identificadas de forma consistente famílias específicas em todos os órgãos, incluindo Enterococcaceae e Enterobacteriaceae, principalmente nas últimas fases de decomposição, e Bacillaceae, que resistiram frequentemente até ao último intervalo avaliado, enquanto Staphylococcaceae foi detetada de forma variável. A contaminação precoce e substancial observada no músculo esquelético, estômago e intestino, torna-os inadequados para cálculo do PMI. *E. faecalis* revelou-se um potencial biomarcador para a invasão dos rins, fígado e, possivelmente, do cérebro em períodos de tempo tardios, enquanto *E. faecalis* e *E. coli* na bexiga, bem como *E. coli* no baço e no coração, justificam uma investigação mais aprofundada. Embora reconhecendo as limitações de não considerar a complexidade da

microbiota, este estudo piloto apresenta uma abordagem inovadora específica para a espécie, abrindo caminho para a identificação de biomarcadores facilmente rastreáveis em contextos *postmortem* reais.

Palavras-chave:

Ciências Forenses, Microbiologia, Microbioma, Bactérias, Tanatomicrobioma, Intervalo *Postmortem*

Abstract

Determining the *Postmortem* Interval (PMI), the time elapsed since death, is one of the most challenging issues in forensic sciences. While factors influencing body decomposition are well-studied, the pivotal role of bacteria in *postmortem* changes has gained recognition only recently. Most studies focus on extensive bacterial sequencing of *postmortem* samples, but culture-based experiments for higher taxonomic resolution of bacteria remain scarce. The work aimed to analyze total bacterial counts and map three key bacterial species (*Enterococcus faecalis, Staphylococcus aureus, Escherichia coli*) in different organs at different *postmortem* periods. Male C57BL/6J SPF mice underwent three independent assays during 11 *postmortem* timepoints, adhering to European and Portuguese regulations for animal sacrifice and organ harvesting at controlled temperatures. Ten organs (intestine, stomach, skeletal muscle, liver, spleen, kidney, bladder, lungs, brain, and heart) were collected, weighed, and instantly frozen in liquid nitrogen. Prior to the experimental assays, we screened mice faecal samples, which confirmed the presence of *E. faecalis* and *E. coli*. Samples from fecal and tissue specimens were homogenized and thoroughly resuspended in buffered peptone water, then plated onto enriched nonselective and selective culture media (n=4). Following routine aerobic incubation, Colony Forming Units (CFU) per gram of tissue or per mL of sample were quantified for total and individual bacterial loads. Bacterial species were identified by MALDITOF-MS (matrix assisted laser desorption ionization-time of flight) mass spectrometry, and statistical analysis performed in GraphPad Prism 10.0.1. A total of 44 different bacterial species from 13 families and 3 phyla were identified in the 10 organs, with notable consistency in the presence of species such as *Staphylococcus xylosus, E. faecalis,* and *E. coli* across the three experiments. Particular families were consistently identified across all organs, including Enterococcaceae and Enterobacteriaceae mostly in the later stages of decomposition, and Bacillaceae resisting often until the last timepoint, whereas Staphylococcaceae was variably detected. The early and substantial contamination observed in skeletal muscle, stomach, in addition to the intestine, makes them unsuitable for PMI calculations. *E. faecalis* has shown promise as a potential biomarker for kidney, liver, and, possibly, brain invasion at later timepoints, whereas *E. faecalis* and *E. coli* in the bladder, as well as *E. coli* in the spleen and heart, warrant further investigation for similar biomarker potential. While recognizing the limitations of not considering the

complex microbiota network, our pilot study brings an innovative species-specific approach paving a way to identify easily traceable biomarkers in real *postmortem* contexts.

Index

Index of Figures

Index of Tables

List of abbreviations and acronyms

American Type Culture Collection	ATCC
Buffered Peptone Water	BPW
Colony Forming Units	CFU
Columbia Blood Agar	CBA
European Congress of Clinical Microbiology and Infectious Diseases	ECCMID
Hospital-acquired infections	HAIs
MacConkey Agar	MAC
Mannitol Salt Agar	MSA
Matrix-assisted laser desorption/ionization imaging mass spectrometry	MALDI-IMS
Matrix-assisted laser desorption/ionization time-of-flight mass spectrometry	MALDITOF-MS
National Ethics Council for Life Sciences	CNECV
Organization Responsible for the Animal Welfare of the University Institute of Health Sciences	ORBEA-IUCS
Postmortem interval	PMI
Postmortem submersion interval	PMSI
Revista Científica Internacional da Rede Académica das Ciências da Saúde da Lusofonia	RevSALUS
Slanetz & Bartley Agar	SLB
Specific and opportunistic pathogen-free	SOPF
Specific pathogen-free	SPF
Sudden infant death syndrome	SIDS
Triphenyltetrazolium Chloride	TTC
Tryptone Soy Broth	TSB
World Health Organization	WHO

1. Introduction

The beginning of Microbiology occurred in the late 17th century by van Leeuwenhoek with the first microscopic observations of bacteria ("little animals"). However, it was only affirmed as a distinct science almost 200 years later, during the middle 1800s, when Louis Pasteur demonstrated that microorganisms were not spontaneously generated (Opal, 2009). After the global recognition that microorganisms were indeed responsible for human and animal diseases, they have been used as physical evidence along with the beginning of Forensic Science at the end of the century XIX when the presence of a given infectious agent could be attributed to a specific infection with subsequent death (Maccallum & Hastings, 1899). Since then, microorganisms have been mostly used to associate humans/animals with diseases, fomites, or locations (Metcalf et al., 2016; Pechal et al., 2014). But it was only after the anthrax bioterrorist attack on September 11, 2001, in the USA, that the forensic value of microbiology became a reality with microbiologists being able to apply their experimental results, as trace evidence, for a forensic investigation (in this case, to attribute the source of bacterial spores) (Kuiper, 2016). Indeed, the once limited vision on using microorganisms for forensic investigations has gradually changed, running parallel to an unprecedented era of technological sequencing advances since the 2000s – this transformation showed that microorganism can also serve as temporal evidence once they quickly adapt to environmental changes (Opal, 2009). Even in the presence of variable conditions (e.g., temperature, oxygen availability, moisture, pH, light), those changes seem temporally predictable, allowing the establishment of a timeline, which could be useful in providing information on cadaveric decomposition. One could say that a dead body is a perfect cocktail for several microorganisms like the chemoorganotrophic bacteria that consume organic compounds (e.g., decomposing remains) to generate energy (Carter et al., 2007). Also called decomposers, different bacterial species represent the bulk of microorganisms associated with decomposing remains and trace evidence, and, as microbial signatures are unique, they can be associated with specific hosts or habitats (Carter et al., 2017).

The development of technologies associated with molecular biology and the large-scale sequencing of microorganisms in recent years, accompanied by advances in bioinformatics and the availability of well annotated genes/genomes, catapulted Forensic Microbiology as an emerging discipline with the possibility of multiple applications, namely: i) providing

information on cadaveric decomposition, causes of death and *postmortem* interval calculation; ii) facilitating the investigation of a bioterrorist attack, biocrimes, outbreaks or product authenticity; and iii) supporting in crimes of violence, sexual abuse, medical neglect and agri-environmental contamination (Blondeau et al., 2019; Carter et al., 2017).

With the human microbiome playing a key role in the decomposition of *postmortem* tissues, the estimation of the *postmortem* interval (PMI), which refers to the time elapsed since death, is one the most promising applications of the emerging forensic microbiology area (Hauther et al., 2015). PMI calculation is one of the main points of investigation of forensic expertise, being, however, influenced by several biotic and abiotic factors that preclude reliable conclusions, at least for now. Traditional methods for estimating PMI calculations commonly rely on taphonomic processes or the assessment of decomposition stages, but as the cadaver undergoes degradation, these approaches become less reliable and challenging to implement effectively (Dong et al., 2019; Guo et al., 2016; Roy et al., 2021). While different factors that affect the speed of body decomposition (e.g., temperature, moisture, oxygen, etc.) have been extensively studied, the key role of microorganisms in *postmortem* changes has been only recognized and started to be explored more recently (Burcham et al., 2017). While we witness the continuous improvement of next-generation sequencing methodologies, the occurrence and abundance of particular microbial communities may be at least a complementary tool to obtain more accurate PMI estimations and other forensic investigations, in order to be used in medical-legal contexts.

In the following sections, the growing knowledge of the human microbiome composition (both *antemortem* and *postmortem*), its related concepts, and the potential applications in diverse forensic scenarios, with a special focus on the body decomposition process and PMI calculations, are explored.

1.1. Human microbiota and microbiome.

The human body is inhabited by trillions of diverse symbiotic microbial cells, including bacteria, archaea, fungi, protists, and viruses. Estimated numbers roughly point to a similar number of microbial and human cells (1:1) with microbial cells including a high number of unique bacterial strains at a given time during life (Gilbert et al., 2018). The colonization of our body is a continuous process, starting in the early neonatal state and succeeding throughout life intimately affected by factors such as ethnic/racial background, diet, lifestyle,

host genetics, environment, antibiotic usage, immunity status, among others (Consortium, 2012; Walker at al., 2023). The term microbiome describes the entire "ecological community of commensal, symbiotic and pathogenic microorganisms that share our body space" and undergoes intra- and interindividual time variations in terms of number and abundance distribution in different body locations (Clarke et al., 2017; Flores et al., 2014; Gouello et al., 2021; Lutz et al., 2020). Microbiota and microbiome terms have been commonly used indistinguishably, though they currently have clear different meanings. While microbiota refers to the assembly of all living microorganisms (bacteria, archaea, fungi, protists, algae and possibly viruses) encountered in a given habitat/environment, microbiome refers to the broad collection of all microbial structures, genomes, genetic elements and metabolites carried by the present microorganisms and embedded within the environmental conditions of that habitat/environment. We will from now on only consider the term "microbiome" to generally include both the microbiota and their "theatre of activity" (structural elements, metabolites/signal molecules, and the surrounding environmental conditions), as previously suggest by Berg *et al.* (Berg et al., 2020).

1.1.1. Core microbiome.

The diversity and abundance of human microbial profiles vary significantly from person to person, but there exists a shared group of microorganisms known as the core microbiome. These microorganisms encompass all functional bacterial and genomic taxa that play a crucial role in the proper functioning of the body. They help maintain regulation of essential functions related to health, including nutritional acquisition, but which, on the other hand, can also be associated with human diseases due to imbalances within such microbiome (Consortium, 2012; Gouello et al., 2021; Neu et al., 2021). The development of the core human microbiome is a gradual process that begins at birth and continues throughout the first years of life (Wernroth et al., 2022). Even though continuingly evolving across life influenced by diverse factors, it remains relatively constant across time and amongst individuals if strong microbiota deviations do not occur. However, the definition of a "core" healthy microbiome is debatable, and more research is needed to define it in terms of common sets of taxa or metabolic modules or other functions. In any case, it should always be considered in the context of its environment, including body parts (as microbial profiles vary between different body sites, including within the same organ), diet and geography (Sharon et al., 2022; Turnbaugh et al., 2007).

Human microbiota comprises hundreds of bacterial genera and species mainly clustering into four different phyla: the Bacteroidota (former Bacteroidetes), the Bacillota (former Firmicutes), the Actinomycetota (former Actinobacteria) and the Pseudomonadota (former Proteobacteria) (Dekaboruah et al., 2020). The greatest abundance and diversity of microorganisms resides in the gut, which has been the organ more deeply studied regarding microbiome research (Costello et al., 2009). The gut microbiome protects against pathogens, provides nutrients and energy, is in constant communication with the immune system, and is involved in many chemical reactions (e.g., drug's metabolism) having complex effects on human metabolic pathways with implications in several diseases (e.g., inflammatory bowel disease, autoimmune disorders, obesity). Within the gastrointestinal tract, the stomach, duodenum, and ileum have low microbial densities, whereas the jejunum, caecum, and colon are densely populated. The human intestine microbial communities are dominated by the phyla Bacteroidota (e.g., *Bacteroides fragilis*) and Bacillota (e.g., *Lactobacillus* spp., *Faecalibacterium* spp.), with smaller amounts of Pseudomonadota (e.g., *Escherichia* spp.) and Actinomycetota (e.g., *Bifidobacterium* spp.) (Shetty et al., 2017). This composition is quite unique to each person and remains relatively stable, though suffering some evolution with age and environmental factors, after the first 3-4 years of human life (Gilbert et al., 2018). The beginning of gut colonization is mainly due to facultative bacteria (e.g., *Escherichia coli*, *Enterococcus* spp., *Streptococcus* spp., *Staphylococcus* spp.) that, by consuming oxygen, gradually create an anaerobic atmosphere during infancy ready to be colonized with anaerobic bacteria (e.g., *Bacteroides, Bifidobacterium, Clostridium* spp.) from breast milk (Dekaboruah et al., 2020). As an example of the complexity and variety of factors when analyzing human microbiome, also the infant diet greatly influences the evolving microbiota. Since it is known that breast-milk-fed infants have higher abundance of *Bifidobacterium* and *Bacteroides* in comparison to those fed formula who maintain facultative anaerobes (*Enterobacteriaceae*) for longer periods of time (Gopalakrishna et al., 2020). Diet is one of the main factors affecting gut microbiome: for example, in high-fat diets, populations of Bacteroidota and Actinomycetota are often found, while in fiber-based diets the microbiome composition mainly includes Bacillota and Pseudomonadota. Animal-based diets translate into a microbiota with decreased Bacillota (*Roseburia spp*., *Eubacterium rectale* and *Ruminococcus bromii*), and herbal diet shows a great abundance of *Bacteroides spp*. and *Bilophila spp.* (Roy et al., 2021).

Mouth seems to be the second most diverse habitat of the human body, mainly carrying bacteria but also viruses, fungi, protozoa and archaea, and gets established in the first year of life. The oral microbiome also maintains a relatively unique composition in each person, although affected at different sites in the mouth (e.g., teeth, tongue, gingiva, saliva). It counts with more than 1000 bacterial species representative of more than 10 phyla (mainly Bacillota, Bacteroidota, Pseudomonadota, Actinomycetota, Spirochaetota, Fusobacteriota) with *Streptococcus* spp., *Fusobacterium* spp., *Lactobacillus* spp., *Actinomyces* spp., *Veilonella* spp. and *Neisseria* spp. among the most abundant genera (Deo et al., 2019; Dewhirst et al., 2010). Saliva, as a sample of the mouth cavity, is particularly important in cases of bite marks, sexual assault, and child abuse. The salivary microbiome is particularity distinct from other sites in the body, but similar among individuals, being, therefore, an indicator of great relevance for PMI estimation. There are approximately 500 million of bacterial cells per mL of salive and this microbiome is highly influenced by individual factors, such as personal oral hygiene and smoking. Saliva naturally contains antimicrobial factors that are no longer produced after death, thus contributing for the *postmortem* microbial invasion in the oral cavity (Guo et al., 2016). Gram-positive oral bacteria (e.g., *Streptococcus salivarius*) seem to be robust markers for excessively degraded saliva samples due to their high resistance to degrading factors (Ohta et al., 2019).

The skin is a remarkable example showing great variations in microbiome composition across different skin anatomy sites, according to variable physical and chemical features (lipid content, pH, sweat and sebum secretion) besides inter-individual variability (e.g., more extensive bacterial diversity in women due to hormonal differences) (Grice et al., 2011). The more represented genera in skin have been generally identified as *Corynebacteria* (Actinomycetota), cutaneous propionibacteria (Actinomycetota) and staphylococci (Bacillota) (Grice et al., 2009). For example, the sebaceous glands of the face, scalp, chest, and back are those where large amounts of oily sebum are produced and the preferred to the lipophilic anaerobe *Cutibacterium* (former *Propionibacterium*) *acnes* proliferate. In forensic analyses, *Cutibacterium acnes* can be particularly important since its presence is highly specific and an indication that the sample taken corresponds to a skin sample (Gouello et al., 2021; Neu et al., 2021). *Staphylococcus* spp. and *Corynebacterium* spp. are the most common in moist areas, whereas dry areas are more enriched with Pseudomonadota (Dekaboruah et al., 2020). Bacillota are abundant in more juvenile hands, while *Cutibacterium* is commonly found in adults. It is evident that this microbiome makes up the

barrier between the body and the environment, showing a dynamic flux due to constant exposure to environmental conditions (Ahannach et al., 2021; Oliveira et al., 2018; Roy et al., 2021). A continuing and dynamic flow of microbiota transfer between the skin and surfaces/objects in close contact remaining in the body for an extended period of time (Ahannach et al., 2021; Oliveira et al., 2018) exists, but whether this unique microbial fingerprint left behind by skin shedding can be used as trace evidence remains to be validated (Ahannach et al., 2021).

The original dogma that the urine is sterile has been knocked down in the last decade and contrarily to what was previously thought and to what some articles still describe, a protective urinary or bladder microbiome exists (Thomas-White, 2016). Although still in its infancy in comparison to other body tracts, studies have described that healthy female urinary microbiome is highly diverse within and between individuals and dominated by specific family/genera (e.g., *Lactobacillaceae, Gardnerella, Corynebacterium*) or a mixed community without a prevalent genus (e.g., *Staphylococcus, Corynebacterium* and *Prevotella*) (Perovic et al., 2022). As so, this must also be taken into account in forensic investigations.

The vaginal microbiome is largely dominated by bacteria having an important role on women's health and that of their newborns. The healthy vaginal microbiome is dominated by hundreds of bacterial species belonging to Bacillota (e.g., *Lactobacillaceae, Streptococcaceae*), Pseudomonadota (e.g., *Enterobacteriaceae*), Actinomycetota (e.g., *Corynebacteriaceae*), and Bacteroidota (e.g., *Prevotellaceae*). A high abundance of *Lactobacillus* species able to produce antimicrobial molecules and lactic acid that maintain an acidic environment against invading pathogens is well recognized (Diop, 2019). Although relatively stable, the vaginal microbiome varies according to individual characteristics, such as health status, ethnicity, sexual habits, contraceptive use and pregnancy. The male genital tract has not been studied so extensively compared to the female one. Available studies demonstrate that sperm has a low biomass with high contamination whereas semen has a specific microbiome in healthy fertile individuals, either *Lactobacillus*- or *Prevotella*-enriched or polymicrobial, possibly including members of Actinomycetota (C*orynebacterium*), Bacteroides (*Prevotella*), Bacillota (e.g., *Lactobacillus, Streptococcus, Staphylococcus*), and Pseudomonadota (*Haemophilus*, *Burkholderia*) (Baud et al., 2019). The presence of possible pathogenic bacteria, such as *Ureaplasma urealyticum*, *Mycoplasma*

hominis and *Prevotella* spp. may be related to a low semen quality in cases where no spermatozoids are observed (Gouello et al., 2021).

Blood is a fluid commonly found at the place of death, which may originate from distinct places in the body, including menstrual blood, venous blood, nasal blood, and blood from the epithelium of the skin. Blood has been traditionally considered sterile in healthy individuals, just as urine; however, 16S rRNA sequencing studies allowed distinguishing four types of blood. Menstrual blood presents large amounts of species of *Lactobacillus*, nasal blood is affected by the nasal breath that can dilute microorganisms and blood from the skin epithelium contains the same microorganisms that compose the cutaneous microbiome (López et al., 2020).Venous blood can present low amounts of bacteria and nonspecific products corresponding to the proteins of the human host. Indeed, human blood is traditionally considered sterile, but the existence of a blood microbiome became a matter of debate in recent years. A very recent study, which is the most robust to date comprising 9.770 healthy individuals, does not support the hypothesis of a core microbiome endogenous to human blood, but instead showed there is a transient translocation of commensal microorganisms from other body sites (Tan, 2022).

Hair is often collected at death scenes for forensic investigations (scalp hair) or sexual assault cases (pubic hair) (Dinis-Oliveira et al., 2013; Dinis-Oliveira et al., 2016). It has been suggested that the microbiome of pubic hair is more stable and less affected by environmental bacteria. As cohabiting and sexually active couples interchange microbiomes, changes in pubic hair patterns may have an impact on the vaginal microbiome. The presence of *Lactobacillus* sp., characteristic of vaginal samples, is very useful for making this distinction, while *Corynebacterium* is often more commonly found in males. Still, there is not a clear distinction in the microbiota that allows to differentiate male from female, and the length of hair may introduce variations in the microbial communities (Gouello et al., 2021; Tridico et al., 2014).

It is now widely accepted that there is considerable inter-individual variability in the composition of the human microbiome (the often called "personal microbiome") and it is increasingly possible to establish new biomarkers of disease (Gilbert et al., 2018). There is also a considerable inter-individual fluctuation in the stability of the human gut, tongue, forehead, and palm microbiome so including temporal variability throughout life is a relevant factor to add to the microbiome composition (Flores et al., 2014). Notably, and despite the inevitable inter-individual variations, the composition of the human gut

microbiome can be distinguished from the communities of other niches such as soil and water (Hauther et al., 2015). A deep understanding of composition and factors influencing the human healthy microbiome is useful to apply in the investigations related to the thanatomicrobiome and recent years have been fruitful in this respect. Among all microorganisms from the human microbiome, bacteria are, due to their diversity and primary role in the decay process, most relevantly associated with the forensic context, ("FAQ: Human Microbiome," 2013; Hyde et al., 2013). Therefore, we will focus on bacterial communities.

1.1.2. The necrobiome: thanatomicrobiome and epinecrotic communities.

The necrobiome concept intends to reflect all organisms (not only microorganisms but also arthropods and vertebrates) and their genes that interact with decomposing remains (carrion) of heterotrophic biomass. Originally focused on vertebrate carrion, Benbow *et al.* recently suggested that the term necrobiome should be extended to include microorganisms and any form of necromass like leaves or wood, for example (Benbow et al., 2018). It has also been recently demonstrated that the interactions between microorganisms and necrophagous arthropods that colonize decomposing vertebrate carrion affect the rate and timing of decomposition (Tomberlin, 2017). Thus, the increasing knowledge about this interactive microorganism-arthropod network may support the evolution of forensic sciences in the future.

The microbial communities of the human necrobiome, or *postmortem* microbiome, have been allocated into two body parts: i) the internal communities have been defined as the ***thanatomicrobiome*** (the microbiome of "death") or the microorganisms found in blood, fluids and internal organs (e.g., brain, heart, liver, lungs, spleen) upon death; and ii) the external or ***epinecrotic communities*** are found on the surfaces or external body surfaces of decomposing cadavers including inside superficial epithelial tissues, the mouth, ears, eyes, or distal orifices of the digestive tract. The latter ones are easier for collection (noninvasive), but are also more affected by abiotic (e.g., humidity, temperature and pH) or biotic (e.g., gases, insects and scavenger activities) factors (Guo et al., 2016; Javan, Finley, Abidin, et al., 2016; Roy et al., 2021; Speruda et al., 2021; Zhou & Bian, 2018). Expectedly sterile in healthy humans, the internal organs start being invaded by microorganisms after death, which follow a microbial succession in and around the cadaver, greatly influencing body decomposition. The term "thanatomicrobiome" was only introduced in 2014 by Can *et al.,*

(Can et al., 2014) to avoid confusion with microbiomes encompassing insects, arthropods or other large organisms that degrade corpses. The knowledge about the thanatomicrobiome composition along the decay process, which is more stable and less biased, may therefore be useful in different forensic contexts (Javan, Finley, Abidin, et al., 2016; Javan, Finley, Can, et al., 2016).

1.1.2.1. Factors triggering microbial invasion after death.

After death, human cells undergo hypoxia, which triggers the activation of autolytic enzymes leading to the degradation of cellular organelles and subsequently breaks down components such as proteins, carbohydrates, and lipids. As a result, an environment rich in nutrients (e.g., nitrogen, carbon, phosphorus, water) propitious for microbial proliferation is created (Can et al., 2014). With the environment getting more hypoxic along the decay process, the degradation shifts to anaerobic fermentation with the release of different gases (e.g., H_2S, CO_2, methane, ammonia, sulfur dioxide), and the accumulation of acids (lactic/formic) initiates the *postmortem* fall in pH within the early *postmortem* period (Donaldson & Lamont, 2013). As soon as the immune system decays, microorganisms originating from inside (the healthy microbiota in most cases or from infections if that's the case) or outside (microorganisms or even flies from the local environment) can enter the body, including into usually sterile organs, and increase the overall microbial load (Metcalf, Carter, et al., 2016). Temperature and anaerobic conditions have been pointed as the main factors driving this decomposition process (Morris et al., 2006).

In addition to the factors aforementioned, changes that occur in the *postmortem* microbiome, namely in organs and fluids usually sterile, are influenced by the existence of migration phenomena, such as the agonal spread of microorganisms (*perimortem*), *postmortem* translocation or contamination (less probable with strict precautions during sampling) (Morris, 2007; Morris et al., 2006; Speruda et al., 2021). Genuine positives can also occur in the case of a *premortem* bacterial infection, but these usually generate a pure culture growth instead of mixed growth populations except in some polymicrobial infections such as most peritonitis involving intestinal microbiota. The damage of the mucosal surfaces' integrity by the agonal spread or invasion of microorganisms into the bloodstream, subsequent to the ischemia/hypoxia, is controversial due to the difficulty of proving its existence during death or when systemic circulation is artificially maintained by resuscitation attempts. Much more evidence is available regarding the *postmortem*

translocation, which is marked by the entry of intestinal and mucosal bacteria into the circulatory and lymphatic systems, progressing later to other organs due to the decay of the immune system at the time of death. This can be avoided, or at least diminished, if corpses are kept at 4ºC as soon as they are found and preferably within 24h after death (Speruda et al., 2021; Zhou & Bian, 2018).

During a person's lifetime, the translocation of different bacterial types (aerobic and anerobic) can occur. This translocation is associated with the migration of viable bacteria or bacterial fragments from the gut to the mesenteric lymph nodes where bacteria are typically eliminated, preventing their further dissemination. However, in certain cases, translocated bacteria can bypass this elimination process and reach the systemic circulation ultimately leading to sepsis (Balzan et al., 2007). Some bacteria seem to have a particular potential of translocation (e.g., *Enterobacteriaceae, Enterococcus*, *Clostridia*), which can also happen in healthy individuals without negative outcomes if the immune system is able to eliminate them. Different damages/conditions may account for this phenomenon both during life or after death (Mesli, 2017): i) intestinal mucosa alteration (the mucus composition or secretion changes similarly to specific conditions - for example bowel inflammatory diseases, Crohn's disease); ii) modification of the intestinal microbiota (haemorrhagic shock or antibiotherapy); and/or iii) immunodeficiency (e.g. alterations of T lymphocytes signal, decrease of IgA). *Postmortem* translocation may be facilitated by an increased permeability of gut wall due to a long agonal phase, the absence of blood supply responsible for ischemia, the absence of mucus secretion or even a medical history, such as an intestinal bowel disease. The detection of bacteria in organs, such as the brain, liver, spleen and heart that are theoretically sterile unless there is a truly infection, is an indicator of bacterial migration (Speruda et al., 2021; Zhou & Bian, 2018).

1.1.2.2. Body decomposition and microbial succession after death.

Cadaveric decomposition is a dynamic ecological system that undergoes continuous evolution, primarily driven by microbial and necrophagous activities. This process can be broadly divided into five main stages, each with distinct characteristics [fresh decay (autolysis), bloat (putrefaction), active decay (black putrefaction), advanced decay (butyric putrefaction) and skeletonization or dry (diagenesis)] that provide us with essential information for PMI knowledge, location, circumstances and cause of death (Ahannach et al., 2021; Burcham, Pechal, et al., 2019; João, 2006; Lauber et al., 2014; Metcalf, 2019). The

rate and pattern of decomposition are an irreversible mosaic system of physical and biochemical changes associated with biotic factors, such as pathologies and personal individualities, intrinsic bacteria and abiotic factors (Ahannach et al., 2021; Dong et al., 2019; Guo et al., 2016; Hyde et al., 2013; Roy et al., 2021). Bacteria occupy several internal and external sites of the body and derive not only from the inside of the cadaver but also from the vertebrate scavengers, arthropods and soil where it is located, thus having a redoubled influence on the decomposition process. Different factors and scenarios (e.g., weather conditions, season, *antemortem* individuality, corpse *postmortem* manipulation, etc.) combine to generate unique scenarios of decomposition. (Adserias-Garriga, Hernández, et al., 2017; Ahannach et al., 2021; Burcham, Pechal, et al., 2019; Hyde et al., 2013; Lauber et al., 2014; Metcalf, 2019). Notably, it has been shown that the interactions between microbes and the scavenging arthropods that colonize the carcass of decomposing vertebrates affect the rate and time of decomposition and can influence the postmortem microbiome. As so, the growing knowledge about this microbe-arthropod interactive network can support the evolution of forensic science in the future (Tarone et al., 2022).

Initial insights into the microbial communities associated with decomposition were made in nonhuman models in the 1980s (Hyde, 2017). Though the first studies assessing bacterial gene markers, so using non-culturable methods, in human cadavers only started in 2013 (Hyde et al., 2013). Hyde *et al.* (Hyde, 2017) described that rectal/stool samples contained the most diverse bacterial community, while the stomach contained the least diverse bacterial community (dominated by the acid-tolerant *Morganella,* a Pseudomonadota). In general, available studies provide a description of microbial taxa and characterize decomposition patterns during the decomposition process, because it is hard to test different experimental manipulations that can be compared to control conditions. Still, such pattern-oriented data generate relevant information to conduct future studies.

Although still in its infancy, if compared to the extensive knowledge made on forensic entomology, the number of studies addressing the microbial composition during cadaver decomposition is exponentially increasing. Such boom is greatly attributed to the modern culture-independent methods providing more complete and robust data, and because most bacteria from the decomposing community are non-cultivable by traditional culture techniques (Hyde, 2017). The ongoing amount of data that is daily generated is currently higher than ever and strongly dependent on the sequency technology and model used (explored in section 4.3).

Decomposition starts quickly after death with the activity of microorganisms, pancreatic enzymes and gastric acids hypothetically by a certain order, such as larynx and trachea, stomach, intestine, spleen, liver, pancreas, pregnant uterus, heart, lungs, kidneys, urinary bladder, while the skin, muscles, tendons, bones and nulligravid uterus are the last elements to degrade (Javan et al., 2019; Eden et al., 2022). During fresh decay, bacteria inside the body initiate the digestion of surrounding tissues through cell autolysis or self-digestion, resulting in the release of nutrients and macromolecules that are then metabolized by resident microorganisms, especially those from the gut, facilitating the decomposition process. Moreover, a marked shift from aerobic (requiring oxygen to grow) to anaerobic (not requiring oxygen) species occurs, with the latter fermenting sugar in body tissues and producing gaseous by-products (e.g., methane, ammonia). These fermentative processes, characterized by the accumulation of gases and the distension of the body, trigger the beginning of the swelling, inflating or bloat phase, especially in the abdomen, eventually forcing fluids out of the body (purge). Such purging events mark the transition from early to late decomposition and are not necessarily uniform among the different body sites. This enables breakdown of proteins, wet tissue decomposition, and the release of byproducts leading to discoloration and the strong odor typically associated with decaying bodies. The advanced decay stage is marked by the breakdown of fats and the production of volatile fatty acids, contributing to the unique smell of decomposition. Putrefaction is accelerated by vertebrate scavengers or necrophilous arthropods consuming the soft tissues and gradually leading to the dry stages of decomposition (the carcass is reduced to bone, cartilage, and any unconsumed tissue or hair) (Gouello et al., 2021; Pechal et al., 2014). Microorganisms usually start spreading from the gut, digest the intestines, and then the surrounding tissues using the chemicals leaked from the damaged cells. Afterwards, they invade the digestive system and lymph nodes, spreading first to the liver and spleen, followed by the heart and brain (Speruda et al., 2021; Zhou & Bian, 2018).

Different studies showed an increase in bacterial richness and a decrease in diversity from early to late decomposition stages (Table 1) (DeBruyn & Hauther, 2017; Hauther et al., 2015). These studies have also consistently demonstrated an increase in Pseudomonadota and a decrease of Actinomycetota and Bacteroidota, with particular relevance in the rectum (Campobasso et al., 2022; Pechal et al., 2018). Additionally, another study has reported a negative linear relationship between the overall phylum and family taxa with PMI. For instance, Moraxellaceae showed an increase on the day of death, while Aerococcaceae and

12

Enterobacteriaceae were no longer detectable after the fifth day *postmortem* (Pechal et al., 2014). This shift in the cadaveric microbial composition from early to late stages happens during bloating, which is often used as a marker for such transition (DeBruyn & Hauther, 2017; Hyde et al., 2013). When the cadaver enters in the **fresh** stage, the microbial community associated is, at the level of phylum, Bacillota and Actinomycetota, and Lactobacillaceae, Staphylococcaceae, Gemellaceae, Carnobacteriaceae, Aerococcaceae, Veillonellaceae, Streptococcaceae, Campylobacteraceae, Micrococcaceae, Bifidobacteriaceae, Actinomycetaceae, Corynebacteriaceae in the level of family (Adserias-Garriga, Quijada, et al., 2017). Entering in **bloat phase,** a phase of fermentation and proteolysis, the abundant phylum's is Bacillota and Tenericutes, having the class of Clostridiales, families of Peptostreptococcaceae, Bacteroidaceae, Enterococcaceae and the genus *Ignatzschineria* (Adserias-Garriga, Quijada, et al., 2017). In the **active decay**, there is a change from the aerobic *Staphylococcus* and Enterobacterales to anaerobic environment where bacteria able to survive in these conditions dominate, such as Pseudomonadota, Bacteroidota*, Clostridium*, *Bacteroides, Enterococcus, Proteus* and many others from the surrounding environment (Carter, 2008; Dash & Das, 2020; Janaway, 2009; Li et al., 2021; Vass, 2001). When the corpse reaches the **advanced stage**, there are changes in the microbial community in the cadaver, frequently encountering Bacillota, Gammaproteobacteria, Pseudomonadaceae, Alcaligenaceae and Planococcaceae (Adserias-Garriga, Quijada, et al., 2017). When the remains are practically skeletal**,** the bacterial communities associated with them are close to the intestinal communities, being *Bacillota* and *Bacteroidota,* as well *Acidobacteria, Actinomycetota, Pseudomonadota, Planococcaceae*, *Enterococcus, Vagococcus, Clostridium, Corynebacterium, Proteus* and *Acinetobacter* (Dash & Das, 2020; Hyde et al., 2015; Li et al., 2021; Pechal et al., 2014). In this **dry stage**, bacterial communities are similar to soil communities (Dash & Das, 2020; Roy et al., 2021). After 420 days of burial, the succession of bacterial communities to the soil is complete (Adserias-Garriga, Hernández, et al., 2017; Oliveira & Amorim, 2018; Roy et al., 2021).

Importantly, some studies addressed statistically significant time-, organ-, and sex-dependent changes, a variability that is also seen in current microbiome studies analyzing healthy live samples (Javan, Finley, Can, et al., 2016). Some of the largest efforts to assess microbial diversity of internal components of the human thanatomicrobiome showed that Bacillota (former Firmicutes) could be potential biomarkers (Javan, Finley, Can, et al., 2016; Metcalf et al., 2013). Still, bacteria belonging to this phylum may face a decrease instead of

an increase in particular body sites such as the mouth and rectum. Adding to the confusion, contrasting data are also available: while Hyde *et al.* (Hyde et al., 2015) described an increase abundance of Bacillota in mouth over time, Guo *et al.* (Guo et al., 2016) reported a decrease. Besides the inter-individual variability and the possible differences in environmental and biological conditions (weather, clothing…), they used different timepoints and DNA extraction methods. In any case, different studies point to similar bacterial groups as being key *postmortem* taxa involved in decomposing cadavers, which mainly belong to Gammaproteobacteria, *Lactobacillaceae*, and *Clostridiaceae* (Can et al., 2014; Hyde et al., 2013; Kakizaki et al., 2012; Metcalf et al., 2013; Pechal et al., 2014).

Gastrointestinal Tract

Dominant normal gut bacteria from the phyla Bacillota and Bacteroidota start changing in abundance and diversity: closely related bacterial species from the Bacteroidales order (e.g., Bacteroides spp.) significantly decline over time, whereas Clostridiales (Clostridioides spp., Anaerosphaera spp.) and Lactobacillales (Enterococcus spp.) within phylum Bacillota increase [9,70]. Liu et al. [86] proposed significant biomarkers for gut Lactobacillus, Dubosiella, Enterococcus, and Lachnospiraceae. At the later decomposition stages, fecal/rectal samples are dominated by Bacillota and Actinomycetota despite starting/new communities including a high abundance of Bacteroidota (more than skin/mouth). Reports of na increase in Actinomycetota in the drier phases of decomposition are also available [79]. Less dominating Gammaproteobacteria bacteria in live, belonging to the Pseudomonadota phylum (e.g., Acinetobacter spp., Ignatzschineria spp.), also become more abundant, but the increase seems less consistent between individuals [75,79]. In this case, some bacterial genera (Ignatzschineria spp., Wohlfahrtiimonas spp.) have been previously identified in flies or fly larvae visiting the bodies, highlighting the contribution of insects on carrion in the evolution of microbial communities during decomposition. Other environmental bacteria such as Acinetobacter spp. have been commonly found in soil and dry cadavers [79,87]. Although presenting some inter-individual variability, DeBruyn *et al.* suggested specific bacterial genera as potential PMI biomarkers linked to increase (*Clostridia* and *Anaerosphaera*) or decrease (*Bacteroides* and *Parabacteroides*) in abundancy during postmortem time (DeBruyn & Hauther, 2017).

Table 1. Literature evidences on microbial signatures before death and along the body decomposition process.

Body site	After death		
	Overall changes[a]	**Model used and timepoints**	**References**
	Richness ↑ Diversity↓	Human (n=6); 0-20d; Human (n=4) 0-30d	(Hauther et al., 2015); (DeBruyn et al., 2017)
	Richness↓ (except in the rectum) Actinomycetota and Bacteroidota ↓ Pseudomonadota ↑	Human (n=188); <48h/>49h (2 timepoints)	(Pechal et al., 2018)
	S. aureus KUB7 5d - 7d↑and then decrease until undetection at 30d *S. aureus* highest concentrations by culture on 5d for surface sterilized mice *S. aureus* highest concentrations by culture on 7d for non-surface sterilized mice	Mice (n=90); 1h-60d (9 timepoints)	(Burcham et al., 2016)
Body	Dominance of *Clostridium* spp. in internal *postmortem* communities; **Bacillota suggested as a stable biomarker** Female: high abundance of *Pseudomonas* and Clostridiales Male: high abundance of Clostridiales and *Streptococcus*; exclusive presence of *Rothia* *Clostridium* and *Prevotella* species as predictive of different periods of decomposition	Human (n=27); 3.5-240h (66 timepoints)	(Javan et al., 2016)
	Richness ↓ Bacteroidaceae and Moraxellaceae good indicators in the initial sampling; Bacillaceae/Clostridiales were significant after 5d Pseudomonadota was dominant followed by Bacillota Pseudomonadota ↓ over time until 5d Bacillota ↑ over time Moraxellaceae ↑0d Aerococcaceae, Enterobacteriaceae ↑3d and no presence after 5d Planococcaceae, Clostridiales, Clostridiaceae - dominant at 5d	Swine (n=3); 0-5d (4 timepoints)	(Pechal et al., 2014)

	Ignatzschineria and *Wohlfahrtimonas* were common at bloat and purge and until tissues began to dehydrate *Acinetobacter* were common after dehydration and skeletonization *Ignatzschineria* dominated during the wettest phases and ↓ until to skeletonization *Ignatzschineria* was less abundant and less persistent *Wohlfahrtiimonas* associated with myiasis	Human (n=2); 1-20d (10 timepoints)	(Hyde et al., 2015)
	Bacteroidota (Sphingobacteriaceae), Alphaproteobacteria (Brucellaceae, Phyllobacteriaceae, and Hyphomicrobiaceae), and Betaproteobacteria (Alcaligenaceae) ↑ during the advanced decay. Taxa in Rhizobiales were among the most important predictive taxa at each sample site.	Mouse (n=40); 0-48 days (8 timepoints)	(Metcalf et al., 2013)
Skin	Dominated by Pseudomonadota at first 2d ↑ Bacillota, Actinomycetota during the later phases *Pseudomonas and Acinetobacter* were dominant before purge ↑ *Ignatzschineria* after purge and ↓ at dry stage *Clostridium* dominated in the later phases	Human (n=2); 1-20d (10 timepoints)	(Hyde et al., 2015)
	Clostridium ↑ max. at 5d and 7d	Mice (n=90); 1h-60d (9 timepoints)	(Burcham et al., 2016)
	At 5min, 25% of culture positive to enterococci, lactobacilli, and/or *Bacteroides/Prevotella spp.* At 1h, bacterial translocation rates were lowest (virtually no bacterial growth) Culture-positive until 30 min, ↓ at 1h, ↑ to max. at 48h and 72h At 72h, culture-positive for *E. coli* (100%), enteroccci (75%) and lactobacilli (62.5%)	Mice; 0-72h (10 timepoints)	(Heimesaat et al., 2012)
Blood	Dominated by *MLE1-12 (Candidatus Melainabacteria), Saprospirales* and *Burkholderiales* ↑ Relative abundance in ASVs belonging to the order *Clostridiales* ↓ Relative abundance in ASVs belonging to the order MLE1-12 (not significant)	Human (n=40); 24-432h	(Lutz et al., 2020)

Brain	Bacteroidota and Pseudomonadota showed different succession patterns At the genus level, *Ochrobactrum* and *Sediminibacterium* were dominant and ↓ with PMI progression ↑ *Acinetobacter*, *Cupriavidus* and *Agrobacterium (were dominants)* At the phylum level, **Pseudomonadota was the most prevalent** ↑ *Deinococcota* during 12 h At the order level, Rhizobiales was dominant ↓ Saprospirales, Caulobacterales and Thermales ↑ Burkholderiales and Pseudomonadales during 1d ↑ *Acinetobacter* at 8h; ↑ *Cupriavidus* and *Agrobacterium* after 8h	Mice (n=30); 0:30h-1d (5 timepoints)	(Liu et al., 2023)
	↑ *Streptococcus* early in PMI ranges (<24 h, 25–48 h)	Human (n=188); <48h/>49h (timepoints)	(Pechal et al., 2018)
Eyes	↑ Pseudomanodota followed by ↑ Bacillota *Pseudomonas* and Enterococcaceae dominated before purge Planococcaceae dominated after purge and then dropped off as ↑ Clostridium	Human (n=2); 1-20d (10 timepoints)	(Hyde et al., 2015)
Oral cavity/ Mouth	*Pseudomonas* was detected in pre-bloat but was not in any end-bloat At end-bloat, *Pseudomonas* was replaced by common GI tract bacteria (Clostridia, *Lactobacillus*, etc.) Streptococcus, Prevotella and Veillonella detected in pre-bloat swab and scrape Pre-bloat swab and end-bloat scrape was predominated by Bacillota Pre-bloat scrape was predominated by Pseudomonadota	Human (n=2); 0-30d (8 timepoints)	(Hyde et al., 2013)
	Pseudomonadota showed a positive linear correlation with PMI **↓ Alpha diversity over decomposition time** **Pseudomanodota and Bacillota were dominant** Pseudomanodota ↓ first and then ↑ Bacillota ↑ first and then ↓ Actinomycetota and Bacteroidota ↓ At 0h, abundance of Pseudomonadota (*Acinetobacter, Pseudomonas, Phyllobacterium, Photobacterium, Vibrio, Arcobacter, Muribacter*) and Actinomycetota (*Propionibacterium, Rhodococcus*), Bacillota (*Ruminococcaceae*_UCG-014, *Clostridium* sensu_stricto_1, *Paeniclostridium, Lactobacillus, Christensenelaceae*_R-7_Group), Bacteroidota (*Alistipes, Prevotella* _9, *Marinitilum*) and Fusobacteria (*Fusobacterium, Psychrilyobacter*). At 24h, abundance of Bacillota (*Blautia, Enterococcus, Streptococcus, Faecalbacterium*), Pseudomonadota (*Pasteurella*), Bacteroidota (*Bacteroides*), Actinomycetota (*Bifidobacterium*).	Mice (n=24); 0-240h (4 timepoints)	(Dong et al., 2019) (Figure 3 and 4)

17

At 144h, abundance of Actinomycetota (*Staphylococcus, Subdoligranulum, Romboutsia*) and Pseudomonadota (*Morganella, Escherichia shigella, Enterobacter*). At 240h, abundance of Pseudomonadota (*Citrobacter, Proteus*) ↓ Alpha-proteobacteria and Bacteroidia ↑ Gammaproteobacteria Bacilli and Clostridia ↑ first and then ↓ ↑ Enterobacterales, ↑ *Proteus* ↓ *Pasteurellales, Bacteroidales* and *Rhizobiales* *Lactobacillales* ↑ first and then ↓ ↓ Pasteurellaceaeae and Phyllobacteriaceae Streptococcaceae, Ruminococcaceae and Bacteroidaceae ↑ first and then ↓ *Muribacter* and *Phyllobacterium* ↑ first and then ↓		
Microbial communities were similar in diversity over decomposition time **↓ Alpha diversity over decomposition time** *Haemophilus parainfluenzae* and *Streptococcus* were most abundant at <24h and 25–48h Bacteroidota (e.g., *Prevotella*) during the earlier stages of decomposition *Streptococcus* was a predominant taxon during pre-bloat and during the first 4d ***Streptococcus* as a potential biomarker during the first 2d** *H. parainfluenzae* **potential bioindicator <48h after death**	Human (n=188); <48h/>49h (2 timepoints)	(Pechal et al., 2018)
Bacillota and Actinomycetota are the predominant phyla in the fresh stage *Tenericutes* **presence corresponds to bloat stage** **Peptostreptococcaceae and Bacteroidaceae were predominant families in the bloat stage** **Bacillota is the predominant phyla in advanced decay** (different community from fresh stage) Fresh stage was characterized by *Lactobacillaceae, Staphylococcaceae, Gemellaceae, Carnobacteriaceae, Aerococcaceae, Veillonellaceae, Streptococcaceae, Campylobacteraceae, Micrococcaceae, Bifidobacteriaceae, Actinomycetaceae* and *Corynebacteriaceae.* Bacillota and Actinomycetota predominant 1d to 5d, but their relative abundances ↓ from 1d to 5-6d ↑ Bacillota 6-12d (Clostridiales and Bacillaceae - representative Bacillota from bloat to advanced decay stages) ↑ *Tenericutes* transiently between 5d and 7d, just at bloat stage ↑ *Ignatzschineria* and Clostridiales in the bloat stage Gammaproteobacteria, Pseudomonadaceae, Alcaligenaceae, Planococcaceae are predominant families in advanced decay Bacillia nd Clostridia presence in skeletonization/dry stage	Human (n=3); 1-12d (7-8 timepoints)	(Adserias-Garriga et al., 2017)

18

	↑ Alpha diversity after death At 4h, Bacillota and Actinomycetota were dominant Bacillota gradually ↓ At 1d, ↑ Pseudomonadota (predominant phylum) and ↑ Moraxellaceae (predominant family) and gradually ↓ At 2d, Enterobacteriaceae dramatically ↑ and ↓ at 4d Xanthomonadaceae gradually ↑ (dominant taxon from 3d) At 6d, ↑ Pseudomonadaceae Streptococcaceae and Pasteurellaceae gradually ↓	Rat (n=18); 1-9d (9 timepoints)	(Guo et al., 2016)
Buccal Cavity	Dominated by MLE1-12 *(Candidatus Melainabacteria)*, Saprospirales and Burkholderiales ↑ Relative abundance in ASVs belonging to the order Burkholderiales ↓ Relative abundance in ASVs belonging to the order MLE1-12 (not significant)	Human (n=40); 24-432h	(Lutz et al., 2020)
Heart	*S. aureus* remained at 0 until 7d, ↑ to max. after 14d↑ and ↓ to levels near zero at 30d At 5h, a sample showed 100% *Escherichia* and other have *Candidatus Arthromitus, Parabacteroides, Anaerostipes* and *Dorea* At 7d, *Clostridium* dominated (72,1%) with *Lactobacillus* and *Peptostreptococcaceae* spp.	Mice (n=63); 1h-30d (7 timepoints)	(Burcham et al., 2019)
	Varying numbers of *Clostridium* from 1h to 24h, that reached and remained at max. countable limits 5d to 14d; *Clostridium* isolates were also recovered at 30d and 60d	Mice (n=90); 1h-60d (9 timepoints)	(Burcham et al., 2016)
	At the genus level, *Thermus* was more abundant ↓ *Enhydrobacter and Caulobacter, belonging Alphaproteobacteria* and *Methyloversatilis* during 1d ↑ *Pseudomonas* at 8 h ↑ *Sphingomonas* and *Cupriavidus* to peak values at 12h At the phylum level, Pseudomonadota and Deinococcota were dominant *perimortem* ↑ Bacillota and ↓ Actinomycetota during 1d At the order level, *Pseudomonadales, Thermales* and *Burkholderiales* were dominant ↑ *Sphingomonadales* to a peak value at 12h ↑ *Rhizobiales* during 1d ↑ *Deinococcales* at 12h ↓ *Rhodocyclales, Rhodospirillales* and *Caulobacterales* during 1d	Mice (n=30); 0:30h-1d (5 timepoints)	(Liu et al., 2023)

19

	Streptococcus sp. isolates found 5-7d *Clostridium sp.* isolates found 1-3d *Clostridium sp., Enterobacter sp., Bifidobacterium sp., Bacteroides sp.* ↑	Human (n=33); 1-7d (3 timepoints)	(Tuomisto et al., 2013)
Pericardial Fluid	*S. aureus* at 5h *postmortem* ↓ to 0, after 5h ↑↑ to max. at 14d and ↓ up to 30d At 5h PM, contained 100% *Lactobacillus* At 7d, contained 44% *Clostridium* and 55% *Staphylococcus*	Mice (n=63); 1h-30d (7 timepoints)	(Burcham et al., 2019)
Lungs	Varying numbers of *Clostridium* from the 1h to 24h, that reached and remained at max. countable limits 5d to 14d *Clostridium* isolates were also recovered at 30d and 60d	Mice (n=90); 1h-60d (9 timepoints)	(Burcham et al., 2016)
	Bacillota (Lactobacilaceae, e.g. *Lactobacillus*) and Bacteroidota (Bacteroidaceae, e,g, *Bacteroides*) ↑ during the bloating stage (6–9d) Bacillota (Lactobacilaceae, e.g. *Lactobacillus*) and Bacteroidota (Bacteroidaceae, e,g, *Bacteroides*) ↓ after rupture occurs (~9d) Rhizobiales (Alphaproteobacteria) in the families Phyllobacteriaceae, Hyphomicrobiaceae, and Brucellaceae (e.g., *Pseudochrobactrum* and *Ochrobactrum*) to dominate *Serratia*, *Escherichia*, *Klebsiella*, and *Proteus* become abundant after rupture	Mouse (n=40); 0-48 days (8 timepoints)	(Metcalf et al., 2013) (Figure 2)
Abdominal cavity	Total bacteria load ↑ Relative abundances ↓ ↓ *Bacteroides* and *Lactobacillus* over time *Bifidobacterium* no significant change over study	Human (n=6); 0-20d	(Hauther et al., 2015)
Gut	Enterobacterales and *Escherichia* were detected in the lower GI tract for both pre-bloat and endbloat *Clostridium* is abundant at the end of the bloat stage	Human (n=2); 0-30d (8 timepoints)	(Hyde et al., 2013)
	Bacteroidales (*Bacteroides, Parabacteroides*) ↓ Clostridiales (*Clostridium, Anaerosphaera*) and Gammaproteobacteria, *Ignatzschineria* and *Wohlfahrtiimonas* ↑ Relative abundances and diversity ↓ *Bacteroides, Parabacteroides* and *Lactobacillus* ↓	Human (n=4);0-30d	(DeBruyn et al., 2017)

Total bacterial load ↑ 12h and 24h post sacrifice with high levels of enterobacteria and lactobacilli Total bacterial load ↓ 15 and 30min post sacrifice with ↓ Enterobacteria, enterococci, bifidobacteria, and *Clostridium* spp. Enterobacteria, enterococci, bifidobacteria, and *Clostridium* spp.↑ to de max. levels from 30min until the end of the study Varying numbers of *Clostridium* from the 1H to 24H, that reached and remained at max. countable limits 5d to 14d *Clostridium* isolates were also recovered at 30d and 60d	Mice (n=90); 1h-60d (9 timepoints)	(Burcham et al., 2016)
Until 5h postmortem *Parabacteroides*, *Mucispirillum* and *Lactobacillus* dominated At 24h ↓ relative abundance *Parabacteroides*, disappearance of *Mucispirillum* and ↑ *Lactobacillus* At 7d ↓ *Lactobacillus* and ↑ *Anaerostipes*, *Clostridium* and *Enterococcus* *Staphylococcus aureus* - stable 1-5h, ↓ at 24h, ↑ to max. after 7d and ↓↓ to min. at 14-30d	Mice (n=63); 1h-30d (7 timepoints)	(Burcham et al., 2019)
***Lactobacillus, Dubosiella, Enterococcus, Lachnospiraceae* - proposed as significant biomarkers** *Bacillota (Lactobacillus reuteri/johnsonii, Clostridium tetani, Enterococcus faecalis), Bacteroidota, Actinomycetota*- dominant Bacteroidota e Actinomycetota 2d↑ - 2d-4d↓ *Bacillota bacterium M10-2* - appeared on 2d and 2d-4d↑ *Enterococcus faecalis* - appeared on 2d and 2d-10d↑ *Tenericutes* (bloat phase) *Lactobacillus reuteri* ↑ - peak values 7d and 15d *Clostridium tetani* E88 - appeared on 7d until 15d and then ↓ *Lactobacillus johnsonii* ↑ 1 week after death *Helicobacter* ↓ gradually during 15d *Gordonibacter, Bifidobacterium, Enterorhabdus, Lactococcus, Clostridium sensu stricto, Anaerosalibacter, Enterococcus, Dubosiella, Lactobacillus* - remained at 15d	Mice (n=240); 6-10 w (10 timepoints)	(Liu et al., 2022)
Total bacterial load ↓ between 3h and 6h with ↓ lactobacilli and *Bacteroides/Prevotella* spp. ↑ Enterococci between 6h and 12h and remain stable until 72h Lactobacilli ↓ between mice alive and 72h *Escherichia coli* remain stable at 0 until 72h *Bacteroides / Prevotella spp.*↓ 3-12h	Mice; 0-72h (10 timepoints)	(Heimesaat et al., 2012)

	Bifidobacterium detected at end-bloat	Human (n=2); 0-30d (8 timepoints)	(Hyde et al., 2013)
Colon	↑ Distinct in fast replying aerobic species between 6h and 24h Total eubacterial loads ↑ 72h with max. loads of enterobacteria, enterococci and lactobacilli Enterobacteria ↑ between 3h and 12 h Enterococci ↑ between 6h and 24h Enterobacteriaceae 12h-72↑ Enterococci 24h-72↑ *Lactobacilli* significantly ↓ until 72h *Bacteroides /Prevotella spp.* 3h↑ - 12h↓ - 72h↑ *Clostridium coccoides* and *leptum groups* 3h↑ - 12h↓ - 72h↑ Mouse Intestinal *Bacteroides* 3h↑ - 12h↓ - 72h↑ Bifidobacteria 6h↑ - 24h↓	Mice; 0-72h (10 timepoints)	(Heimesaat et al., 2012)
Ileum	Taxon richness first ↓ and then ↑ Bacillota, Pseudomonadota, Bacteroidota and Actinomycetota were found at all the timepoints At the phylum level, Pseudomonadota and Bacillota showed major shifts At the phylum level, bacterial richness ↓ from 0h to 9d and ↑ from 9d to 15d At the family level, Prevotellaceae, Muribaculaceae, Lachnospiraceae ↓ at 0h, 8h, 16h, 3d, 7d, 15d At the family level, bacterial richness ↓ from 0h to 9d and ↑ from 9d to 15d At the genus level, *Lactobacillus* dominated at 1d and *Enterococcus* from 3d to 13d Bacteroidota ↓↓ after death, but ↑ at 3d and 15d Actinomycetota relative abundances ↓ at 16h, 7d and 15d Bacillota and Pseudomonadota peak values at 8h, 1d and 9d *Helicobacter* was absent at 7d, 9d and 15d ↑ Lactobacillaceae, Enterobacteriaceae and Enterococcaceae, represented the majority from 0h-15d *Enterococcus* and *Vagococcus* relative abundances ↑ at 0h, 8h, 3d, 7d and 15d *Proteus* was most abundant at 15d At the species level, *Enterococcus faecalis* ↓ and *Proteus mirabilis* ↑ after 5d *Clostridium sporogenes* ↓ abundance before 1d and *Falsiporphyromonas_endometrii* after 3d *E. faecalis* and *P. mirabilis*appeared during the whole 15d	Rat (n=8); alive-15d (11 timepoints)	(Li et al., 2021)
Rectum	Bacteroidota and Bacillota were predominant phyla until 2d Prevotellaceae was predominant family until 2d Pseudomonadota was the most abundant phylum after 2d Enterobacteriaceae was a predominant family after 2d	Rat (n=18); 1-9d (9 timepoints)	(Guo et al., 2016)

	Bacteroidota and Bacillota were the most abundant phyla before purge Pseudomonadota dominating after purge until the drier phases ↑ Bacillota and Actinomycetota in dry phases Clostridiaceae, Bacteroides and Porphyromonas presented before purge *Corynebacterium* was the most abundant at dry stage *Ignatzschineria* ↑ to max. after purge and ↓ at dry stage *Clostridium* became the most abundant at dry stage Clostridiaceae were the most abundant at dry stage	Human (n=2); 1-20d (10 timepoints)	(Hyde et al., 2015)
Feces	Bacillota mainly dominated with very few Bacteroidota detected in a sample Pseudomonadota dominated in another sample *Pseudomonas* was detected in pre-bloat but was not in any end-bloat At end-bloat, *Pseudomonas* was replaced by other GI tract bacteria (Clostridia, *Lactobacillus*, etc.)	Human (n=2); 0-30d (8 timepoints)	(Hyde et al., 2013)
	Sterility up to 5d After 5d, *Clostridium* sp., *Streptococcus* sp., *Enterobacter* sp., *Enterococcus* sp., *Escherichia* sp., *Staphylococcus* sp. and *Streptococcus* sp.	Human (n=33); 1-7d (3 timepoints)	(Tuomisto et al., 2013)
Liver	Dominated by MLE1-12 *(Candidatus Melainabacteria),* Saprospirales and Burkholderiales ↑ Relative abundance in ASVs belonging to the order *Clostridiales* ↓ Relative abundance in ASVs belonging to the order MLE1-12 (not significant)	Human (n=40); 24-432h	(Lutz et al., 2020)
	Varying numbers of *Clostridium* from the 1h to 24h, that reached and remained at max. countable limits 5d to 14d *Clostridium* isolates were also recovered at 30d and 60d	Mice (n=90); 1h-60d (9 timepoints)	(Burcham et al., 2016)
	At 1h, bacterial translocation rates were lowest (virtually no bacterial growth) Culture-positive until 30 min, ↓ at 1h, ↑ to max. at 48h and 72h.	Mice; 0-72h (10 timepoints)	(Heimesaat et al., 2012)
	At the genus level, *Thermus* and *Cupriavidus* were dominant ↓ *Microbacterium* to zero at 24h ↑ *Acinetobacter*, *Cupriavidus* and *Pseudomonas* over decomposition Genera *Paracoccus* and *Cryocola* were detected only 0:30h At the phylum level, *Pseudomonadota* and *Deinococcota* were dominant *Actinomycetota, Bacillota, Bacteroidota* and *Cyanobacteria* showed relative abundances of > 1% ↓ *Actinomycetota* during 1d At the order level, *Burkholderiales, Pseudomonadales* and *Thermales* were dominant ↑ Clostridiales during 1d ↓ *Actinomycetales;* ↓ *Rhodobacterales* during 4h Comamonadaceae, a family of Betaproteobacteria, was also significantly enriched	Mice (n=30); 0:30h-1d (5 timepoints)	(Liu et al., 2023)

23

	Varying numbers of *Clostridium* from the 1H to 24H, that reached and remained at max. countable limits 5d to 14d *Clostridium* isolates were also recovered at 30d and 60d	Mice (n=90); 1h-60d (9 timepoints)	(Burcham et al., 2016)
Spleen	Dominated by *MLE1-12 (Candidatus Melainabacteria), Saprospirales* and *Burkholderiales* ↑ Relative abundance in ASVs belonging to the order *Clostridiales* ↓ Relative abundance in ASVs belonging to the order MLE1-12 (not significant)	Human (n=40); 24-432h	(Lutz et al., 2020)
	At 1h, bacterial translocation rates were lowest (virtually no bacterial growth) Culture-positive until 30 min, ↓ at 1h, ↑ to max. at 48h and 72h.	Mice; 0-72h (10 timepoints)	(Heimesaat et al., 2012)
	S. aureus KUB7 detected 1h post sacrifice; not detected at 3h, 5h, 24h post sacrifice of surface sterilized mice and detected again 5d through 14d Surface sterilized mice - *Clostridium* ↑ max. at 5d and 7d and ↓ *at 14d, 30d and 60d* Non-surface sterilized mice - *Clostridium* ↑ max. at 7d and 14d and ↓ at 30d and 60d	Mice (n=90); 1h-60d (9 timepoints)	(Burcham et al., 2016)
Kidney	At 1h, bacterial translocation rates were lowest (virtually no bacterial growth) Culture-positive until 30 min, ↓ at 1h, ↑ to max. at 48h and 72h.	Mice; 0-72h (10 timepoints)	(Heimesaat et al., 2012)
	At the genus level, *Thermus* was dominant ↑ *Acinetobacter* and *Pseudomonas* during 8h; ↓ *Methyloversatilis* during 1d At the phylum level, Pseudomonadota, Deinococcota and Bacillota were dominant ↓ Fusobacteria and Cyanobacteria during 1 day ↑ Pseudomonadota and Actinomycetota At the order level, Pseudomonadales and Thermales were dominant ↓ Streptophyta, Clostridiales and Rhodocyclales during 1d ↑ Burkholderiales, Rhizobiales, Bacteroidales and Actinomycetales	Mice (n=30); 0:30h-1d (5 timepoints)	(Liu et al., 2023)
	S. aureus after 3h *postmortem* ↓ to 0, ↑ after 5h until max. at 7d and ↓ after 14d until to 0 at 30d Until 24h, Propionibacteriaceae, *Staphylococcus, Propionibacterium, Enterococcus, Pseudomonas* detected; At 7d, *Clostridium* dominated with Peptostreptococcaceae spp. and *Pseudomonas*	Mice (n=63); 1h-30d (7 timepoints)	(Burcham et al., 2019)
Bone marrow	↑ *Clostridium* sp., *Enterobacter* sp., *Bifidobacterium* sp., *Bacteroides* sp.	Human (n=33); 1-7d (3 timepoints)	(Tuomisto et al., 2013)
Mesenteric lymph node	Culture-positive until 30 min, ↓ at 1h, ↑ to max. at 48h and 72h. At 5min, lactobacilli have translocated, ↑ until 30min, ↓ at 1h and then ↑ At 12h culture + for lactobacilli (high levels), *E. coli,* enterococci, *Bacteroides/Prevotella spp.,* clostridia	Mice; 0-72h (10 timepoints)	(Heimesaat et al., 2012)

	↑ Alpha diversity; Dominated by Clostridiales and Lactobacillales ↓ Relative abundance of MLE1-12 (*Candidatus Melainabacteria*)	Human (n=40); 24-432h	(Lutz et al., 2020)
Uterus	↑ Alpha diversity Dominated by Clostridiales and Lactobacillales ↓ Relative abundance of MLE1-12 (*Candidatus Melainabacteria*)	Human (n=40); 24-432h	(Lutz et al., 2020)
Prostate	↑ Alpha diversity Dominated by Clostridiales and Lactobacillales ↓ Relative abundance of MLE1-12 (*Candidatus Melainabacteria*)	Human (n=40); 24-432h	(Lutz et al., 2020)

[a]Bacteria phyla are designated according to the List of Prokaryotic names with Standing in Nomenclature (LPSN) and National Center for Biotechnology Information (NCBI): Pseudomonadota (former Proteobacteria), Bacillota (former Firmicutes), Actinomycetota (former Actinobacteria), Bacteroidota (former Bacteroidetes) and Deinococcota (former Thermi). Arrows indicate the increase or decrease of bacterial counts throughout time. Abbreviations: ASVs, absolute sequence variants; max., maximum; w, weeks.

The finding of specific bacteria such as *Clostridium* in the end stages of decomposition is not surprising, since it produces amylases and lipases, converting carbohydrates and lipids into organic acids plus alcohols and facilitating fat hydrolysis. The breakdown of proteins in a cadaver is facilitated by various proteolytic bacteria, including *Pseudomonas, Bacillus* and gut sulphate-reducing bacteria. However, during the later stages of decomposition, such as end-bloat, certain bacteria like *Pseudomonas,* which require oxygen to survive, are replaced by other anaerobic bacteria (e.g., *Clostridium*).This shift occurs due to the reduced redox potential resulting from the absence of oxygenated blood, creating a favorable environment for the growth of anaerobic bacteria (Janaway, 2009). In particular, Guo *et al.* reported an increase in Pseudomonadota (mostly Gammaproteobacteria) and a gradual decrease in Bacillota and Bacteroidota in the mouse rectum (Guo et al., 2016).

Regarding **skin** and **mouth**, Pseudomonadota accounts for the greatest biomass before bloat (first 48h), but Bacillota (skin and mouth) and Actinomycetota (skin) increase in the later stages of decomposition (Hyde et al., 2015; Pechal et al., 2014).

Skin. In forensic investigations, the skin is the most analyzed sample in microbiome studies, including in the sub-nail. The cutaneous microbiome in the palm of a cadaver's hand remains stable up to 60 hours after death and is unique, as only 13% of the bacteria is shared among individuals (Ahannach et al., 2021; Roy et al., 2021). This opens the possibility of establishing a connection for individual identification and PMI estimation. In addition, the commensal bacteria found in the skin are highly resistant to environmental stress, such as humidity and ultraviolet radiation (Ahannach et al., 2021; Roy et al., 2021). Indeed, Huang *et al.* (Huang et al., 2020) found that skin was the best microbiome at yielding predictions of age in adults in agreement with forensic studies showing that the skin microbiome predicts PMI better than microbiomes from other body sites.

Mouth. In contrast to other sites (e.g., rectum), bacterial populations usually found in life in the buccal cavity seem considerably different immediately after death (Guo et al., 2016). Authors described a gradual decrease of Bacillota and Bacteroidota in parallel with an increase of Pseudomonadota (mostly Gammaproteobacteria). After the swollen state, intestinal bacteria, such as *Tenericutes*, can be found in the mouth, which may reflect the migration of bacteria populations from the large intestine (Ahannach et al., 2021; Pechal et

al., 2018; Roy et al., 2021). In the first study using human cadavers as models, Hyde *et al*. (Hyde et al., 2013) reported differences between two cadavers in the pre-bloat and post-bloat oral communities, but in both cases *Clostridium* spp. were present in the post-bloat stage.

Brain, heart, liver, spleen and kidney

Limited research exists regarding postmortem microbial succession in internal organs, which are presumed to be sterile (Can et al., 2014). However, studying the microorganisms present in internal organs associated with corpse decomposition is of utmost importance, because the presence/absence and the abundance of certain bacteria in these organs can potentially serve as bioindicators of early PMI. In forensic practice, estimating PMI accurately, particularly during the early stages, hold significant value, as it enhances case detection efficiency. Historically, there has been a belief that microbial growth in certain organs, such as the heart, spleen, liver and brain, occurs only after 24 hours *postmortem* (Gevers, 2004). Tuomisto *et al*. (Tuomisto, Karhunen, Vuento, et al., 2013) showed that the liver was one of the most sterile samples up to 5 days *postmortem*, after which single isolates *Clostridium* sp., *Streptococcus* sp., *Enterobacter* sp., *Enterococcus* sp., *Escherichia* sp., and *Staphylococcus* sp. were detected in human models. Can *et al.* (Can et al., 2014) demonstrated the earliest detection of microorganisms in the liver from a human cadaver with a PMI of 20 hours and in all sampled organ tissues (heart, blood, liver, spleen, brain) from a human cadaver with a PMI of 58 hours. Annunziata *et al.* (Dell'Annunziata et al., 2022) analyzed internal organs of 10 murine cadavers and showed microbial invasion at 3- and 10-days *postmortem* for the liver-spleen and heart-brain, respectively. However, a recent study revealed in mouse models that these internal organs, including the brain, heart, liver and kidney, can harbor bacteria as early as 0.5 hours after death, up to the 24 hours *postmortem* evaluated (Liu et al., 2023). During this early period, they present a relatively low species richness and abundance of bacteria, the dominant microbial species differ among organs, but they tend to become similar over time. As an example, in brain samples the abundance of *Acinetobacter* increased significantly around the 8-hour mark.

Different studies suggest that microorganisms multiply in blood, liver, spleen, heart and brain, in a time-dependent manner, and their relative abundances are unique to each organ and PMI, meaning that when samples are analyzed, they tend to group based on the cadaver or PMI rather than the specific organ tissue (Can et al., 2014; Javan, Finley, Can, et al., 2016; Liu et al., 2023). As with other external organs and body sites, the *postmortem* microbial

communities within internal organs may experience unique shifts and dynamics, potentially influenced by factors, such as environment and organ-specific conditions.

Other cadaveric samples

At later stages of decomposition, microbial successions of bones or soil should be the main choices (Roy et al., 2021). Emmons *et al.* (Emmons et al., 2022) demonstrated that the *postmortem* bone microbiome is distinct from the human gut and soil, but with similarities to each depending on the depth of the bone in the soil. The unique conditions surrounding the burial site shape the microbial community that develops within the bones, and *Pseudomonas* and phosphate solubilization seem to play a key role in skeletal degradation. Human and soil-associated bacteria unite to create a unique bone microbial profile after death: bacterial communities at the surface are more like soil and those in buried bones more like the gut (more anaerobic), with conditions such as the depth of human remains influencing the composition of the *postmortem* microbiome. Soil microbiome greatly affects human *postmortem* microbiome, especially in the late stages of decomposition.

1.1.2.3. Factors affecting decomposition.

The diversity and inter-individual variability observed in the *antemortem* human microbiome, which are highly influenced by diet, age, sex, ethnicity, country of origin, comorbidities, antibiotic's use, among other factors, potentially affect the thanatomicrobiome composition and subsequently the microbial succession occurring after death. Several different abiotic and biotic factors, either present *antemortem* or *postmortem*, contribute and directly influence the decomposition process: the abiotic factors include conditions as time, temperature, humidity, pH and *antemortem* living habitats (e.g., diet and antibiotics); and the biotic factors include insects, scavengers and *antemortem* infections (Dash & Das, 2020).

Within **abiotic factors**, time is a crucial one since it greatly affects abundance and diversity of bacteria over time, playing an important role in estimating the time since death. Also, temperature and water activity (humidity) strongly accelerate the decomposition process by affecting the thanatomicrobiome composition, both qualitatively and quantitatively, and bacterial tissue colonization. Temperature increase has been linked to changes in detritus availability and necrobiome dynamics, with cadaver decomposition

28

evolving faster in hot climates (Dash & Das, 2020; Roy et al., 2021). In addition, bacteria can present variable resistance to humidity or other environmental conditions, since different species require variable optimum temperature/humidity for growth (for example skin bacteria are highly resistant to humid contexts), highlighting the role of knowing epinecrotic communities as well. Major changes in pH also occur after death, mainly associated with a pH decrease in blood and gastrointestinal tract, enabling acidophilic bacteria to thrive (e.g., *Cutibacterium acnes* in skin). However, there are some reports of pH increase in specific body sites (Dash & Das, 2020) being difficult to assess and that control all changes induced by the innumerous by-products generated after death. *Antemortem* intake of drugs, namely antibiotics, is one of the major factors influencing the *postmortem* microbiome. Thus, it is crucial to know the medical and epidemiological history of the person in question. It is well known that the prolonged use of antibiotics, for example, disturbs healthy microbiome, meaning that the thanatomicrobiome will also be affected. But an increasing number of different scenarios, such as drug overdose cases, for which the *postmortem Clostridium* effect has been described, are being explored (Dash & Das, 2020; Javan et al., 2022). Finally, daily diet and lifestyle habits also directly influence the composition and diversity of the gut microbiome, hardening the generation of robust microbiome databases to be used and applied in forensic investigations (Clarke et al., 2017; Mansour et al., 2021).

The decomposition of human carrion is primarily achieved by necrophagous invertebrates (mostly insects) and large scavengers (like other vertebrates such as opossums or vultures), apart from the present microorganisms – the **biotic factors** (Dash & Das, 2020; Mondor, 2012). The microbial interactions on human remains themselves can dictate which insects are attracted to and colonize them. For example, along the decomposition process, bacteria produce large amounts of gases through fermentation and those volatile chemicals (called apeneumones, e.g., H_2S, CO_2, NH_3) attract many of the invertebrates and vertebrates that help decompose the remains. A series of scavenging activities succeed with the successive attraction of different predators and parasites to survive on the conditioned human remains, such as dry skin, bones, and hairs. The physical condition of the dead individual is also key in the decomposition process. A body with a higher amount of fat maintains the inside temperature for longer resisting more to the degradation process. However, at the same time, it provides more nutrients like nitrogen for bacterial growth, meaning that decomposition starts quickly, but bloating takes longer, a slower mass loss occurs and skeletonization is prolonged. Overall, because it is not linear but multifactorial, smaller

carcasses decay significantly faster than large ones and this must be taken into account when testing decomposition-related models and methods to assess PMI (Matuszewski et al., 2014).

The existing *antemortem* microbial abundance also plays a key role in decomposition. An elderly body has approximately 40 trillion microbial cells and, for this reason, has a much faster decay rate than a fetus or a newborn that eventually dies (Lutz et al., 2020). The same is true in deaths from infection where the number of microorganisms is obviously higher. When there were nutritional disorders, such as anemia, or death by poisoning, during life, degradation is slower since the environment is not favorable to microbial growth(Roy et al., 2021; Speruda et al., 2021).

1.2. Microbiome-based analysis for forensic *antemortem* and/or *postmortem* applications.

Due to the widespread presence of microorganisms in the environment and intrinsic to the cadaver, bacteriology and mycology have been applied as a tool for a wide range of forensic techniques (Gouello et al., 2021; Hyde et al., 2013; Oliveira & Amorim, 2018; Speruda et al., 2021). In fact, since the human microbiome project launched in 2007 (https://hmpdacc.org/), our knowledge about the thousands of microbial species colonizing us does not stop growing. From a forensic point of view, particular or a bunch of microorganisms can provide clues as trace evidence in different scenarios (Who? What? When?), from personal identification to cause of death or PMI calculations (Swayambhu et al., 2023). The sections below describe the main applications of microbiome analysis in *antemortem* and/or *postmortem* forensic studies (Figure 1).

1.2.1. Microorganisms or microbiome analysis in *ante/postmortem* forensic studies.

1.2.1.1. Human identification.

Given the similar or even greater number of bacterial cells compared to human cells in particular body sites, it is conceivable that as many bacterial cells and their genes are deposited in touched items in comparison to human markers. The characterization of the personal microbiome and the microbial transfers noticed between people and objects can be used to identify a suspect when their bacterial community is left at the scene of crime or directly on the victim.
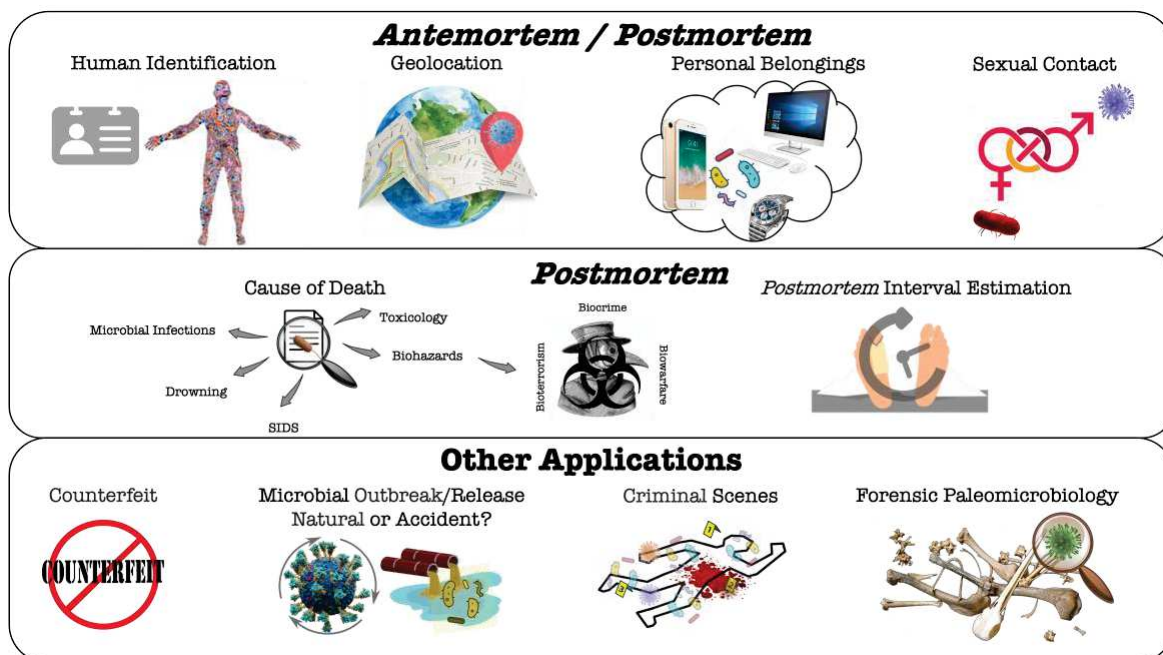
Figure 1. Graphic representation illustrating possible microbial forensic applications to answer criminal/legal cases. *Antemortem* and *postmortem* applications are addressed in more detail in the text. The acronym SIDS stands for Sudden Infant Death Syndrome.

This is achieved through the characterization of microorganisms in the sample, enabling the identification and correlation of the microorganisms present with the sourced tissue, and taking in account the tissue' unique structure and composition, according to the area concerned, on the intervener and on the geolocation (Clarke et al., 2017; Gouello et al., 2021; Lax et al., 2015). Existing transfers can be classified as direct transfers, between human and objects (for example, through a handshake or between the site and the body), or indirect transfers that occur between humans, using an object as a bridge. However, the applicability of this method in forensic sciences requires a high preciousness to avoid contaminations (Gouello et al., 2021). Most studies exploring the skin microbiome indicate a large potential from the palm microbiome as a "fingerprint" for human identification even after months, provided that the objects remain untouched since dominant skin species (e.g., *S. epidermidis*), in case not typed at the species level, are less ideal as biomarkers compared with minor species, since the latter can be linked to specific individuals (Park et al., 2017; Schmedes et al., 2018; Wilkins et al., 2017). An idea gaining strength is the combination of human microbiome analysis with traditional human DNA testing (e.g., short-tandem-repeat [STR] analyses) to provide complementary data for stronger associations and exclusion of

31

individuals falsely associated with biological evidence (Schmedes et al., 2016). For example, by using a new tool for saliva identification with three oral bacterial markers, Jung *et al.* verified the existence of specific oral bacteria in 91.4% of samples with high sensitivity (with very low DNA levels and with residual effects after tooth brushing) and specificity (by comparison with faecal samples) (Jung et al., 2018).

1.2.1.2. Geolocation.

Previous studies carried out on the human microbiome have revealed the variations that exist in the microbial ecology of different populations on our planet. These differences may be due to distinct factors, such as the level of industrialization in each geographic region and/or the lifestyle of each population, which has increased the forensic interest in finding microbial signatures that characterize each geographical area. Indeed, microbial populations are highly dependent on their geographical location, which is directly affected by variations in altitude, latitude, climatic conditions and soil composition (Gouello et al., 2021; Ossowicki et al., 2021). In this context, the Earth Microbiome Project was created in 2010 (https://earthmicrobiome.org/) to sample the whole planet's microbial communities and, thus, to assess biogeographic variations of microbial communities. Each city shows unique microbial profiles contributing with high accuracy to geographical identification of the place of death or surrounding areas (Haarkötter et al., 2021). Available studies exploring the use of microbial profiles for geolocation showed, among other promising data, clear differences in the most common species in people from different cities in different countries. They also showed that scalp hair samples seem to more robustly predict geolocation than pubic hair samples (a result of great forensic relevance), and that gut microbiota differs significantly between European, North American, Japanese, Korean and Colombian populations (Brinkac et al., 2018; Escobar et al., 2014; García et al., 2020). An important constraint of using the microbiome to determine geographic origin is that microbial indicators associated with location can vary by interacting with new environments or by sudden changes in a person's lifestyle. This indicates that longitudinal studies should evaluate different variables.

1.2.1.3. Personal belongings.

Humans have a unique skin microbiome that is generally stable over time and transfers to objects they interact with, generating a microbial signature on personal objects and

surfaces that is stable for forensic scenarios. Different studies, both *antemortem* and *postmortem*, in corpses were able to link microbiomes of hands/shoes with those present on objects/surfaces, including different geographical areas (Kodama et al., 2019; Lax et al., 2015; Phan et al., 2020). Interestingly, particular bacteria from donor's hands could be correlated with lifestyle, estimation of gender and ethnicity (e.g., the absence of *Alloiococcus* indicated female gender, Asian ethnicity, and use of hand sanitizer), corresponding to personal features of a potential large forensic relevance. The finding of stable skin microbiomes from corpses and personal items during transport and storage in the morgue is promising whereas precision of results varied between the different objects (e.g. mobile phones, glasses, etc.) analyzed (García et al., 2020). Naturally, there are some difficulties of using such data since the microbiome of hands and footwear changes over the day and the same occurs for the microbiome of floors and other surfaces that may alter depending on how many people walk/touch it. In *postmortem* studies, in particular, it remains unknown how long the time period is when the human skin microbiome is no longer viable as a personalized signature (Metcalf, 2019).

1.2.1.4. Sexual contact.

For years that molecular/serological identification supports investigations of sexual assault by identifying unusual pathogens (absent from the human microbiome) in the victim and the suspect (e.g., *Neisseria gonorrhoeae, Chlamydia trachomatis*) (Jauréguy et al., 2016). More recently, and owing to the improvement of sequencing technologies, phylogenetic analysis is able to identify with higher precision (at the strain level) the pathogens potentially transferred in sexual assault cases, including with several possible victims (Francés-Cuesta et al., 2019). Now we are entering a different era where the entire microbiome of both the suspect and victim(s) can be explored. Given the uniqueness of the microbiome from person to person and that microbiomes of couples with sexual contacts tend to be more similar to each other than to those of unrelated people, the occurrence of some transfer during sexual contact may allow the human microbiome (genital and/or pubic hair) to be used in investigations of sexual assault when there is no other evidence. The most robust studies showed the stability of the pubic microbiome for 6 months, including at variable storage times and temperatures, which seems not to be influenced by an increased frequency of sexual activity, but with particular gender differences (Bacillales or *Corynebacterium* are more abundant in men, while Bifidobacteriales and/or Lactobacillales

are more abundant in women) (Dixon et al., 2023; Williams et al., 2017, 2019). Moreover, in cases of sexual assault, the evaluation of a woman's microbiome predicted with high accuracy the expected proportion of the aggressor when a single suspect or a small group of suspects were investigated.

1.2.2. Microorganisms or microbiome analysis in postmortem forensic studies.

1.2.2.1. Cause of death.

Different studies established the microbial communities in association with the cause of death and found that the beta dispersion differed significantly between anatomical body sites and modes of death, namely dysbiosis, drowning or sudden infant death syndrome (Roy et al., 2021). The presence of specific microorganisms can act as evidence or bioindicator for the cause of death, which may be useful in confirming the diagnosis of an *antemortem* infection or a previously undiagnosed infectious disease, or in identifying microbial markers for particular types of death (Blondeau et al., 2019; Heimesaat et al., 2012). It has been proven that the different etiologies of death, including natural, accidental, suicide and homicide, also significantly influence the distribution of microbial communities in the different regions of the cadaver (Lutz et al., 2020). Though so far clinical microbiology hasn't started using microbiome techniques to identify infectious causes of death, sequencing tools to characterize human microbiome could be of use in the future in the medico legal field.

Hospital/Community-Acquired Infections and other biorisks

A manifold of reasons can contribute to microbiota disequilibrium (dysbiosis) and this may not always be easy to distinguish from the changes that occur in the human microbiome after death. Generally, the detection of a single microbial species in body fluids, especially those leading as causal agents of hospital-acquired or community-acquired human infections (such as *Streptococcus pyogenes, Streptococcus pneumoniae, Staphylococcus aureus* or *Candida albicans*), indicates an *antemortem* infection. By contrast, a mixed profile points to a *postmortem* invasion, as a consequence of a contamination from the skin or intestine (Neu et al., 2021). However, a true pathogen can be isolated as more frequent in a mixture with other contaminants. The presence of *Propionibacterium acnes*, *Corynebacterium sp*. or

Bacillus sp. (except *B. anthracis*), is much less often associated with an infection (Speruda et al., 2021).

Chronic diseases, for example, can have a significant impact on human microbiome, which may occur as a result of changes in the host's physiology or lifestyle or as a consequence of medical treatments, such as antibiotics. In forensic sciences, the understanding of the relationship between chronic diseases and microbial dysbiosis can be important in reconstructing the medical history of a deceased individual and in determining the cause of death. In the early stages of liver disease, there is an increased intestinal permeability, which occurs independently of changes in the microbiome or endotoxins. Cholestatic liver injury is characterized by a translocation of bacteria from the families *Enterobacterales*, *Enterococcaceae* and *Bacillaceae* primarily to the mesenteric lymph nodes (Fouts et al., 2012). In cases of death from cardiac arrest, there are sex differences in the populations of microorganisms. *Clostridium* spp. and *Streptococcus* spp. are highly abundant in men and Clostridiales and *Pseudomonas* spp. in women. This demonstrates that the hearts of males and females form distinct bacterial niches after death (Bell et al., 2018). In another study, it was shown that a decreased phylogenetic diversity represents a highly significant predictor of heart disease, with a dominant presence of *Streptococcus, Prevotella, Fusobacterium*, and *Rothia* (Pechal et al., 2018).

Hospital-acquired infections (HAIs: infections that first appear 48 hours or more after hospitalization or within 30 days after having received health care) or nosocomial infections are a common cause of death even in industrialized countries with advanced healthcare systems. The World Health Organization (WHO) estimates that 1.4 million people suffer from HAIs worldwide and that particular pathogens are more often involved in these scenarios (e.g., *S. aureus, S. pneumoniae, E, coli, K. pneumoniae, C. albicans*), some of which belong to the human healthy microbiome. As most of them are opportunistic pathogens, taking advantage of particular situations, namely patients with dysbiosis from chronic diseases, elderly people, invasive surgeries, immunosuppression, etc., strict preventive and hygienization measures followed by healthcare institutions are crucial to avoid outbreak and human transmission events through contact with contaminated medical equipment, surfaces, or healthcare workers. In this context, microbial forensics is important for clinical diagnostics and public health protection, for example in an event of an infectious disease outbreak scenario in which the accurate identification (ideally until the strain level) of the agent is highly relevant, namely for hospital tort litigation-lawsuits by patients against

hospitals arising from a HAI (Oliveira et al., 2018). Naturally or community-acquired infections (e.g., pneumonia) are infections contracted outside of a healthcare setting, originating naturally from an individual event of dysbiosis/immunosuppression or spread through contact with infected people, contaminated objects, or the environment. They need to be distinguished from those that result from malicious transmission and, in all cases, infections can be traced back to the patient's activities, environment, and contact with others together with genotyping/sequencing data from human and environmental/clinical samples to determine the source of the infection. The final goal is always to determine the source of the infection, the method of spread, and the parties responsible, in order to prevent future infections and hold those responsible accountable. As we are facing an unprecedent revolution in sequencing and other analytic methods, we never know what Microbiology still reserves under this context: for example, by combining laser microdissection and 16S rRNA sequencing, osteomyelitis caused by *Pseudomonas aeruginosa* was identified as the cause of death of a child from the 18th century (D'Argenio et al., 2017).

Drowning

Drowning is a usual cause of death for victims recovered from watery environments and determining this type of death is, whenever possible, based on pathological findings. Diatoms are aquatic algae from the phytoplankton and, as long as their density is high enough, their analysis can be useful to estimate the type and amount of diatom-rich water aspirated into the lung before death. This approach is limited if diatoms are too large and they cannot reach the bloodstream and organs, if they are present in low concentrations or simply because they can also be found in non-drowned bodies (false positives) (Piette et al., 2006). For these reasons, smaller aquatic microorganisms (bacteria, cyanobacteria and bacterioplankton) present in large amounts have been increasingly explored as markers of death by drowning (García et al., 2020). The established knowledge of the usual aquatic habitats of particular microorganisms, such as *Aeromonas* in freshwater, *Vibrio* and *Photobacterium* in saltwater, and all three genera in brackish water, facilitates their future use as markers to support the diagnosis of drowning deaths (Uchiyama et al., 2012). Kakizaki *et al.* (Kakizaki et al., 2011) demonstrated, by culturomic experiments, that the detection of bacterioplankton in a blood sample may support the assumption of death by drowning, since commensal bacteria do not readily invade the bloodstream after drowning. As so, the location and circumstances of the drowning can be established after identification of the

bacteria present in the water where a drowning occurred, which can be compared to bacteria found in a victim's lungs to determine if the victim was indeed exposed to that specific water source. These findings, together with other medico legal investigations that include strontium (Azparren et al., 2003) other chemical markers, diatoms and histopathology as well as the victim's medical history and the circumstances of the incident, , must also be taken into consideration in determining the cause of death.

Sudden infant death syndrome (SIDS)

SIDS is defined as the sudden and unexpected death of an infant <1 year during sleep that remains unexplained after a thorough investigation that includes the examination of the site and circumstances of death, a complete autopsy, the revision of the clinical history of the victim and their relatives, and an interview with the parents. The complete autopsy should include ancillary analyses: histopathology, microbiology, toxicology and biochemistry among others. but there is growing evidence that microbiota dysbiosis may play a role in SIDS (Goldwater, 2015). Available studies indicate greater colonization of SIDS cases with different species of *Clostridium* and Bacteroides, babies sleeping in a prone position seem to be more heavily colonized with *S. aureus* and a significant association is shown between SIDS cases and infections by bacterial and viral pathogens (Highet et al., 2014; Leong et al., 2017). An alternative hypothesis relies on the development of the infant gut microbiome after birth in interaction with the brainstem serotonergic system (Praveen et al., 2016).

Toxicological effects imposed by microbial metabolism

Postmortem microbial activity may interfere with autopsy toxicological results. It is known that during decomposition some microorganisms are responsible for the degradation of drugs (e.g., antidepressants, benzodiazepines, cannabinoids, cocaine) or other xenobiotics (e.g., cyanide) and for the neoformation of other metabolites (e.g., alcohol, methamphetamines and amphetamines, opioids) (Oliveira et al., 2018). This is of particular concern if the body has been exposed to higher temperatures favoring microbial growth, since it increases the corpse's degradation prior to autopsy. Some remarkable examples include the bioconversion of nitrobenzodiazepines (e.g., clonazepam, diazepam) into their 7-amino-metabolites by several species (e.g., *Bacillus cereus, Staphylococcus epidermidis, Clostridium perfringens* and *Bacteroides fragilis*); the *N*-demethylation of

37

methamphetamine into amphetamine by intestinal bacteria (e.g., enterobacteria, enterococci, *Lactobacillus, Clostridium*); or the production of ethanol or other byproducts, from sugars, amino acids, fatty acids, among others, by a variety of bacteria (*Corynebacterium spp., Escherichia coli, Enterococcus faecalis, Klebsiella spp.*), yeasts (e.g., *Candida* spp, *Saccharomyces cerevisiae*) and fungi (e.g., *Aspergillus* spp.). Ethanol is a well-explored example and, even though forensic toxicologists have established ethanol values in blood for different situations, determining whether blood ethanol concentrations originate from *antemortem* ingestion or from *postmortem* production can prove to be very difficult even using preservative agents. This is particularly relevant in advanced cases of decomposition, which may be favored by warm and moist environments (Castle et al., 2017).

Other circumstances may be taken in account when evaluating a possible ethanol intoxication scenario. For example, the auto-brewery syndrome, which is a rare underdiagnosed condition, implies a gut microbiota dysbiosis in which illegal levels of ethanol are detected in the blood even without ethanol consumption (Dinis-Oliveira, 2021). As so, the deep and increasing knowledge of the human *antemortem* and *postmortem* microbiome can provide a full snapshot of the microorganisms present in different organs and body sites, and so a better understanding of the changes in drug metabolism occurring after death (either by degradation, production of bioconversion) and how they may impact autopsy and the interpretation of toxicology *postmortem* results.

1.2.2.2. Estimation of *postmortem* interval.

The estimation of the PMI, i.e., the time elapsed since death, is probably the most studied application of the *postmortem* microbiome and a fundamental part of a criminal investigation (Metcalf et al., 2013; Pechal et al., 2014). There are pieces of evidence that *postmortem* microbiomes do not significantly change within 24-48 hours of death and can reflect *antemortem* health status (Pechal et al., 2018). In fact, *antemortem* conditions, such as drug/ethanol or another stressful lifestyle (e.g., dumping) linked to homicide, for example, greatly influence *postmortem* microbiome composition (Pearson, 2019). Despite the existence of a great diversity of methods with potential to predict, in a certain way, the PMI, their accuracy remains limited and none of them can be recognized as an accurate and universal tool. The selection of one in detriment of another is based on each case, on the available data and the particular circumstances of each case. Thus, in order to get a more

rigorous prediction, several methods have been employed in parallel, thus reducing the margin of error of each method individually.

Evolution of methods for PMI estimation

Several methods have been implemented over the years to estimate PMI (Figure 2) (Franceschetti et al., 2023; Pittner et al., 2020). The PMI estimation is primarily based on the visual inspection of the cadaver (e.g., *algor*, *livor* and *rigor mortis*) in early *postmortem* periods, which are the standard tools in routine practices, and on alternative methods such as histopathological and biochemical methods that remain relatively imprecise. In later *postmortem* periods, PMI calculations with such classical methods are harder to apply and other methods as forensic entomology and molecular tests may be more relevant (Pittner et al., 2020; Roy et al., 2021). Forensic entomology has provided a reliable evidence-based alternative for PMI calculation based on invertebrates' biomarkers found in the cadaver or the surrounding environment (Dong et al., 2019; Guo et al., 2016; Metcalf, 2019; Roy et al., 2021; Sampaio-Silva et al., 2013; Speruda et al., 2021). Studies on changes in the bacterial communities of internal organs, aiming to establish a relationship between bacterial interactions and the time elapsed after death (the so-called microbial clock), have been increasingly employed in the PMI calculation. This relies on the fact that bacterial communities experience a dynamic alteration over time after death, showing, therefore, potential as biomarkers for PMI calculation (Ahannach et al., 2021; Burcham et al., 2019; DeBruyn et al., 2017; Lutz et al., 2020).

Microbiome, Microbial communities or Microbial succession

Bacterial predictors are generally related to the different events of cadaveric decomposition. Particularly, in the calculation of the PMI the microbial clock is more accurate in the first 48 hours after death, as the cadaver is still in a fresh stage with limited contamination by soil microorganisms. Even though there are some descriptions of PMI estimates errors varying from 2 to 7 days (Dong et al., 2019; Gouello et al., 2021; Metcalf, 2019), the accuracy and precision of PMI estimates is unknown, as error can arise from sources of variation, such as measurement error and environmental factors. Microorganisms actively engage in decomposition owing to their ability to use available nutritional sources and their inherent resistance features. Furthermore, in contrast to human cells, bacteria possess a circular shape and robust cell walls, affording them protection against degradation

(Ahannach et al., 2021; Blondeau et al., 2019; Gouello et al., 2021; Metcalf, 2019; Roy et al., 2021). It is in the decay period, in particular, that a fundamental role for bacterial action in the decomposition of the human body is verified (Adserias-Garriga et al., 2017).
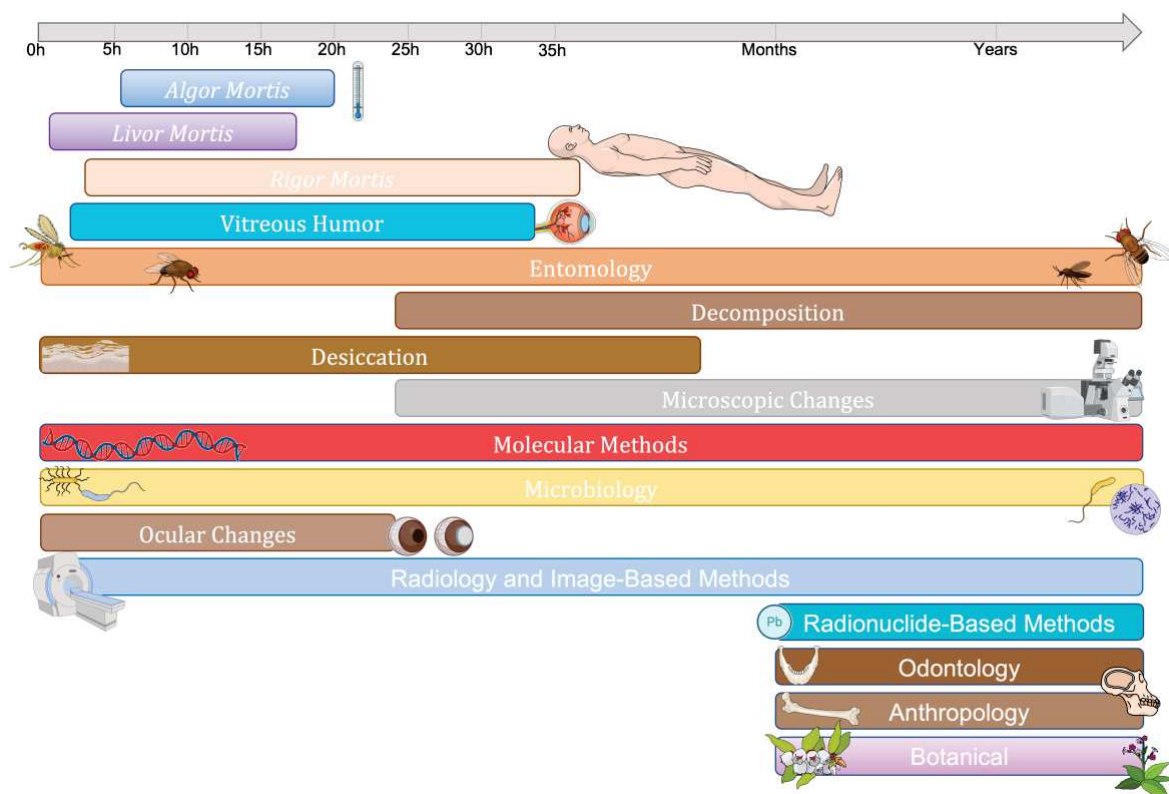
Figure 2. Graphic representation illustrating main methods to estimate PMI and the time frame within which can be employed (adapted from Costa et al., 2015). Algor mortis, the cooling of the body after death, is probably the most widely used method for estimating PMI and is based on the decrease in rectal temperature (Eden et al, 2022). Livor mortis corresponds to the change in skin color due to the deposition of stagnant blood in the lower parts of the body after death and be assessed by the color and fixation of lividity through the bleaching test (Brooks, 2016; Eden at al., 2022). Rigor mortis, also called *postmortem* rigidity, represents the third stage of death characterized by the stiffening of muscles due to the binding of actin and myosin filaments (starts around 2-3 hours after death) (Eden et al., 2022). The vitreous humor, a clear and colorless fluid that fills the space between the lens and the retina of the eye, offers an alternative biological matrix for estimating the PMI through a valuable biochemical method (Cordeiro et al., 2019; Roy et al., 2021). Entomology, the study of insects and their interactions with other organisms, humans, and the environment, has been used for forensic purposes since the thirteen century, providing insights into PMI through the analysis of insect colonization and life cycle evolution on decomposing cadavers (Amendt et al., 2004). The process of decomposition after death involves the degradation of soft tissues through autolysis (cellular breakdown) and putrefaction (bacterial consumption), with various factors influencing its progression; there is a somewhat predictable sequence of stages, including fresh, bloat, decay, and dry (Brooks, 2016). Desiccation, the process of drying of the skin and mucous membranes after death, leads to changes in color and texture, with notable

effects observed in the eyes as well as in the skin where the lips and genitalia are particularly affected (Brooks, 2016). Microscopic changes, including alterations in tissue histopathology, immunohistochemical, and protein densities, can provide valuable information for estimating the PMI based on the decrease or increase of specific proteins and compounds (Brooks, 2016). Molecular methods, including RNA and DNA analysis, offer valuable tools for PMI estimations by assessing nucleic acid integrity, measuring degradation rates, and quantitatively amplifying target genes, although DNA degradation poses limitations for longer PMIs (Brooks, 2016). Microbiology, the main focus of this section is discussed in detail in the next section. Ocular *postmortem* changes include variations in corneal opacity, pupil diameter, blood vessel striation, retinal color, and intraocular pressure (Brooks, 2016). Forensic radiology is an emerging area of forensic sciences that deals with the utilization of imaging techniques such as radiography, computed tomography and magnetic resonance imaging for the examination and analysis of deceased individuals (Brooks, 2016). Radionuclide-based methods, commonly employed in forensic anthropology for skeletonized remains, utilize radionuclides like 210Pb and 210Po, 14C radiocarbon, as well as measurements of citrate and nitrogen content (Amadasi et al., 2017; Brooks, 2016; Ubelaker et al., 2020). Forensic odontology uses dental evidence to provide expert analysis and answers to forensic inquiries, serving both the field of justice and anthropology (Mohammed et al., 2022). Forensic anthropology analyzes bone evidence, whether fragmented or intact, to respond to the law in several aspects, including identification, gender or age estimation, and PMI calculation (Ubelaker et al., 2020). Through botanical classification and traditional knowledge of plant species, the relationships between their development, specific habits, and geographical origins can be established, adding in the PMI estimation (Coyle, 2005).

Table 1 comprises the current knowledge about the fluctuating microbial communities along cadaver decomposition with the different studies using different strategies/technologies essentially varying in: i) the organism used (human, mouse, swine) and its individual characteristics (e.g., sex, age, weight); ii) the DNA extraction method and sequencing technology; iii) the sampling method; iv) the time points tested; v) the body sites tested even within the same organ (e.g., skin); and vi) the number of samples and replicas. Although the influence of these variables on changes in microbial communities is not well established, available studies suggest that succession of bacterial communities may be used to estimate PMI, since they could associate common bacterial groups (predominately bacteria from Gammaproteobacteria, Lactobacillaceae, and Clostridiaceae) with decomposition corpses (Can et al., 2014; Hyde, 2017). Therefore, and as aforementioned within section 2.2.2., particular bacterial phyla, families and/or genus are key *postmortem* taxa involved in the body decomposition process. Particular bacterial families or genera have even been proposed as potential PMI indicators, such as those belonging to Pseudomonadota and Bacillota. Javan *et al.* (Javan et al., 2016) proposed some species from the Bacillota

phylum (*Clostridium* sp., *Bacillus* sp., *Peptoniphilus* sp., *Blautia* sp. or *Lactobacillus* sp. strains) as potential biomarkers in estimating time of death. Adding to the challenges of definitively identifying bacterial biomarkers is the description of contradictory reports across different studies (e.g., increase versus decrease of bacterial richness; Table 1). These inconsistencies can be attributed to variations in study models, the inclusion of different body parts, the intricate microbial and metabolic networks involved, and the multitude of factors influencing human body decomposition.

In one of the very first studies addressing PMI using gene markers by high-throughput sequencing, Pechal *et al.* (Pechal et al., 2014) used swine remains over 5 days to describe that the ability to differentiate bacterial communities throughout physiological time depends on the level of taxonomic resolution. While the best results were observed using a model built on the four phyla (Bacillota, Bacteroidota, Pseudomonadota, Actinomycetota), specific bacterial families, including *Campylobacteriaceae, Enterococcaceae, Moraxellaceae, Prevotellaceae,* and *Pasteurellaceae*, retrieved even better results. By using a similar approach by Pechal *et al* (Pechal et al., 2014) with building regression models informed by the Random Forest classifier but in a mouse model, Metcalf *et al.* (Metcalf et al., 2013) showed that PMI can be estimated within 3 over 48 days (with the highest accuracy before 34 days) and that combining skin and soil microbial communities (16S rRNA and 18S rRNA datasets, respectively) provided the most accurate PMI prediction models, at least compared to the abdominal cavity where during the rupture stage microbial changes are more variable. For bacteria, taxa in the order *Rhizobiales* (Pseudomonadota) were among the most important predictive taxa at each sampling site. In a follow-up by the same authors (Metcalf et al., 2016), they found the greatest PMI accuracy (2–3 days over the first 25 days of decomposition) from microbial samples of the caecum, soil, and skin over the first 2 weeks of decomposition, and that the soil type did not affect the accuracy of the "microbial clock". Another remarkable exciting result was achieved by Metcalf *et al.* (Metcalf et al., 2016) describing accurate time estimates since placement across different seasons, meaning an advantage in using microbial communities that can circumvent some of the factors affecting body decomposition and entomology tools (Carter et al., 2017). Even after the corpse has completely decomposed, the microbial signatures belonging to the body remain in the soil for months or even years, allowing clandestine graves to be found (Carter et al., 2017).

Since these first descriptions, an increasing number of studies describe potential microbial signatures or biomarkers of human decomposition suitable for *postmortem*

calculations (Table 1; (García et al., 2020)). Most studies used 16S rRNA gene sequencing to detect a wide range of bacteria with the limitation of generally reaching only phyla or family taxonomic levels. Independently of the methodological approach, different studies showed *Clostridium* as a strong positive predictor of PMI (DeBruyn et al., 2017; Janaway et al., 2009; Percival, 2009). *Clostridium* species are known to play a crucial role in facilitating decomposition by breaking down lipids and complex carbohydrates associated with human tissue. *Clostridial* lipases are believed to significantly aid in fat hydrolysis, particularly in hot and humid environments characterized by low oxygen levels and limited redox conditions, while their hydrolytic enzymes convert carbohydrates into organic acids and alcohols, further contributing to the decomposition process (the *postmortem Clostridium* effect). When the body is recovered from water, the time of death is often defined by the *postmortem* submersion interval (PMSI), which is the time elapsed since the body was immersed in water. The marine barnacles *Notobalanus decorus decorus* have been used as promising bioindicators (Speruda et al., 2021), but PMSI and microbial communities will not be further explored.

1.3. Methods and technical issues.

Microbiological analysis can be carried out by two distinct metagenomic techniques: by culture-dependent or by genetic approaches. It is important to note that these methods are commonly applied to daily situations, ranging from microbe identification in hospital routine, outbreak resolution, food quality control, academic research, among others. Depending on the final goal and available resources, one or several methods can be simultaneously employed, from the classical Microbiology (e.g., culture media, biochemical tests) to high-throughput sequencing methods (Roy et al., 2021; Zhang et al., 2022).

1.3.1 Culture-dependent methods.

The culture dependent-method relies on cultivating bacterial species in specialized microbiological media, enabling the isolation of viable microorganisms from samples. This approach provides a means to characterize these microorganisms with a high degree of accuracy and taxonomic resolution (Zhou et al., 2018). While this method is relevant in forensic analysis due to its ability to precisely identify taxa, it does have limitations, including the prolonged cultivation periods required by some microorganisms (Speruda et

al., 2021). In addition, considering that approximately 99% of environmental bacteria cannot be successfully grown in laboratory conditions, and that up to 80% of bacterial species inhabiting the human body are considered "unculturable", the identification of bacteria using these methods can present a challenge in forensic analysis (Guo et al., 2016; Hyde et al., 2013; Zhou et al., 2018).

Na *et al.* (Joo-Young et al., 2017) examined *postmortem* body fluid samples from human Korean autopsy cases to identify various bacterial genera and species that are typically part of human normal microbiota together with C-reactive protein testing to identify the presence of *antemortem* inflammation. However, the authors employed a combination of genetic and biochemical tests for bacterial identification, resulting in a lack of a definitive and comprehensive list of results. Tuomisto *et al.* (Tuomisto et al., 2013) analyzed 33 human autopsy cases by bacterial culturing and concluded that liver and pericardial fluid were the most sterile samples up to 5 days *postmortem* (the latest being invaded). This research has also shown that the relative amounts of intestinal bacterial DNA (Bifidobacteria, Bacteroides, enterobacteria, and Clostridia) increase with time. Burcham *et al.* (Burcham et al., 2016) used reinforced clostridial medium and mannitol salt agar to, respectively, count colony growth and analyze *postmortem* dynamics of *Clostridium perfringens* and *Staphylococcus aureus* in a mouse model. Dell'Annunziata *et al.* (Dell'Annunziata et al., 2022) analyzed, on 10 murine cadavers, microbiological swabs from external anatomical sites and internal organs during 16 and 30 days. The resulting swabs were plated on blood, MacConkey, Chocolate, Sabouraud and Schaedler agar plates, allowing to infer that the initially sterile internal organs showed signs of microbial invasion at 3- and 10-days *postmortem* for the liver-spleen and heart-brain, respectively, and the *postmortem* microbiota was mainly dominated by Bacillota and Pseudomonadota.

Despite the limitations associated with culturomics, its accessibility in routine microbiology makes it a valuable tool. Further studies exploring this field can yield important insights into key bacteria or identify useful biomarkers derived from these bacteria with the potential to be incorporated into routine analyses using simple methods.

1.3.2. Culture-independent methods.

Current methods for the genetic profiling of the thanatomicrobiome greatly aim to elucidate the microbial communities present in a given sample (often called thanatogenomics). Microbial community sequencing is achieved by two methodological

approaches: 1) **amplicon (marker gene) sequencing**, a method that amplifies variable regions of a highly conserved bacterial gene, such as the 16S rRNA genes, enabling to infer taxonomic/genomic relationships based on their phylogeny; and 2) **whole genome shotgun sequencing or metagenomics**, an approach that sequences all ("meta") of the DNA present in a given sample (Jo et al., 2020). It is important to highlight that analyzing specific gene markers after sequencing (e.g., the 16S rRNA gene) is not metagenomics (a common literature misinterpretation) as this corresponds to gene amplicon sequencing. These methods are based on the extraction of genetic material from samples by using DNA commercial extraction kits that greatly facilitate the process, and represent rapid, precise, and very informative methods for identification of bacterial populations.

Regarding amplicon sequencing, the most common marker genes include 16S rRNA gene for prokaryotes (bacteria and archaea), 18S rRNA gene for eukaryotes, and internal transcribed spacer for microscopic fungi (Zhou et al., 2018). In fact, most available studies here explored addressed microbial taxa by the bacterial genetic marker 16S rRNA gene. This can provide an in-depth coverage due to the relatively short sequence with hypervariable regions appropriately sized for the sequencing platforms. In addition, given its conserved regions, it allows for designing universal primers to target the hypervariable regions that denote the variable microbial diversity. Moreover, 16S rRNA sequencing provides consistent and longitudinal results, is cost/time-saving, and suitable for large numbers of samples simultaneously for estimating time and location of death (Jovel et al., 2016). The V4 hypervariable region seems the most sensitive for microbial signatures, while the overlap between the V2 and V4 hypervariable regions shows the highest accuracy for taxonomic determination. Nevertheless, the greatest limitation is that 16S rRNA gene profiling has low discriminatory power for some bacterial groups, enabling the identification of bacteria until the genus level, occasionally until the species level. Nevertheless, this limitation can be bypassed by sequencing the entire 16S gene and the intragenomic variation between 16S gene copies (Johnson et al., 2019). Metagenomics is, on the other hand, able to provide strain-level characterization by producing sequence reads of strain-specific markers, and to quantify the taxa diversity within the sample analyzed (α-diversity) as well as the diversity among distinct samples (β-diversity) (Adams et al., 2015; Roy et al., 2021; Speruda et al., 2021; Zhou et al., 2018). Different methods and bioinformatic tools, requiring efficient and accurate computational pipelines besides robust and updated reference databases, have been applied to profile the human thanatomicrobiome communities. However, it poses a big

45

current challenge given the massive scale of data generated (Roy et al., 2021; Speruda et al., 2021; Tu et al., 2014; Tu et al., 2017; Zolfo et al., 2018) . The future may rely on machine learning methods (boosted algorithms, random forests, neural networks, or new ones that may appear) for modeling *postmortem* microbiomes, overcoming the different analytical challenges and performing reliable predictions in death investigations (Zhang et al., 2019).

Other approaches involving transcriptomics and proteomics, which provide functional community information and/or a global snapshot of physiological and biochemical state of a sample, can be highly valuable (e.g., when DNA is absent or degraded as in hair or bones samples) and are increasingly explored (Burcham et al., 2019; Van-An et al., 2021). Also, flow cytometry (evaluating DNA degradation) and MALDITOF-MS (Matrix-assisted laser desorption/ionization time-of-flight mass spectrometry) or MALDI-IMS (Matrix-assisted laser desorption/ionization imaging mass spectrometry), respectively able to accurately identify bacteria at the species level and profiling the proteins and peptides in tissue sections, have been explored as promising tools for PMI calculation (Campobasso et al., 2022; Li et al., 2017; Williams et al., 2015).

1.4. Advantages and limitations of microbiome analysis in forensic investigations.

It is currently undeniable that microbial markers may complement routine forensic tests. The huge technological advances over the last two decades made it possible to overcome significant challenges as identifying unknown or hoax microorganisms, either non-cultivable in the laboratory, present in low numbers, in complex matrices or even genetically modified, or in cases where samples are degraded and human cellular components are limited and where the abundance and resistance of microorganisms may be an advantage (Roy et al., 2021; Swayambhu et al., 2023). Current methodological approaches allow faster diagnostics and monitoring independent of culture media, the reduction of time and associated costs, and surveillance of outbreaks and epidemics in real time. An extraordinary example is the fast and real time vigilance and monitoring during the COVID-19 pandemic. The management of this crisis was only possible due to the current sequencing and bioinformatic technologies we have nowadays available in many countries, enabling to identify and characterize, at the strain (SARS-CoV-2 variants) and subcellular (mutations in the spike surface of the virus, among others) levels, the virus circulating worldwide. At the same time, knowing the strains

circulating in many human and non-human sources in different areas allowed to deeply investigate if this pandemic started naturally or if the virus was yielded in the lab.

Despite the obvious advantages, many limitations to the implementation of forensic microbiology in legal contexts, especially with regard to knowledge of the human microbiome, still need to be overcome: most studies are small-scale; human microbiome show inter and intra-variability and temporal variations; the microbiome can be a mixture of different sources (suspect, victim, environment…); the variability of methods used (e.g., DNA control protocol, sequencing platform); the lack of standardization, standards and guidelines that can be universally and legally applied; the lack of databases, genome references, and metadata; the lack of sufficient representative genetic and geographic coverage (e.g., most PMI studies are from the USA); the limited access to human cadavers (most often animal models are used) in *postmortem* studies. Probably, one of the greatest obstacles that is common to the general Microbiology is the lack of a unique protocol with standard procedures both for DNA extraction and sequencing processes. Paradoxically, this lack of uniformity can also serve as an opportunity for fostering novel discoveries that might not have materialized if everyone adhered to the same rigid procedures (Walker et al., 2023). In fact, the sequencing technology, itself, and computational resources can provide a technical bias hampering the accurate determination of microbial composition (454 technology, Illumina, Nanopore) (Nearing et al., 2021; Pechal et al., 2014).

With respect to the studies on *postmortem* microbial succession in particular, the vast majority of them are performed in animal models, as the access to human cadavers is very limited. Thus, the translation of animal studies to the human scenario may be difficult to establish, making the interpretation of the results challenging (Speruda et al., 2021). Indeed, the most realistic approach of studying forensic microbiology during decomposition is to make use of human cadavers, but there are several reasons limiting their access and secured research. In addition, donated human cadavers can represent a highly variable initial microbiome, as already described. Different nonhuman animal models have been used as a proxy for humans in forensic decomposition (e.g., domesticated swine, rodents), especially in PMI estimation by forensic entomologists, as they are crucial to establish significant patterns in microbial communities, taxonomy, and different variables under controlled lab settings. Some manipulation studies can even control, for example. the presence/absence of arthropods (Benbow et al., 2017).

During the collection of samples for the calculation of PMI, the bacterial species isolated could have no cadaveric provenance due to sample contaminations. These contaminations can arise from different sources, including from non-sterile collection instruments or from the environment surrounding the cadaver. Therefore, because each sample presents specific traits, it is important to establish a contamination scale, which should be taken in consideration during data analysis (Speruda et al., 2021). The environmental variables that impact the accuracy of the models for PMI estimation remain largely unknown. Currently the temperature represents the only environmental variable tested and considered by the models for PMI estimation; however, other variables, such as humidity, oxygen, and precipitation, greatly impact the bacterial profile overtime. Thus, it is of great importance to include such variables for the development of novel models for PMI calculation. In addition, it remains largely unknown which type of samples and which body location has the most accurate bacterial population for PMI estimation. All this knowledge will certainly help in developing of novel, more robust and accurate models for the estimation of the PMI (Metcalf, 2019; Roy et al., 2021). A major limitation in the study of PMI using microbial succession is the fact that the most accurate period of the microbial clock remains unknown. It is considered that the microbial communities of decomposers should provide the most accurate estimative during periods of rapid microbial succession (early/active decay stage of decomposition), since bacteria have a large amount of nutrients available. However, large-scale data sets, with continuous sampling, for a long period of time, and taking into account temperature and humidity conditions, should be considered to validate such hypothesis (Metcalf, 2019). Overall, a large barrier to creating robust PMI models for the thanatomicrobiome knowledge is the lack of human cadaver-associated data sets from different environments, encompassing diverse populations and derived from standardized procedures.

2. Objectives

The crucial role that bacteria play in the body decomposition process is now well established and their use for forensic identification presents a compelling alternative to traditional methods. Despite the numerous challenges in the analysis of the *postmortem* complex microbial network, existing research underscores the potential of *postmortem* microbial succession, promising in both animal and human models, particularly for forensic purposes, such as estimating the PMI. The complexity of identifying distinctive *postmortem* microbial signatures to build comprehensive databases underscores the value of detailed knowledge about specific bacterial species serving as accurate PMI indicators during decomposition. While limited, some studies highlight the greater significance of particular bacterial genera over others in this context (Heimesaat et al., 2012; Roy et al., 2021).

Given the limited studies using routine culturomics approaches in murine models to investigate the natural bacterial evolution, this work aimed to map three key bacterial species (*Escherichia coli, Enterococcus faecalis, Staphylococcus aureus*) in different biological tissues of mice under natural conditions to understand how they evolve during a specific *postmortem* time period. These bacteria are natural inhabitants of the intestinal microbiota (*E. coli, E. faecalis*) or can be part of the skin and mucosal microbiota (*S. aureus*), all of which are commonly associated with significant human infections (e.g., endocarditis, urinary tract infections). Specific goals included:

- To assess the reliability of classical culturing approach combining different culture media for detecting key bacterial species and families across different *postmortem* timepoints;
- To identify and quantify the initial microbiota present in the different organs (time zero) for which scarce data is available;
- To determine if any of the bacterial species detected can serve as a reliable biomarker for calculating the *postmortem* interval.

3. Material and Methods

3.1. Ethics statement. Animal experimentation was carried out according to the European Guidelines for animal welfare (2010/63/EU), transposed into Portuguese law (Law No. 113/7, August 2013) and in accordance with the guidelines of the National Ethics Council for Life Sciences (CNECV)". All animal experiments were approved by the Organization Responsible for the Animal Welfare of the University Institute of Health Sciences (ORBEA-IUCS), reference ORBEA/IUCS/CESPU-001/2023.

3.2. Animal model, sacrifice and timepoints. Male C57BL/6J SPF (specific pathogen-free)-immunocompetent mice (*Mus musculus*), weighting 23-28 g (6-7 weeks of age), were acquired from Charles River Laboratories and co-housed at the Bioterio of the University Institute of Health Sciences under standard conditions of lighting (12-hour light/dark cycles), temperature (21.0 ± 1.5 °C), and relative humidity (50.0 ± 7.0%) with *ad libitum* access to food and water.

They were maintained under these conditions for at least 15 days prior starting the experiments (9-10 weeks old at the beginning of the experiments). Three independent assays were performed. In the first assay (pilot study), 12 mice were used, and organs were harvested at 11 different *postmortem* time points: 0 h (2 animals for control), 2 h, 4 h, 6 h, 8 h, 10 h, 11 h, 12 h, 24 h, 48 h, and 72 h. This assay served to refine the timepoints for the subsequent experiments. The remaining two assays (Experiment 1 and Experiment 2) served as the definitive study for our project, and 11 *postmortem* time points were selected: 0 h (2 animals for control), 2 h, 4 h, 8 h, 10 h, 12 h, 16 h, 20 h, 24 h, 36 h, and 48 h.

Animals were sacrificed in an isoflurane chamber followed by cervical dislocation (Figure 3). After death, animals were maintained at a controlled environment temperature of 21 ºC. The desired *postmortem* time points, different organs were collected: brain, heart, lungs, liver, spleen, stomach, kidneys, bladder with urine, intestines, and skeletal muscle from the hind limbs.
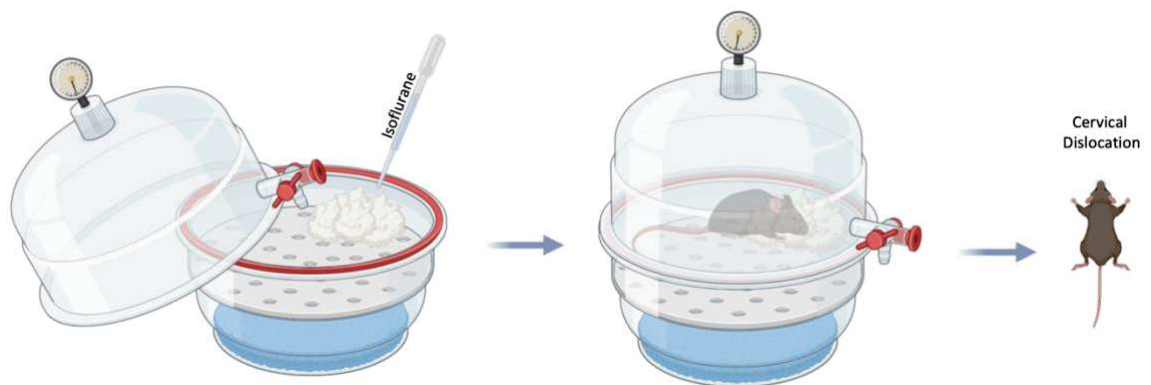
Figure 3. Illustration of the procedure used for animal sacrifice In an Isoflurane chamber followed by cervical dislocation.
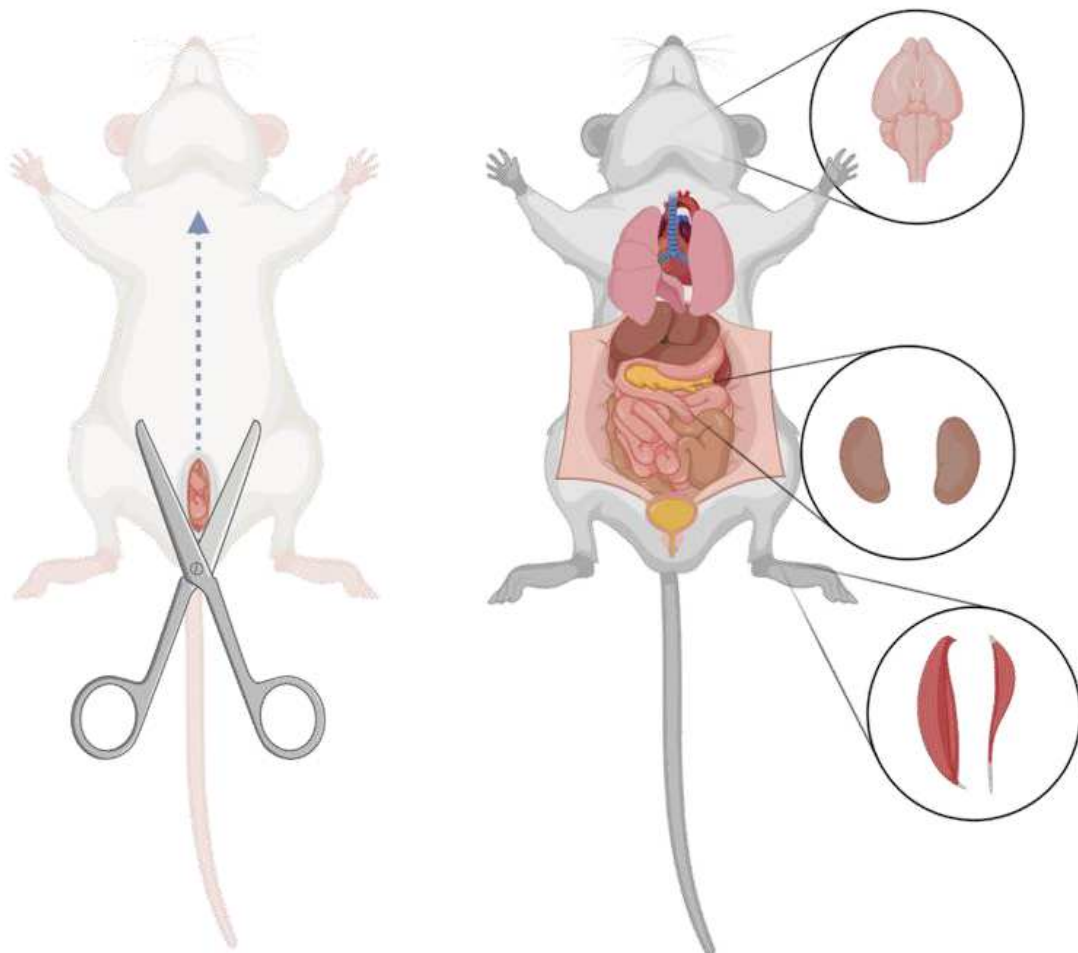
Figure 4. Procedure used for organ collection.

All surgical instruments were emerged in 70 % ethanol before organ harvesting. The collection of all organs was performed on a clean and disinfected dissecting board.

3.3. Sample collection.

All samples were weighed after harvesting and immediately frozen in liquid nitrogen in individual 15 mL tubes to prevent contamination between samples. Samples were stored at -80 °C until the microbiological (Pilot Assay and Experiments 1 and 2) and biochemical assays (Experiments 1 and 2).

3.3.1. Bladder + urine.

The collection of bladder (with urine) was performed by removing the entire sample from the abdominal cavity, avoiding bladder rupture.

3.3.2. Lungs, heart, liver, kidneys, spleen, and stomach.

The mouse carcass was placed in a dorsal recumbent position. The abdominal cavity was opened with an incision along the midline, extending cranially to the level of the thorax and caudally to the pubis, and the abdominal walls were laterally retracted. With the relevant tissues exposed, each tissue was collected using sterile forceps and scissors. All unnecessary fat and connective tissue were removed (Dinis-Oliveira et al., 2010; Parkinson et al., 2011).

3.3.3. Intestine.

The colon was segmented distal to the pubis level, and the colon was retracted out of the carcass. The mesenteric attachments were removed to straighten the large and small intestines. An almost complete collection of the colon and small intestine was performed.

3.3.4. Brain.

Using small scissors, the lower blade was inserted into the opening where the skull opens towards the spinal canal, and a straight upward cut was made through the midline of the skull. With forceps, the two halves of the skull were separated to expose the brain. The entire brain was collected.

3.3.5. Skeletal Muscle.

Tissue was collected from the hind limbs, both right and left.

3.4. Cultural analysis. Analysis of total aerobic bacterial load and counts of *Escherichia coli*, *Staphylococcus aureus*, and *Enterococcus faecalis*.

I. Before starting the experiments, fecal pellets available in the box housing the mice were collected to confirm their colonization by the bacterial species *E. faecalis, S. aureus* and *E. coli*. This procedure was done prior all three assays. Fecal samples (Table 1) and the extracted tissues (Table 2) during the pilot assay were resuspended and homogenized in Buffered Peptone Water (BPW at 1:10) (Figure 5). Serial 1:10 dilutions (100 μL of the solution in 900 μL of saline solution) were prepared. One hundred microliters of each dilution were Inoculated In different selective culture media for *Enterococcus* (Slanetz & Bartley agar), *Staphylococcus* (Mannitol Salt Agar), and enterobacteria (MacConkey agar), which were used for the quantitative detection of *E. faecalis, S. aureus,* and *E. coli*, respectively (Heimesaat et al., 2006). For the total bacterial count, samples (100 μL) were inoculated onto blood agar medium under aerobic conditions.
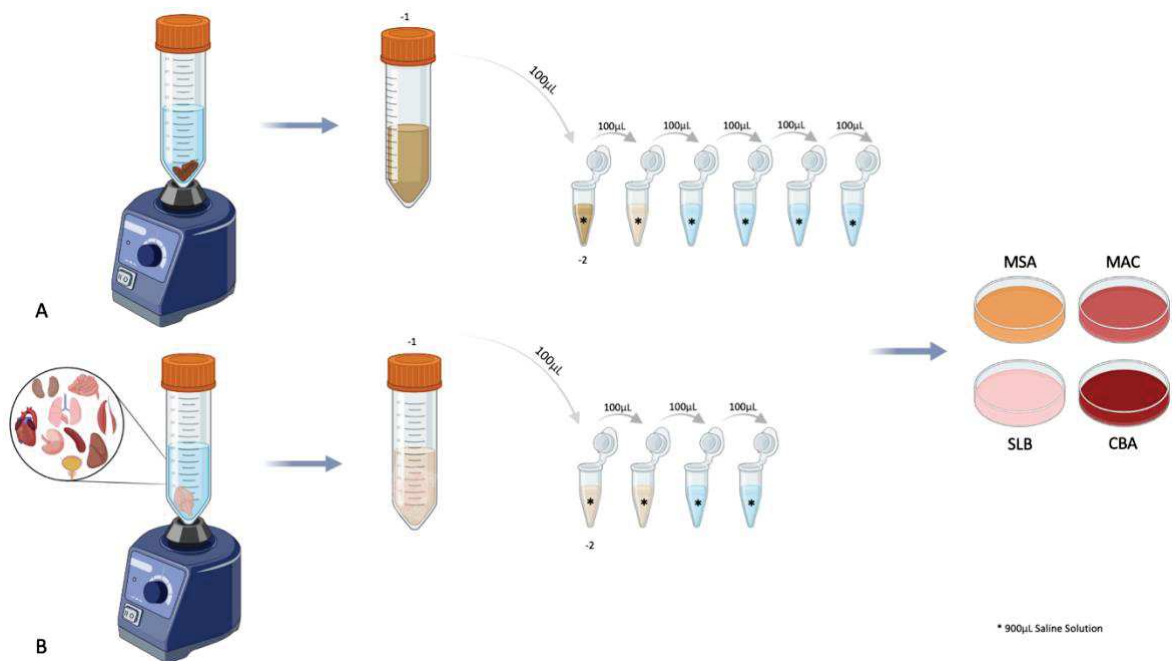
Figure 5. Illustration of the sample processing protocol for microbiological quantifications in fecal (A) and tissue samples (B). Processed samples were Inoculated in different media, including Mannitol Salt Agar (MSA), MacConkey Agar (MAC), Slanetz & Bartley Agar (SLB), and Columbia Blood Agar (CBA).

II. For experiments 1 and 2, collected samples were divided into 2 different portions (stored in 1.5 mL tubes) to be used for microbiological analyses (Figure 6) and to store at -80°C for future studies. For microbiological analysis, BPW was added at the 1:10 ratio, tissue was

homogenized by vortex followed mechanical rupture with a pellet pestle homogenizer. Samples diluted and further inoculated in selective media as described in I).
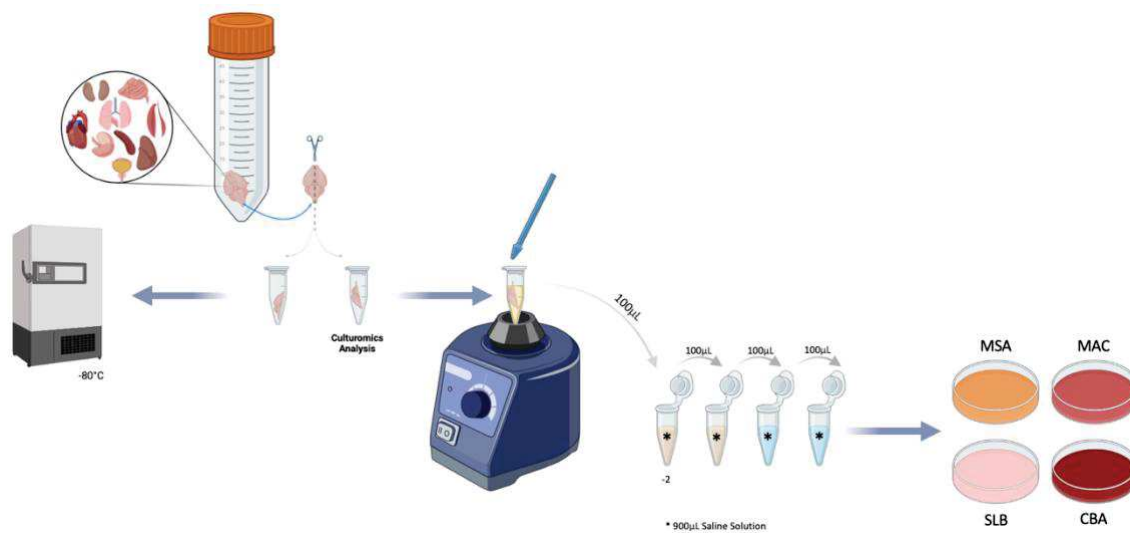
Figure 6. Illustration of the sample processing protocol for microbiological quantifications in tissue samples collected in experiments 1 and 2. Samples were first split in 2 fractions. One fraction was restored at -80 ºC and the remaining tissued was processed for microbiological analysis. Processed samples were then cultured on different media: Mannitol Salt Agar (MSA), MacConkey Agar (MAC), and Slanetz & Bartley Agar (SLB), and Columbia Blood Agar (CBA).

All culture media were incubated aerobically in a Memmert 4032/3 incubator at 37°C. The total bacterial count and the count of the three bacterial species of interest were expressed as Colony Forming Units (CFU/mL) per gram of tissue or per mL of sample, considering the initial amount of tissued used (grams). *Enterococcus faecalis* ATCC 29212*, Staphylococcus aureus* ATCC 29213, and *Escherichia coli* ATCC 25922 (American Type Culture Collection) were used as control strains.

For each condition, colonies with distinct morphologies were selected for further identification. These colonies were purified on Brain Heart Infusion agar media and preserved at -80 °C in Tryptone Soy Broth (TSB) medium with 15% glycerol. Each frozen isolate was assigned with a code number for subsequent studies.

Table 2. Organs collected in each assay and their respective masses (in grams) used for the microbiological assays.

		Brain	Heart	Lungs	Kidney	Liver	Spleen	Stomach	Intestine	Skeletal muscle	Bladder + urine
0 h (1)	Pilot Assay	0.4961	0.2096	0.1688	0.3627	1.5558	0.0961	0.4327	1.1704	0.4943	0.1257
	Experiment 1	0.2725	0.1462	0.1688	0.2303	0.482	0.0554	0.1540	1.1320	0.4465	0.0371
	Experiment 2	0.0930	0.0631	0.0488	0.0847	0.0866	0.0366	0.0831	0.0935	0.0768	0.1246
0 h (2)	Pilot Assay	0.3	0.0	0.0	0.3	0.9	0.0	0.3	0.9	0.4	-
	Experiment 1	0.2281	0.1472	0.1443	0.2316	1.6034	0.0459	0.2301	1.924	0.8038	0.1705
	Experiment 2	0.1422	0.0918	0.0645	0.1198	0.1171	0.0565	0.0889	0.1132	0.1436	0.1070
2 h	Pilot Assay	0.5543	0.1749	0.1917	0.4190	1.5244	0.1127	0.5543	0.9897	0.5931	0.1393
	Experiment 1	0.0723	0.0919	0.0491	0.1197	0.0772	0.0409	0.0901	0.1133	0.1112	0.0815
	Experiment 2	0.0819	0.1137	0.0787	0.0899	0.1192	0.041	0.1115	0.0628	0.1100	0.1236
4 h	Pilot Assay	0.4293	0.1270	0.2302	0.4495	1.4360	0.1109	0.3932	1.3780	0.5462	0.0424
	Experiment 1	0.1365	0.0957	0.1224	0.1075	0.0751	0.0382	0.1038	0.0571	0.1199	0.1364
	Experiment 2	0.1186	0.1026	0.1144	0.0913	0.1216	0.0488	0.1221	0.1158	0.0906	0.0842
6 h	Pilot Assay	0.4783	0.1947	0.3199	0.5134	1.8026	0.3158	0.4150	1.0702	0.8033	0.0657
8 h	Pilot Assay	0.5304	0.2643	0.2586	0.4193	0.9958	0.2074	0.8408	1.1229	0.7831	0.2158
	Experiment 1	0.1377	0.0821	0.118	0.1014	0.1733	0.045	0.136	0.0941	0.0976	0.0709
	Experiment 2	0.1106	0.113	0.0921	0.1081	0.114	0.0455	0.0663	0.083	0.1058	0.0632
10 h	Pilot Assay	0.3639	0.2531	0.2678	0.3863	1.6783	0.2826	0.5306	1.2824	0.7174	0.2109
	Experiment 1	0.1461	0.0854	0.0842	0.1588	0.1659	0.0361	0.1268	0.0979	0.1245	0.0391
	Experiment 2	0.1275	0.1267	0.0756	0.1213	0.1064	0.1008	0.0918	0.1468	0.0801	0.0913
11 h	Pilot Assay	0.3811	0.1957	0.2580	0.3917	1.7480	0.1158	0.5679	0.7543	0.5559	0.0976
12 h	Pilot Assay	0.4989	0.2169	0.2526	0.4789	1.6619	0.2359	0.4524	0.9898g	1.0942	0.1566
	Experiment 1	0.0842	0.1031	0.0735	0.1204	0.0606	0.0465	0.1295	0.0981	0.1309	0.0311
	Experiment 2	0.1135	0.1036	0.0929	0.0829	0.1104	0.0471	0.0645	0.1374	0.1113	0.1743

Table 2. Organs collected in each assay and their respective masses (in grams) used for the microbiological assays (continuation).

		Brain	Heart	Lungs	Kidney	Liver	Spleen	Stomach	Intestine	Skeletal muscle	Bladder + urine
16 h	Experiment 1	0.0875	0.0854	0.0588	0.0936	0.124	0.0412	0.1301	0.1517	0.1207	0.1248
	Experiment 2	0.0905	0.0974	0.0833	0.1133	0.0917	0.0434	0.0912	0.0604	0.0994	0.0363
20 h	Experiment 1	0.1304	0.0689	0.0955	0.0647	0.147	0.0371	0.0917	0.1375	0.1246	0.158
	Experiment 2	0.11	0.1067	0.0773	0.0901	0.104	0.0519	0.119	0.1012	0.0956	0.0969
24 h	Pilot Assay	0.4919	0.2048	0.3251	0.4811	1.8121	0.1422	0.7093	1.3370	1.1494	0.1353
	Experiment 1	0.1325	0.0871	0.0882	0.0808	0.099	0.0418	0.066	0.0631	0.0903	0.1298
	Experiment 2	0.0737	0.0795	0.0618	0.1024	0.0786	0.0675	0.1011	0.0728	0.0834	0.0751
36 h	Experiment 1	0.1139	0.1134	0.0857	0.1176	0.1056	0.0495	0.1409	0.1445	0.0831	0.1102
	Experiment 2	0.1275	0.0785	0.0643	0.0977	0.0851	0.0348	0.1106	0.0939	0.1019	0.0808
48 h	Pilot Assay	0.3373	0.1859	0.2339	0.4438	2.0876	0.1537	0.4790	1.5636	1.2245	0.2683
	Experiment 1	0.0749	0.0815	0.0911	0.0877	0.1173	0.0438	0.1415	0.1102	0.1336	0.0907
	Experiment 2	0.1197	0.0754	0.0723	0.1002	0.0652	0.0448	0.0937	0.0984	0.0915	0.0688
72 h	Pilot Assay	0.3945	0.1916	0.2147	0.3726	1.3639	0.1092	0.4303	1.3000	1.3032	0.1914

*Masses equal to "0.0" due to the use of a semi-analytical balance incapable of measuring such small masses, which was replaced by an analytical balance as soon as the collection was completed. The "-" symbol was used to indicate the absence of mass, as the biologic sample (Bladder + urine) was not collected.

3.5. Bacterial species identification.

Bacterial identification was performed by the reference spectroscopy method using a MALDITOF-MS device (Figure 7). This technology generates characteristic mass spectra that serve as unique microbial fingerprints. It allows for precise identification at the species level for most Gram-positive and Gram-negative bacterial strains (Croxatto et al., 2012). The device uses a laser to dissociate the sample into its constituent particles and molecules, measuring the time they take to fly through a certain space until they reach the detector. The created spectrum is then compared to a comprehensive reference database (Gao et al., 2022).
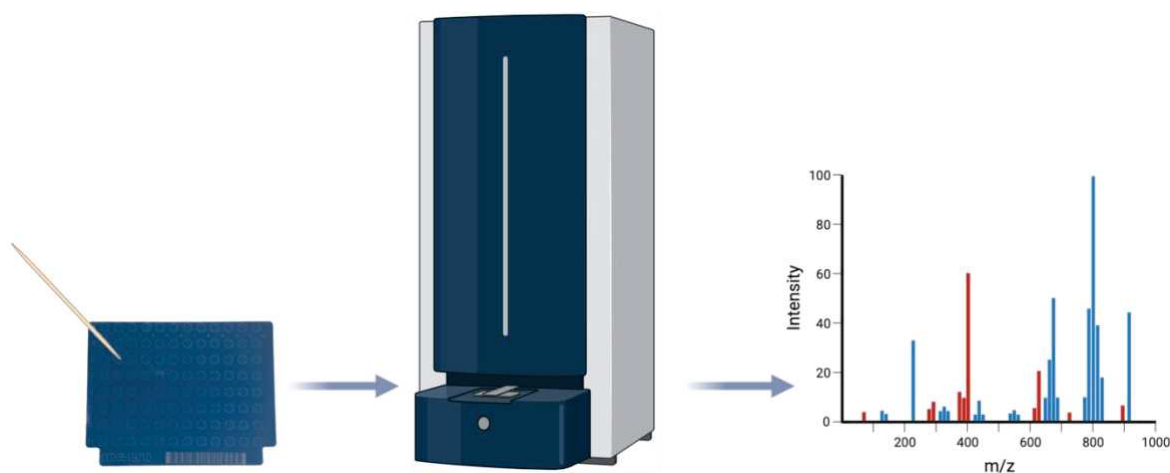
Figure 7. Schematic of the procedure used for using MALDITOF-MS analysis, including the preparation of the plate (by inoculating a fresh pure colony with a loop) and the final spectrum acquisition.

3.6. Culture media used.

Culture media, including MacConkey Agar, Mannitol Salt Agar, Slanetz & Bartley Agar, and Brain Heart Infusion Agar, used for bacterial growth, were prepared as follows:

i) For Brain Heart Infusion Agar (Frilabo, 61007), 26 g of powder were solubilized in 500 mL of distilled water, autoclaved, and dispensed in 90 mm diameter plates. Brain Heart Infusion Agar, a non-selective medium, is employed to grow and isolate a diverse array of microorganisms such as bacteria and fungi. This medium is adaptable and nutrient-rich, offering the necessary nutrients for fostering the growth of a wide spectrum of microorganisms. In this project, it was utilized to replicate bacteria and generate fresh colonies.

ii) For <u>MacConkey Agar</u> (Frilabo, 610028), 25.75 g of powder were solubilized in 500 mL of distilled water, autoclaved and dispensed in 90 mm diameter plates. MacConkey agar is a specialized medium that allows the selective growth and selection of gram-negative bacteria. It can also differentiate gram-negative bacteria based on their ability to metabolize lactose. As a result, gram-negative lactose fermenters will produce pink colonies as *Escherichia coli* (Jung et al., 2023).

iii) For <u>Mannitol Salt Agar</u> (Frilabo, 610029), 55.5 g of powder were solubilized in 500 mL of distilled water, autoclaved, and dispensed in 90 mm diameter plates. was used for each 500mL of distilled water. The Mannitol Salt agar medium is a selective for bacteria tolerant to high salt levels, specifically *Staphylococcus* genus and *Staphylococcus aureus*. It differentiates *Staphylococcus* species based on mannitol fermentation, where bacteria growth lowers the medium's pH and results in yellow-colored colonies (typical of *S. aureus*).

iv) To prepare <u>Buffered Peptone Water</u> (Scharlau, 02-277-500) 2 g of the powder were solubilized In 100 mL of distilled water, autoclaved and dispensed In 90 mm diameter plates. Buffered Peptone Water medium is a versatile microbiological medium used for the pre-enrichment of samples to recover sub-lethally injured bacteria. Its neutral pH and nutrient-rich composition make it suitable for promoting the repair and growth of these bacteria before their isolation on selective media.

v) For <u>Slanetz & Bartley Agar + Triphenyltetrazolium Chloride (TTC)</u> (Liofilchem, 610147), 22.25 g of powder were dissolved in 500 mL of distilled water. The mixture was boiled until complete dissolution, but not autoclaved, as this process would lead to the oxidation of TTC, rendering the medium nonviable. Slanetz & Bartley Agar + TTC is a specialized microbiological medium used for the detection and enumeration of *Enterococci*, as they generate distinctive red or pink colonies through the fermentation of TTC l to create a red formazan compound inside the bacterial cell. The agar plates were then incubated at 37°C for 48 hours, to allow bacteria growth and color change. *Enterococcus faecalis*, the target enterococci species of our study, shows dark wine-coloured colonies instead of pink colonies (more common for *E. faecium* species).

vi) The <u>blood agar</u>, Columbia Agar 5% sheep blood, used for total bacterial growth and counting, was ordered pre-plated from Frilabo (FRI0066P) or bioMérieux AS (43041). It is a microbiological culture medium used for cultivating a wide range of microorganisms. It is nutrient-rich, containing agar, nutrients, and 5% sheep blood. It allows the differentiation of bacteria through hemolytic activity, leading to distinct patterns of red blood cell breakdown, including alpha-hemolysis, beta-hemolysis, and gamma-hemolysis. Additionally, this medium can be used for bacterial isolation to obtain fresh cultures.

vii) For the preparation of <u>Tryptone Soya Broth</u> medium (Oxoid, CM0129) with glycerol, 15 g of TSB were diluted in 500 milliliters of distilled water, along with the addition of 15% glycerol. The solution was then sterilized by autoclave. Glycerol works as an additional carbon source for microbial growth and as a cryoprotector for long-term storage. This medium is used in distinct microbiological scenarios, including the cultivation and maintenance of bacterial cultures, and the preservation of those cultures for long periods of time.

4. Results and Discussion

4.1. *Enterococcus faecalis* and *Escherichia coli* are gut colonizers of the C57BL/6J SPF-immunocompetent mice.

SPF, and then specific (and opportunistic) pathogen-free (SOPF) inbred lines (lacking specific opportunist pathogens, such as *Staphylococcus aureus* or *Pseudomonas aeruginosa*) now represents the common health standard for experimental mouse breeding (Convenor et al., 2014). Still, and given the numerous factors that may influence mice microbiota post-weaning, we performed an initial evaluation of the fecal microbiota in the animals before initiating the experimental assays. This practice, as previously recommended (Guo et al., 2022), is advantageous in mouse studies, providing valuable insights into the variations between different mouse strains. To confirm the colonization of the C57BL/6J SPF-immunocompetent mice used in this study by the target bacterial species *E. faecalis, S. aureus* and *E. coli*, fecal samples were cultivated on specific media Slanetz & Bartley, Mannitol Salt Agar, and MacConkey, respectively. The total bacterial load (total countable colonies growing in blood agar) ranged between 1.0×10^5 and 3.6×10^8 CFU/g for the mice enrolled in the pilot assay, between 1.0×10^7 and 2.0×10^7 CFU/g for the experiment 1 and 2.0×10^7 CFU/g (twice) for the experiment 2 (Table 2).

We confirmed the presence of Gram-positive *E. faecalis* and Gram-negative *E. coli* bacterial species, among other common commensal species typically found in mice. A positive growth of *E. faecalis* and *E. coli* was observed in all (only one was negative for *E. coli*) of the samples analyzed, which was expected since they are common gut colonizers of animals, including mice, beside humans (Wang et al., 2019). Notably, and given the high bacterial load occurring in the gut, these two species could not be detected in the blood agar plates in all cases, highlighting the importance of using selective culture media to maximize the number of bacterial species isolated. In contrast, *S. aureus* could not be detected in any fecal sample, which is not surprising since this species, if present, is more associated with murine skin rather than the intestine (Tavakkol et al., 2010). In addition, *S. aureus* can be recovered from murine skin, but not all mouse colonies seem to carry *S. aureus* (Schulz et al., 2017). Although not all mice naturally host *S. aureus*, it has occasionally been considered an organism introduced by human caretakers, rather than a native commensal of mice. Adding complexity to this issue, staphylococcal species like *S. aureus* and *Staphylococcus xylosus* can propagate swiftly within groups of

cohoused animals (Gimblet et al., 2017), which means that the transfer of *S. aureus* from caretakers to just a few animals could potentially result in its widespread dissemination throughout the entire colony.

For long that the mice models used (C57BL/6J SPF) have been recommended for biomedical research as 'animals that are free of specific microorganisms and parasites, but not necessarily free of others not specified' (O'Rourke et al., 1988). As so, researchers using SPF rodents are encouraged to determine the baseline loading of these bacteria in the animals used due to the undefined composition, fluctuation (with diet or environment) and interindividual diversity of the microbiota of laboratory mice. Thus, this remains a limitation since the scientific community still lacks a common SPF standard cocktail (Appendix 7.1). The richness of the mouse gut microbiota is typically estimated to encompass over 300 bacterial genera (Nguyen et al., 2015). Among the common colonizers of the mouse intestine, seven bacterial phyla are prevalent, with Bacillota, Bacteroidota, and Pseudomonadota being the most predominant (Clavel et al., 2016; Xiao et al., 2015). A recent and comprehensive study analyzing the minimal microbiota containing representative and prevalent bacteria from the gut of the same rodent model of our study showed, by whole-genome sequencing (WGS), that 20 different families were consistently present in all tested mice. Although not present with the highest loads, some of these families were common to our findings, such as Enterobacteriaceae (e.g., *E. coli*), Lactobacillaceae (e.g., *Ligilactobacillus murinus*), and Bacillaceae (e.g., *Bacillus pumilus*) (Darnaud et al., 2021). We further identified in fecal pellets *S. xylosus* (7/7 of the fecal samples) and *Acinetobacter lwoffii* (1/7 of the fecal samples), which belong to Staphylococcaceae and Moraxellaceae families, respectively (Table 2). This does not imply that these species cannot be found in these mice because the cited study only refers to the bacterial families occurring in all mice samples. In fact, *S. xylosus* has been identified as a major colonizer in both mouse ear skin from wild mice and C57BL/6 laboratory raised mice, whereas human prevalent species, such as *S. epidermidis* and *S. aureus,* were not identified as major species on murine skin (Belheouane et al., 2020; Tavakkol et al., 2010). *S. xylosus* is a commensal of murine skin, but can become pathogenic when there are disruptions to the skin barrier and/or when the host immune response is compromised (Battaglia et al., 2023). It is also curious that apparently there are inherent features of murine skin promoting the colonization by *S. xylosus*, while features of human skin disfavor *S. xylosus* colonization. Furthermore, *S. xylosus* has been

repeatedly associated with infected skin wounds in mice, both in immunocompromised mice and in non-immunocompromised ones (Battaglia et al., 2023).

Table 3. Record of fecal samples collected for microbiological analysis.

	Sample (*n* of mice)	Weight	CFU/g CBA	CFU/g MAC	CFU/g MSA	CFU/g SLB	Species ID
Pilot assay	1 (4 mice)	4.62 g	3.6×10^8	3.0×10^8	1.6×10^5	2.0×10^7	*Enterococcus faecalis* *Escherichia coli* *Staphylococcus xylosus* *Acinetobacter lwoffii*
	2 (4 mice)	3.28 g	1.7×10^6	2.0×10^2	1.5×10^6	1.9×10^4	*Enterococcus faecalis* *Escherichia coli* *Staphylococcus xylosus* *Pantoea agglomerans* *Bacillus pumilus* *Ligilactobacillus murinus*
	3 (4 mice)	3.00 g	1.0×10^5	6.0×10^3	9.0×10^4	6.0×10^4	*Enterococcus faecalis* *Escherichia coli* *Staphylococcus xylosus*
Experiment 1	4 (6 mice)	1.21 g	2.0×10^7	1.2×10^5	1.6×10^7	1.3×10^6	*Enterococcus faecalis* *Staphylococcus xylosus* *Escherichia coli*
	5 (6 mice)	1.17 g	1.0×10^7	7.0×10^5	9.5×10^6	6.0×10^5	*Enterococcus faecalis* *Staphylococcus xylosus*
Experiment 2	6 (6 mice)	1.25 g	2.0×10^7	4.0×10^5	1.5×10^7	3.0×10^6	*Enterococcus faecalis* *Staphylococcus xylosus* *Escherichia coli*
	7 (6 mice)	1.24 g	2.0×10^7	1.0×10^6	1.2×10^7	7.0×10^5	*Enterococcus faecalis* *Escherichia coli* *Staphylococcus xylosus*

Abbreviations: CFU, Colony Forming Units; CBA, Columbia Blood Agar; MAC, MacConkey Agar; MSA, Mannitol Salt Agar; SLB, Slanetz & Bartley Agar; ID, identification.

4.2. Analysis of *postmortem* bacterial communities after death reveals a dominance of Bacillota and increase of particular bacterial species.

Before harvesting each organ, a photograph was taken of the respective mouse at each time point. This allowed for closer examination and consideration of the anatomical changes initially observed. Essentially, a reduction in blood concentration within the organs was evident, causing them to become paler, particularly noticeable in the liver (Figure 8). In the intestine, the presence of air bubbles begun to appear at 20 h, becoming more pronounced from 48 h *postmortem* onward. The brain became a gelatinous paste from 24 h after death.

Regarding the cultural analysis, a total of 1304 samples were collected from 36 animals along 11 timepoints that spanned 2 days (experiments 1 and 2) or 3 days (pilot assay) of decomposition. The microbial variation observed in the different organs analyzed after death was visually registered and quantified in terms of CFU/g of tissue (brain, heart, lung, kidney, liver, spleen, urine + bladder, stomach, gut and skeletal muscle). For a clear quantification of CFU In each organ along the different timepoints, we considered that there should be a clear reduction in the number of colonies as the dilution factor becomes higher, such that counting distinct CFU is possible for at least two dilutions. It is important to highlight that our phenotypical approach, which exclusively focused on aerobically growing bacteria, has limitations. This method does not allow us to observe numerous fastidious species, including obligate anaerobic bacteria that are commonly found in the complex intestinal microbiota. Additionally, it may fail to detect bacteria that have died in the meantime, which can only be captured using molecular methods.

Regardless of the organ or time point examined, our methodological approach detected a total of 44 different bacterial species belonging to 13 families and 3 phyla. The majority (36 out of 44) were associated with nine families within the Bacillota phylum, while the remaining species were assigned to the Pseudomonadota (3 out of 44) and Actinomycetota (5 out of 44) phyla (Figure 9). These results are consistent with other studies (Li et al., 2021; Liu et al., 2020) also referring these among the top phyla present in all or most timepoints.
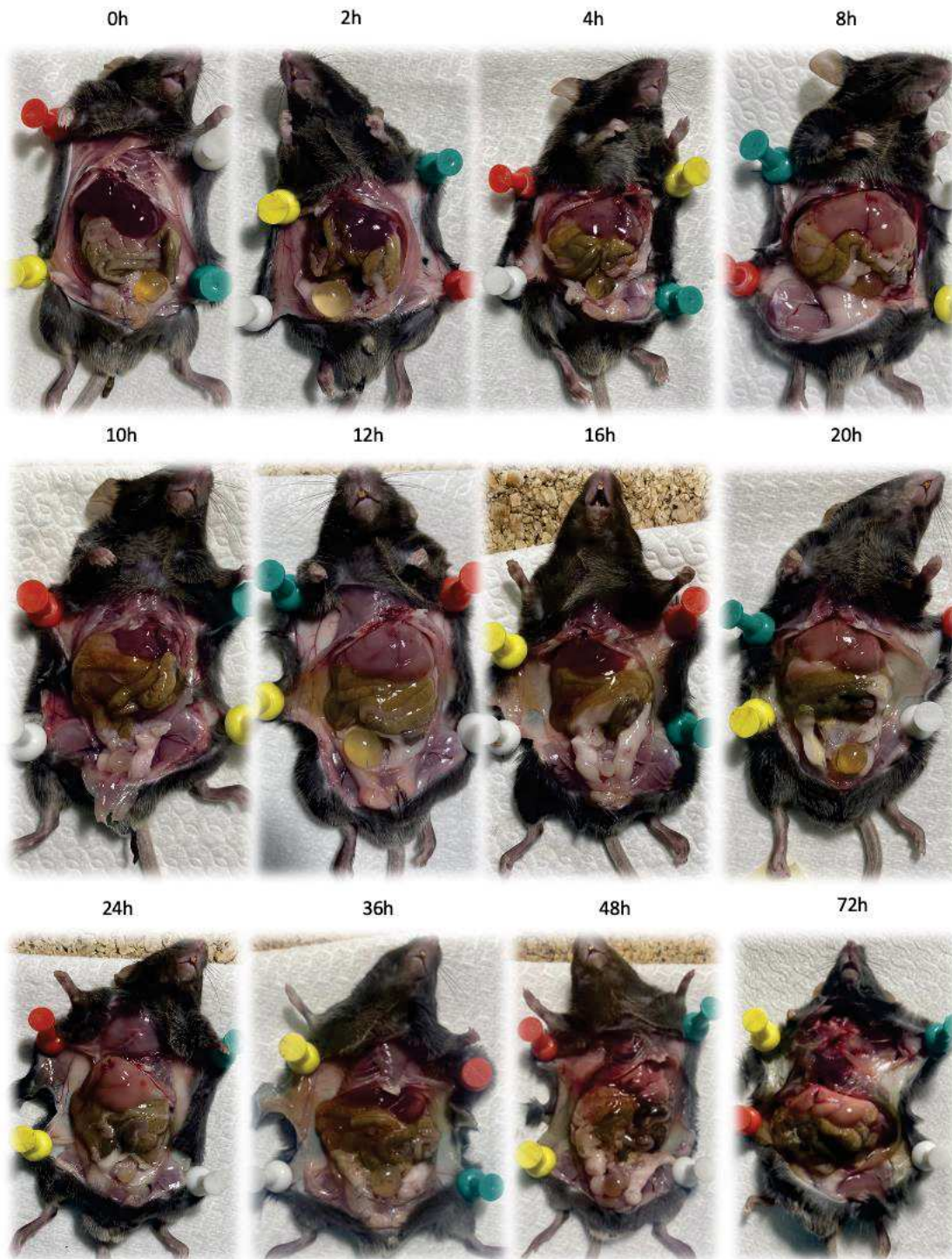
Figure 8. Photographic record of the anatomical changes visible after animal sacrifice at different timepoints.

The usually dominant anaerobic Bacteroidota phyla could not be detected in our study since we were limited to a routine-based culturomic assay made aerobically. Species that were consistently present in all organs analyzed included *S. xylosus, E. faecalis* and *E. coli*. Other species of *Staphylococcus*, *Bacillus* spp, and *L. murinus,* were identified in most organs and samples, whereas some species were only identified in a particular organ (e.g., *Pseudomonas* in the stomach or *Ureibacillus* in the kidney) (Figure 9). Consistent with our findings, other studies have similarly identified *E. faecalis* and *Escherichia* spp as among the most abundant species (Liu et al., 2020).

Taking in account the evolution of bacterial occurrence along time in all the ten organs analyzed, major variations at the family level are illustrated in Figure 10. It is crucial to note that this figure does not provide information on bacterial counts (quantification), but instead it illustrates the frequency (presence/absence) of the different bacterial families in the various samples throughout the decomposition process.

Main fluctuations are described as follows:

- **Staphylococcaceae** were dominant and showed a decreasing abundance over PMI progression. The dominance of members of this family, essentially *Staphylococcus* spp, has been previously reported (Heimesaat et al., 2012; Tuomisto et al., 2013). These minor gut bacteria are mainly linked to mice skin and mucosa as mentioned in the previous section and, as already suggested in other studies (Tuomisto, Karhunen, Vuento, et al., 2013), the presence of non-*S. aureus* staphylococci species may indicate sample contamination.

- **Enterococcaceae** and **Enterobacteriaceae** showed similar trends: while Enterococcaceae exhibited some fluctuations until 12 h, but clearly became dominant after 24 h, Enterobacteriaceae remained relatively stable until 12 h and also showed an increase after 24 h. The notorious increase of *Enterococcaceae* and *Enterobacteriaceae* through decomposition has been previously shown in different studies (Heimesaat et al., 2012; Hyde et al., 2015; Li et al., 2021; Liu et al., 2020), with Li *et al.* (Li et al., 2021) describing these bacteria as representing the major proportion from 0 h to 15 days.
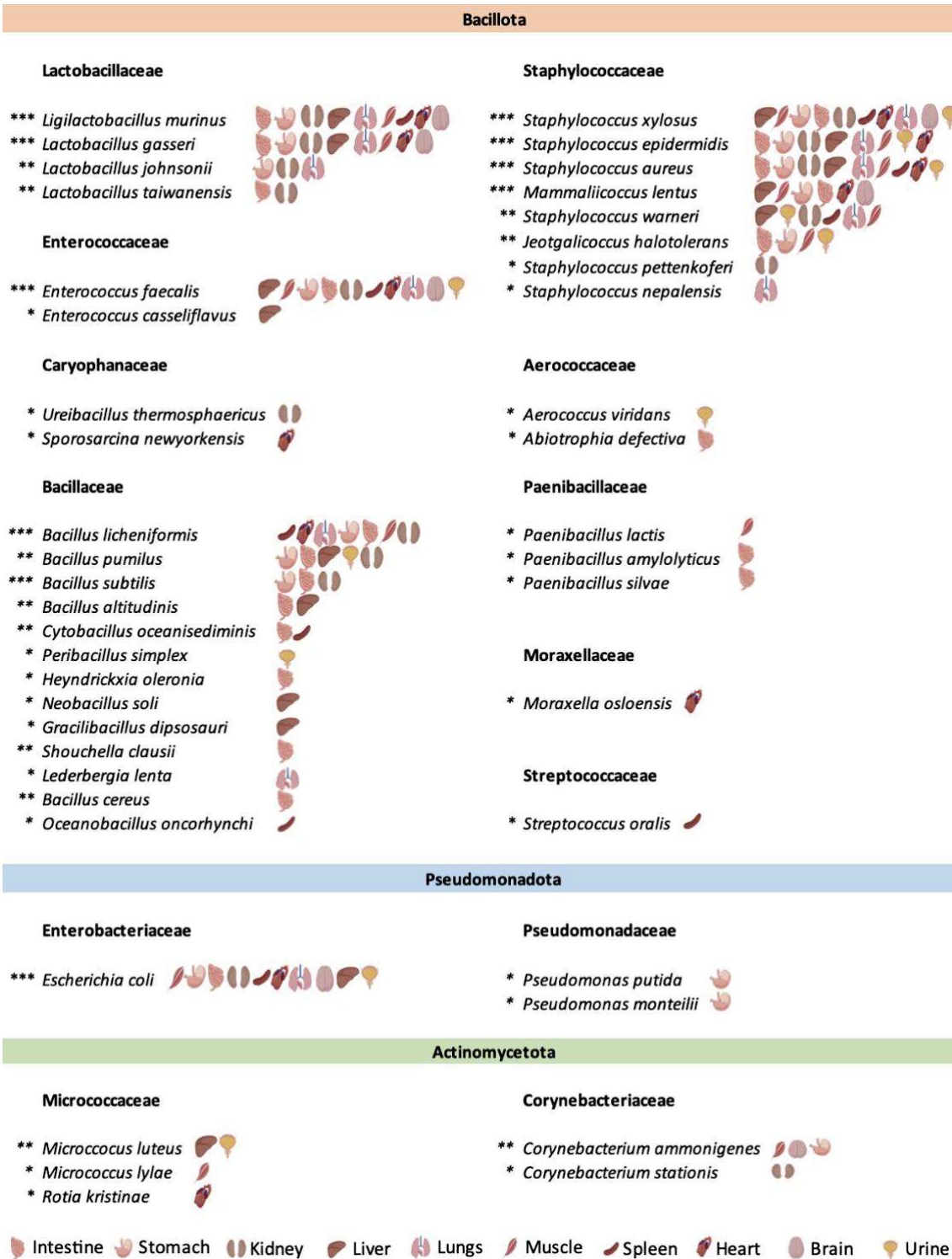
Figure 9. Distribution of the bacterial species found in the analyzed samples, organized by families and their respective phyla. *Species found only once (one sample); **Species found in 2 to 10 samples; ***Species found in more than 10 samples.

Figure 10. Distribution of all bacterial families detected at the different timepoints during 48 h of decomposition. The size of each portion is proportional to the frequency of each family's occurrence across the different samples, regardless of the organ analyzed. The overall sample size (n=1304) was not factored into this analysis; instead, only the presence or absence of bacterial families in each organ was considered in all of the experiments. Bacterial families are categorized by different colours according to the phylum they belong to (Bacillota in gradients of orange, Pseudomonadota in gradients of blue, and Actinomycetota in gradients of green).

- **Bacillaceae** was relatively stable over time. While this family was not the focus of our study, it has been described as dominant after 5 days *postmortem* and as the main representatives within Bacillota from bloat to advanced decay (Adserias-Garriga et al., 2017; Pechal et al., 2014). This observation is in line with their resilient and, in several cases, endospore-forming nature, enabling them to resist until the stage of dry remains (García et al., 2020).

- **Lactobacillaceae** were present since 0 h and showed a slight increase until 12 h, and then started decreasing. This initial increase has been described by Metcalf and colleagues (Metcalf et al., 2013; Metcalf, Xu, et al., 2016) who demonstrated that the relative abundances of anaerobic gut bacteria (such as Lactobacillaceae) increased at the bloat stage. Afterward, significant decreases of the microaerophilic lactobacilli populations are well described in association with an overall drop in the total bacterial load in the intestinal microbiota of mice (Hauther et al., 2015; Heimesaat et al., 2012; Li et al., 2021; Metcalf et al., 2013). Notably, lactobacilli can be both aerobic and anaerobic, and their metabolism can be influenced by the presence of oxygen, which partly explains the fluctuations observed (Tuomisto et al., 2013). Even though we did not use specific culture media and atmospheric conditions to culture members of this fastidious bacterial family, our results corroborate one of the highest occurrences of Lactobacillaceae at 12 h (Figure 10), their occurrence in different organs (Figure 9), and so the swift translocation of intestinal bacteria, which could prove valuable in differentiating between primary pathogenic agents and secondary putrefactive contaminants.

- Specific families, such as Caryophanaceae (8 h e 12 h), Micrococcaceae (0 h, 8 h, 24 h, 36 h, 48 h), Aerococcaceae (16 h, 24 h), Paenibacillaceae (0 h, 24 h), Corynebacteriaceae (0h, 8 h, 16 h, 36 h), and Pseudomonadoceae (8 h, 48 h) were punctually observed. Those observed at 0 h most probably correspond to contaminants from skin/mucosa (Micrococcaceae) or normal habitants of the intestine (Paenibacillaceae) (Guo et al., 2022). Aerococcaceae family has been identified in the fresh stage of decomposition before (Pechal et al., 2014).

When examining the changes in bacterial frequencies over time across all ten analyzed organs, significant variations at the species level are depicted in Figure 11. Species that appeared only once have been excluded from the analysis.
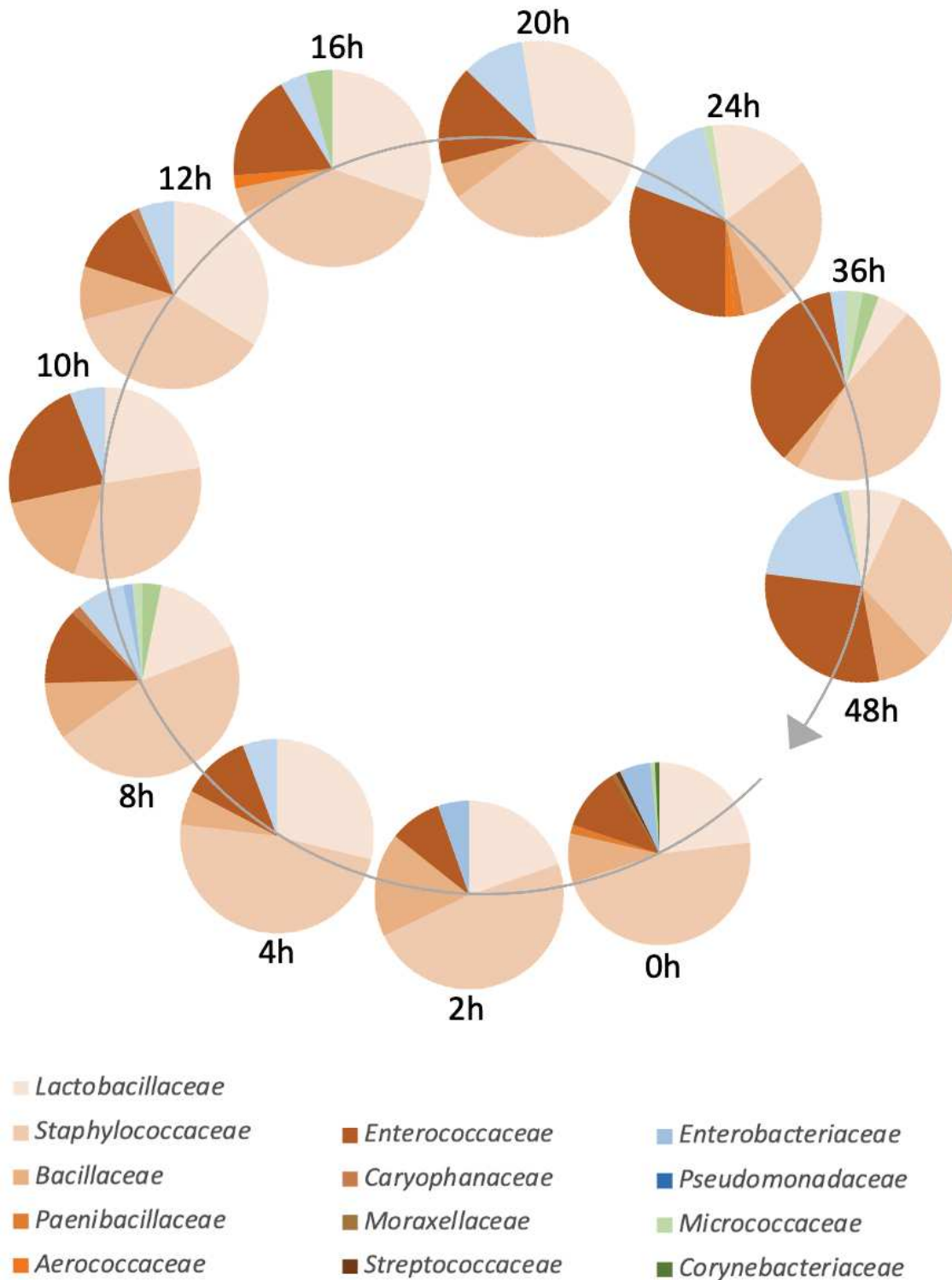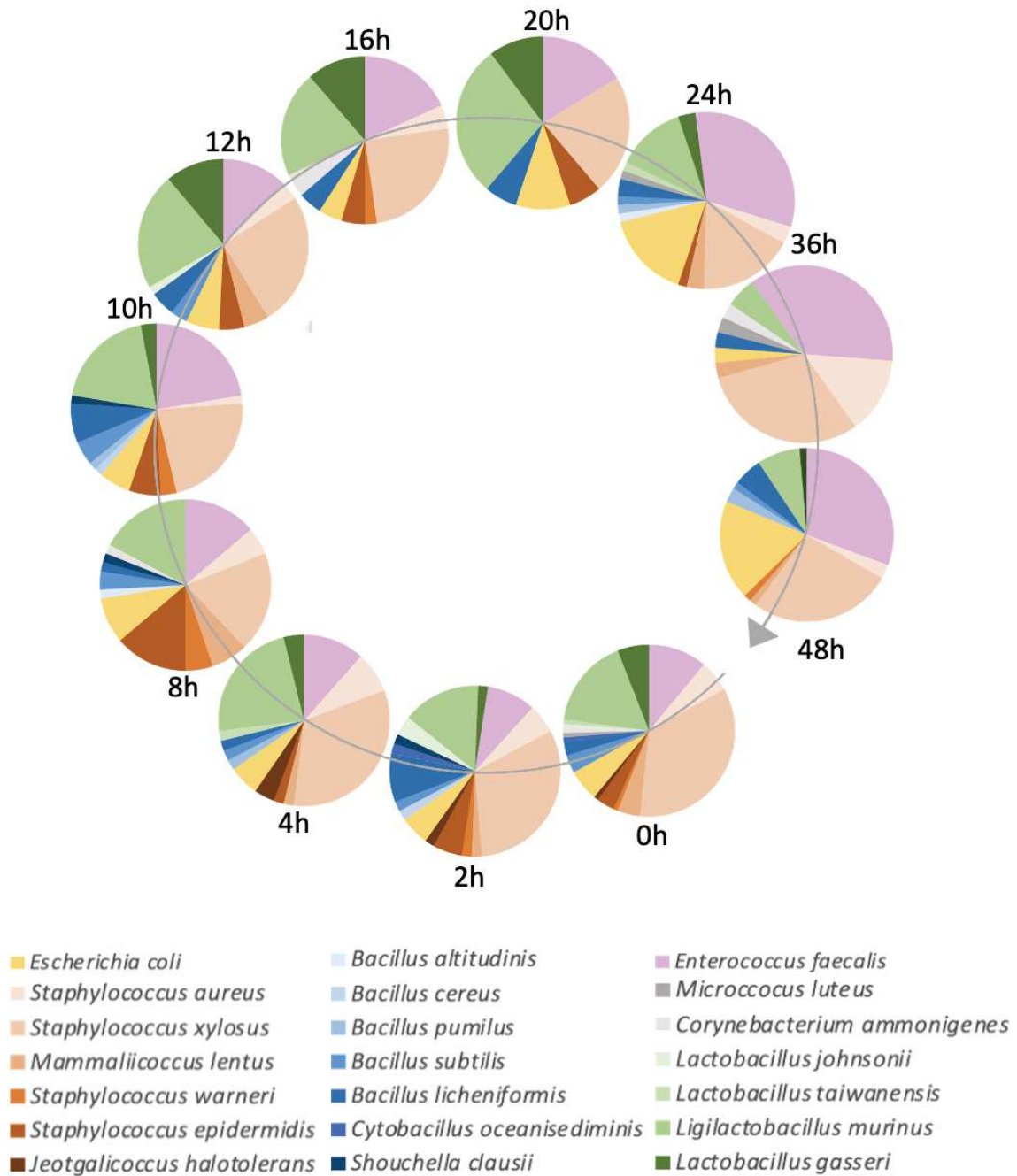
Figure 11. Distribution of all bacterial species detected at the different timepoints during 48 h of decomposition. The size of each portion is proportional to the frequency of each family's occurrence across the different samples, regardless of the organ analyzed. The overall sample size (n=1304) was not factored into this analysis; instead, only the presence or absence of bacterial families in each organ was considered in all experiments. Only species appearing more than once were included in this figure – they are categorized by different colours according to the family they belong to (Staphylococcaceae in gradients of orange, Bacillaceae in gradients of blue, and Lactobacillaceae in gradients of green).

The noticeable increase in both *E. faecalis* and *E. coli* species up to 48 h *postmortem* was prominent. However, it is essential to acknowledge that this increase is somewhat

overrepresented compared to other species. This overrepresentation is due to our method, which specifically targeted these bacterial species using dedicated culture media. According to Liu *et al*. (Liu et al., 2020), *E. faecalis* was one of the most abundant species detected in different samples in the advanced decomposition stages. Li *et al.* (Li et al., 2021) also showed a much higher relative abundance of *E. faecalis* at 0 h, 16 h, and 3, 7, and 15 days after death than in alive samples. Also, Tuomisto *et al.* (Tuomisto et al., 2013) reported that *Enterococcus* spp and *Escherichia* spp were among the most abundant bacteria in human autopsy cases. Therefore, these data support our results.

Different species of *Staphylococcus* spp. were commonly identified throughout the timepoints studied, in accordance to previous studies (Tuomisto et al., 2013). The consistent recovery of the dominant species, *S. xylosus*, from the initial 0-hour time point in most of the analyzed samples may indicate sample contamination with non-*S. aureus* species. This is further reinforced by its decline over the course of decomposition, as it becomes overshadowed by other species that rapidly increase in later *postmortem* intervals. The case of *S. aureus* will be particularly better explored in the sections below.

Different species of *Lactobacillus (L. johnsonii, Lactobacillus taiwanensis, Lactobacillus Gasseri*) and especially *L. murinus* (former *Lactobacillus*) are maintained relatively stable until the 24 h timepoint, after which they started decreasing. In a previous kinetic *postmortem* survey of the microbiota within culture-positive extra-intestinal tissues, bacterial translocation to extra-intestinal compartments was observed as early as 5 minutes after death with the highest frequent detection rate corresponding to *Lactobacillus* at 3 h and 12 h *postmortem* marks (Heimesaat et al., 2012). A subsequent decrease of facultative *Lactobacillus* spp is described due to hypoxia after death (Tuomisto et al., 2013).

4.3. Culturomics analysis.

The analysis of bacterial growth in the different culture media used enabled us to categorize the cases into three groups: non-growing indicating the absence of colony growth), monoculture (growth of a single colony morphology), and polyculture (growth of two or more colony morphologies) (Table 3).

When focusing solely on the CBA medium (328 samples; 280 presenting growth and 48 non-growing), which supports the growth of several bacterial species, including fastidious microorganisms, the majority of samples showing growth were categorized as

mixed cultures (227/280; 81%), with only a small number considered monocultures (53/280; 19%) (Figure 12). Monoculture samples were identified in all organs except the intestine, and they greatly corresponded to species typical of skin microbiota in early *postmortem* timepoints (e.g., *S. xylosus*) or gut microbiota (*E. faecalis* or *E. coli*) at later timepoints (24 h or 48 h). This clearly illustrates that monocultures are more easily observed in a highly nutritive medium like blood agar during later time intervals. This phenomenon arises from the overgrowth/invasion of particular species that inhibit the growth of less dominant ones.
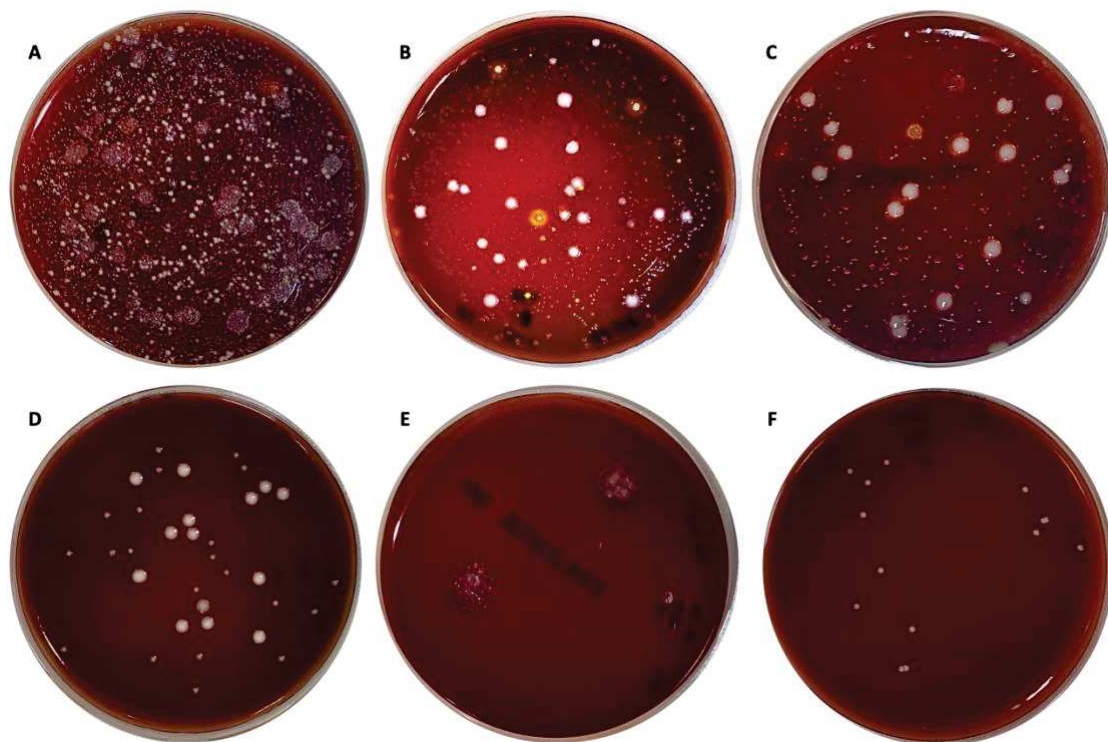
Figure 12. Representative blood agar plates illustrating the bacterial growth typical of polycultures (A-E) and monoculture (F). A, Intestine sample (12 h); B, Stomach sample (16 h); C, Spleen sample (48 h); D, Skeletal Muscle sample (36 h); E, Kidney sample (20 h); F, Intestine sample (8 h).

Concerning the cultures obtained using the MacConkey agar medium (n=329; 274 non-growing and 55 presenting growth), specifically designed for Gram-negative bacteria, the majority of positive samples retrieved were identified as monocultures of *E. coli* (53 out of 55, 96%). There were two exceptions, both originating from plates associated with stomach samples, where the growth of the Gram-negative *Pseudomonas monteilii* and *Pseudomonas putida* species was observed at 8 hours and 48 hours, respectively.

71

Mannitol Salt Agar (MSA) is a selective and differential growth medium used for the isolation of staphylococci, but it is not completely selective for staphylococci, and some other bacterial species (e.g., *Micrococcus* spp, *Bacillus* spp) may grow on it as well, especially after long incubation periods ($\geq$ 48 hours). Out of the 320 samples analyzed in MSA (190 showing growth and 130 non-growing), the 89 cases of monocultures mainly corresponded to *S. xylosus* (70/89, 79%) but in a significant number of samples (19/89, 21%), the mono-growth of *E. faecalis, S. aureus, M. lentus, J. halotolerans, B. licheniformis, B. pumilus, B. altitudinis,* and *C. oceanisediminis*was also observed. In addition to the species mentioned in the monocultures, mixed cultures (n=101) were also detected, which included *C. ammonigenes, S. epidermidis, G. dipsosauri, B. subtilis,* and *S. warneri.*
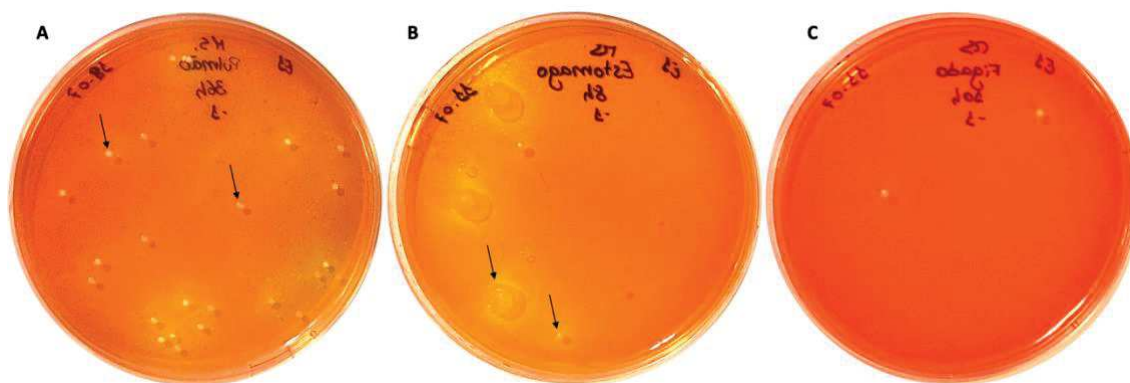
Figure 13. Representative Mannitol Salt Agar (MSA) plates illustrating the bacterial growth typical of polycultures (A and B) and monoculture (C). A, Lungs sample (36 h); B, Stomach sample (8 h); C, Liver samples (10 h). Arrows represent the different colony morphologies observed in the polycultures.

Slanetz-Bartley Agar (n=320) exhibited the highest level of specificity, enabling the growth of monocultures in all cases showing bacterial growth (119/119, 100%) which exclusively corresponded to the growth of *E. faecalis*.

The positive growth that we observed in the different culture media can theoretically be attributed to different reasons such as true positive, agonal spread (controversial), *postmortem* transmigration, and contamination. It is commonly accepted, although not absolute, that a pure culture of a pathogen points to infection and can be considered a genuine result, whereas a mixed culture of non-pathogens is more likely to result from *postmortem* migration (Morris et al., 2006).
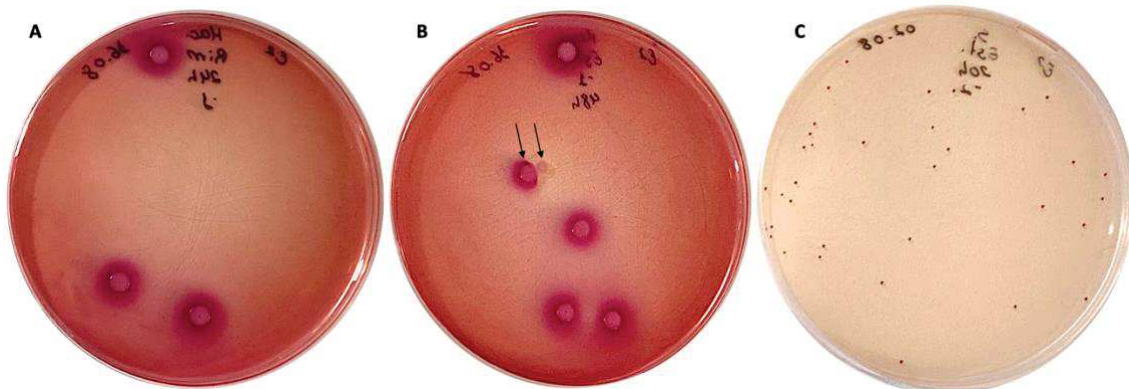
Figure 14. Representative MacConkey Agar (MAC) and Slanetz & Bartley Agar (SLB) plates illustrating typical bacterial growth. Bacterial growth typical of an *E. coli* monoculture in MAC (A), a polyculture in MAC (B), and an *E. faecalis* monoculture in SLB (C). A, Kidney sample (24 h); B, Stomach sample (48 h); C, Stomach sample (20 h). Arrows represent the different colony morphologies observed in the polyculture grown in B.

Therefore, if culturing results indicate the presence of more than one distinct isolate or staphylococcal species, other than *S. aureus*, the sample should be regarded as contaminated or invaded by different bacteria. This is particularly relevant for those species with a greater propensity for *postmortem* migration across organ barriers, epithelia, or mucosa following death (Tuomisto et al., 2013; Weber et al., 2010). Although the possibility that a single bacterial species invades in the agonal period is not excluded, this will depend on factors associated with the specific organism, such as propensity to invade and density of colonization, or to local factors affecting its site of colonization, but not to a general reduction in body defenses or a compromise of mucosal integrity (Morris et al., 2006).

Table 4. Bacterial species identified in 330 samples analyzed in the MSA culture medium.

Organ	Monoculture	n	Polyculture	n	Non-growing culture	n
Skeletal Muscle	*S. xylosus* [0 h (2), 2 h, 4 h, 8 h, 12 h, 20 h, 36 h, 48 h]	9	*S. xylosus*, No ID (10 h)	1	0 h (2), 2 h, 4 h, 8 h, 10 h, 12 h, 16 h, 20 h, 24 h (2), 36 h, 48 h	13
	No ID (0 h)	1	*S. aureus*, No ID (0 h)	1		
		10	*S. epidermidis, S. xylosus* (2 h, 10 h, 12 h)	3		
			S. xylosus, J. halotolerans (4 h)	1		
			S. xylosus, C. ammonigenes, No ID (8 h, 16 h)	2		
			E. faecalis, No ID (24 h)	1		
			S. xylosus, M. lentus, No ID (48 h)	1		
Intestine			*B. licheniformis, L. murinus* (36 h)	1		
			S. xylosus, No ID [0 h (3), 2 h, 4 h (2), 24 h, 48 h]	8		
			S. xylosus, S. aureus (0 h, 2 h)	2		
			S. xylosus, C. oceanisediminis, No ID (0 h)	1		
			E. faecalis, S. xylosus (0 h, 20 h)	2		
			S. aureus, No ID (2 h, 10 h)	2		
			S. xylosus, J. halotolerans (4 h)	1		
			B. licheniformis, B. altitudinis, M. lentus, No ID (8 h)	1		
			M. lentus, No ID (8 h)	1		
			B. licheniformis, S. xylosus [10 h (2), 48 h]	3		
			M. lentus, B.licheniformis (12 h)	1		
			S. xylosus, E. faecalis, B. subtilis (12 h)	1		
			No ID (16 h)	1		
			S. xylosus, L. murinus, No ID (20 h)	1		
			S. epidermidis, E. faecalis, S. xylosus (12 h)	1		
			E. faecalis, No ID (16 h)	1		
			S. xylosus, B. licheniformis, B. subtilis (24 h)	1		
			S. epidermidis, S. xylosus, No ID (24 h, 36 h)	2		
			B. subtilis, S. aureus, No ID (8 h)	1		
			S. xylosus, E. faecalis, S. aureus, B. licheniformis (48	1		
Stomach	*S. xylosus* (0 h, 48 h)	2	*S. xylosus*, No ID [0 h (2), 2 h, 4 h, 10 h, 36 h]	6	2 h, 4 h, 8 h, 12 h, 24 h	5
	B. licheniformis (36 h)	1	*S. aureus*, No ID (4 h, 48 h)	2		
	No ID (0 h)	1	*S. xylosus, J. halotolerans* (0 h)	1		
			B. licheniformis, No ID (2 h)	1		
			S. xylosus, B. licheniformis (10 h)	1		
			E faecalis, B. licheniformis (24 h)	1		
			No ID (10 h, 24 h)	2		
			S. epidermidis, E. faecalis, B. licheniformis, M.lentus, S. xylosus, No ID (20 h)	1		
			C. ammonigenes, S. xylosus, No ID (16 h)	1		
			S. xylosus, S. aureus (0 h)	1		
			S. epidermidis, E. faecalis, S. xylosus, B. licheniformis (20 h)	1		
			S. epidermidis, E. faecalis, S. xylosus (8 h)	1		
			E. faecalis, S. aureus, S. epidermidis, No ID (8 h)	1		
			E. faecalis, S. xylosus, B. licheniformis, No ID (12 h)	1		
			S. epidermidis, S. xylosus, E faecalis, No ID (12 h)	1		
			S. aureus, B. licheniformis (16 h)	1		
			B. subtilis, No ID (48 h)	1		
Bladder	*S. xylosus* [0h (3), 2h, 4h, 12h, 20 h, 24 h, 48h]	9	*S. xylosus*, No ID [4 h, 20 h, 36 h (2), 48 h]	5	(0h, 2h, 4h, 8h (2), 10h (2), 12h, 24h (2), 48h]	11
	J. halotolerans (2h)	1	*S. xylosus, S. aureus* (0 h)	1		
			S. epidermidis, S. warneri (8 h)	1		
			S. epidermidis, No ID (10 h)	1		
			S. epidermidis, S. xylosus (16 h)	1		
Kidney	*S. xylosus* [0 h (3), 2 h, 10 h, 12 h, 16 h, 20 h, 48 h]	9	*S. xylosus*, No ID (2 h)	1	0 h (2), 4 h (2), 8 h, 10 h, 12 h (2), 16 h, 20 h, 24 h (3), 36 h, 48 h	15
	M.lentus (0 h, 36 h)	2	*S. epidermidis*, No ID (2 h)	1		
	S. aureus (4 h, 8 h)	2	*S. xylosus, S. epidermidis* (8 h, 10 h)	2		
			S. xylosus, E. faecalis (48 h)	1		
Liver	*S. xylosus* [0 h (2), 4 h, 10 h, 12 h, 36 h, 48 h]	7	*E. faecalis, M. lentus* (0 h)	1	0 h (2), 2 h (2), 4 h, 8 h (2), 10 h, 12 h (2), 16 h, 20 h (2), 36 h, 48 h	15
	S. aureus (4 h)	1	*S. xylosus*, No ID (2 h)	1		
	E. faecalis (10 h)	1	*G. dipsosauri, S. xylosus* (0 h)	1		
	B. altitudinis (24 h)	1	*S. epidermidis*, No ID (8 h)	1		
	No ID (16 h, 24 h)	2	*S. xylosus, M. lentus* (24 h)	1		
			S. xylosus, E. faecalis (48 h)	1		
Spleen	*S. xylosus* [0 h (3), 2 h, 4 h, 24 h, 48 h	8	*S. xylosus, S. aureus* (0 h)	1	0 h, 4 h (2), 8 h (3), 10 h (2), 12 h (3), 16 h, 20 h, 24h, 36 h, 48 h	16
	C. oceanisediminis (2 h)	1				
Lungs	S. xylosus [0 h (4), 2 h, 4 h, 12 h, 20 h, 24 h]	9	*S. warneri, S. epidermidis* (8 h)	1	0 h (2), 2 h (2), 4 h (2), 8 h, 10 h (2), 24 h, 12 h (2), 36 h	13
	S. aureus (8 h)	1	*S. xylosus, S. epidermidis* (10 h)	1		
	E. faecalis (48 h)	1	*S. xylosus, E. faecalis* (16 h)	1		
			S. aureus, No ID (16 h)	1		
			S. epidermidis, E. faecalis (20 h)	1		
			S. xylosus, No ID (24 h, 36 h, 48 h)	3		
			S. xylosus, B. licheniformis (48 h)	1		
Brain	*S. xylosus* [0 h (2), 2 h, 4 h (3), 8 h, 10 h (2), 12 h, 16 h, 20 h, 48 h]	13	*S. xylosus, C. ammonigenes* (36 h)	1	0 h (4), 2 h (2), 8 h (2), 10 h, 12 h (2), 16 h, 20 h, 24 h (2), 36 h	16
	E. faecalis [24 h, 48 h (2)]	3				
Heart	*S. xylosus* (0 h, 4 h, 10 h, 48 h)	4	*M. lentus, S. epidermidis* (8 h)	1	0 h (5), 2 h (3), 4 h (2), 8 h (2), 10 h (2), 12h (3), 16 h (2), 20 h (2), 24 h (3), 36 h, 48 h	26
			S. xylosus, No ID (36 h, 48 h)	2		

The timepoints when each bacterial species or combination of bacterial species were identified are indicated in brackets.

Non-growing cultures do not necessarily mean total sterility but less than the limit of detection. Abbreviations: No ID, no identification was achieved by the MALDITOF-MS database.

Table 5. Bacterial species identified in 328 samples analyzed in the CBA culture medium.

Organ	Monoculture	n	Polyculture	n	Non-growing culture	n
Skeletal Muscle	*S. xylosus* (0 h, 8 h)	2	*L. gasseri, L. murinus* (0 h)	1	0 h, 2 h, 16 h, 20 h	4
	L. murinus (4 h)	1	*S. xylosus,* No ID [0 h (2), 2 h, 4 h, 8 h, 12 h]	6		
	E. faecalis (8 h, 12 h)	2	*B. licheniformis, S. xylosus* (0 h)	1		
			S. xylosus, E. faecalis, No ID (2 h)	1		
			S. xylosus, E. faecalis, S. aureus (4 h)	1		
			E. coli, E. faecalis (10 h)	1		
			E. faecalis , No ID (10 h)	1		
			S. xylosus, E. faecalis (24 h)	1		
			S. xylosus, S. epidermidis, L. murinus (10 h)	1		
			S. xylosus, L. murinus (20 h)	1		
			S. xylosus, L. murinus, L. gasseri (12 h)	1		
			S. xylosus, S. warneri (16 h)	1		
			E. faecalis, P. lactis, L. murinus, L. gasseri (24 h)	1		
			E. faecalis, L. murinus (24 h, 48 h)	2		
			S. xylosus, M. lentus, No ID (36 h)	1		
			S. aureus. E. faecalis (36 h)	1		
			E. coli, S.xylosus (48 h)	1		
			S. xylosus, M. lylae (48 h)	1		
Intestine			*S. xylosus,* No ID (0 h, 2 h)	2		
			S. xylosus, E. faecalis, L. murinus (0 h, 12 h)	2		
			L. murinus, L. gasseri (0 h)	1		
			B. subtilis, S. xylosus, M. lentus, No ID (0 h)	1		
			S. xylosus, A. clausii, M.lentus, B. subtilis, B. licheniformis, B. cereus, E. coli , No ID (2 h)	1		
			E. faecalis, L. taiwanensis, L. murinus (4 h)	1		
			B. subtilis, E. coli, E. faecalis, S. xylosus (4 h)	1		
			S. xylosus, L. murinus (4 h, 10 h, 12 h)	3		
			L. murinus , No ID (8 h)	1		
			E. faecalis, E. coli, S. xylosus, B. subtilis, A.clausii (8 h)	1		
			L. murinus, B. licheniformis, S. xylosus , No ID (10 h)	1		
			B. cereus, B. subtilis, S. xylosus, E. faecalis, A. clausii, E. coli, B. pumilus (10 h)	1		
			E. faecalis, No ID (12 h, 36 h, 48 h)	3		
			S. xylosus, E. faecalis (16 h)	1		
			E. faecalis, L. murinus (2 h, 20 h)	2		
			E. coli, L. murinus (8 h)	1		
			E. faecalis, L. murinus, L. taiwanensis (0 h)	1		
			S. xylosus, B. subtilis, P. amylolyticus, L. murinus, P. silvae, M.lentus, No ID (0 h)	1		
			E. coli, E. faecalis (24 h, 48 h)	2		
			E. faecalis, S. aureus (36 h)	1		
			E. faecalis, E. coli, L. murinus (16 h)	1		
			S. xylosus, L. murinus, B. licheniformis, L. gasseri, No ID (20 h)	1		
			S. xylosus, S. aureus, A. defectiva, L. murinus, No ID (24 h)	1		
			No ID (24 h)	1		
			E. coli, L. murinus, L. gasseri (48 h)	1		
Stomach	*S. xylosus* (2 h)	1	*B. licheniformis, L. murinus,* No ID (0 h)	1		
			S. xylosus, No ID [0 h (2), 20 h, 24 h]	4		
			E. faecalis, S. xylosus, L. murinus, No ID (0 h)	1		
			S. xylosus, M. lentus, B. subtilis , No ID (0 h)	1		
			B. subtilis, M. lentus , No ID (0 h)	1		
			B. licheniformis, L. johnsonii, No ID (2 h)	1		
			E. faecalis, S. xylosus, No ID (4 h)	1		
			S. xylosus , No ID (2 h)	1		
			S. aureus, No ID (12 h, 24 h)	2		
			L. murinus, No ID (4 h, 8 h, 12 h, 16 h, 20 h)	5		
			No ID (4 h, 8 h)	2		
			E. faecalis, L. murinus (8 h)	1		
			S. xylosus, L. murinus (10 h)	1		
			E. faecalis, S. aureus, L. murinus , E. coli, No ID (10 h)	1		
			B. subtilis, E. faecalis, No ID (10 h)	1		
			L. murinus, L. johnsonii (12 h)	1		
			B. licheniformis, L. gasseri, L. murinus (16 h)	1		
			L. murinus, L. gasseri (24 h)	1		
			L. murinus, B. licheniformis (36 h)	1		
			S. xylosus. L. murinus , No ID (36 h)	1		
			S. xylosus, E. faecalis, B. pumilus, B. licheniformis (48 h)	1		
			E. coli, L. murinus, No ID (48 h)	1		
			E. faecalis, L. murinus (48 h)	1		

Table 5. Bacterial species identified in 328 samples analyzed in the CBA culture medium (continuation).

Organ	Species		Species combinations		Times	
Bladder	*P. simplex* (2 h)	1	*S. xylosus,* No ID [0 h (2), 2 h (2), 20 h, 36 h]	6	0 h, 4 h (2), 8 h (2), 10 h (2), 12 h, 24 h	9
	S. xylosus (4 h, 24 h, 48 h)	3	*M. luteus ,* No ID (0 h)	1		
	S. epidermidis (16 h)	1	*S. aureus, S. epidermidis* (0 h)	1		
	No ID (24 h)	1	*S. warneri,* No ID (8 h)	1		
	E. coli (48 h)	1	*S. epidermidis, S. warneri* (10 h)	1		
			No ID (12 h)	1		
			S. xylosus, A. viridans (16 h)	1		
			S. xylosus, No ID (12 h)	1		
			E. faecalis (20 h)	1		
			E. faecalis, S. aureus, No ID (36 h)	1		
			S. xylosus, B. pumilus (48 h)	1		
Kidney	*S. xylosus* (0 h)	1	*S. xylosus,* No ID (0 h, 2 h, 36 h)	3		
	No ID (4 h, 10 h)	2	*L. murinus, L. gasseri* (0 h)	1		
	B. subtilis (10 h)	1	*S. aureus, L. johnsonii* (0 h)	1		
	U. thermosphaericus (12 h)	1	*L. murinus, S. epidermidis* (0 h)	1		
	L. taiwanensis (24 h)	1	*S. epidermidis, S. pettenkoferi* (2 h)	1		
	No ID (36 h)	1	*S. epidermidis, L. murinus, L. gasseri* (2 h)	1		
	E. faecalis (24 h, 48 h)	2	*S. aureus, B. pumilus, L. murinus, S. epidermidis* (4 h)	1		
			S. xylosus, L. murinus, L. gasseri (4 h)	1		
			L. murinus, No ID [8 h (2), 12 h, 20 h]	4		
			L. murinus, B. licheniformis, No ID (16 h)	1		
			S. xylosus, S. epidermidis, C. stationis, L. murinus, No ID (8 h)	1		
			S. xylosus, S. warneri, L. murinus, L. gasseri (10 h)	1		
			S. xylosus, L. murinus (0 h, 12 h)	2		
			E. faecalis, L. gasseri (16 h)	1		
			B. licheniformis, L. murinus (20 h)	1		
			E. facalis, L. murinus (24 h)	1		
			S. xylosus, E. faecalis (48 h)	1		
			S. xylosus, E. faecalis, S. warneri (48 h)	1		
Liver	No ID (4 h)	1	*S. xylosus* [0 h (2)]	2	0 h, 2 h, 10 h	3
	L. murinus (12 h)	1	*E. coli, L. murinus, L. gasseri* (0 h)	1		
	E. faecalis (36 h)	1	*E. casseliflavus , N. soli* (0 h)	1		
			S. xylosus, S. aureus, S. warneri, L. murinus, No ID (2 h)	1		
			L. murinus, No ID (2 h, 4 h)	2		
			L. murinus, L. gasseri (0 h, 20 h)	2		
			S. xylosus, L. murinus, L. Gasseri (4 h, 10 h, 12 h)	3		
			S. xylosus, L. murinus (16 h, 20 h)	2		
			E. faecalis, No ID (8 h, 10 h, 48 h)	3		
			S. epidermidis (8 h)	1		
			S. xylosus, S. epidermis (8 h)	1		
			S. xylosus, S. aureus. E. faecalis, L. murinus (12 h)	1		
			S. xylosus, L. gasseri (16 h)	1		
			E. faecalis, E. coli, B. pumilus (24 h)	1		
			S. xylosus, M. lentus, M. luteus, L. murinus, No ID (24 h)	1		
			E. faecalis, L. murinus (24 h)	1		
			S. xylosus, M. luteus (36 h)	1		
			E. coli, S. xylosus, E. faecalis (48 h)	1		
			S. xylosus, L. murinus, No ID (48 h)	1		
Spleen	*O. oncorhynchi* (0 h)	1	*S. oralis, L. murinus* (0 h)	1	0 h (2), 2 h, 4 h, 10 h, 12 h (2), 16 h	8
	S. warneri (0 h)	1	*S. xylosus,* No ID (0 h, 16 h, 20 h, 36 h)	4		
	L. murinus (4 h, 20 h)	2	*E. faecalis, B. licheniformis, S. xylosus, No ID* (2 h)	1		
	No ID (8 h, 8 h)	2	*L. murinus,* No ID (2 h, 4 h)	2		
	S. xylosus (12 h, 48 h)	2	*S. xylosus, L. murinus* (8 h, 10 h)	2		
	E. faecalis (24 h, 36 h)	2	*E. faecalis, L. murinus* (10 h, 48 h)	2		
			E. faecalis, No ID (24 h)	1		
			E. coli, S. xylosus, E. faecalis (48 h)	1		
Lungs	*L. murinus* (4 h)	1	*L. murinus, S. epidermidis* (0 h)	1	0 h	1
	No ID (4 h)	1	*S. xylosus,* No ID (0 h)	1		
	E. faecalis (36 h)	1	*S. xylosus, L. murinus, L. johnsonii* (2 h)	1		
			L. murinus , No ID (0 h, 8 h)	2		
			L. murinus, E. faecalis , No ID (10 h)	1		
			S. xylosus, S. warneri, L. murinus (8 h)	1		
			L. murinus, L. gasseri (12 h, 20 h)	2		
			L. murinus, S. xylosus (0 h, 2 h, 16 h)	3		
			L. murinus, L. gasseri, S. xylosus (12 h, 20 h)	2		
			S. xylosus, L. murinus, S. epidermidis (10 h)	1		
			B. licheniformis , S. xylosus, No ID (2 h)	1		
			S. xylosus, L. murinus, L. lenta (4 h)	1		
			S. warneri, No ID (8 h)	1		
			S. xylosus, E. faecalis, B. licheniformis, No ID (10 h)	1		
			L. murinus, L. gasseri (0 h, 12 h)	2		
			E. faecalis, S. xylosus, S. nepalensis, L. murinus, No ID (16 h)	1		
			E. faecalis, No ID (24 h, 48 h)	2		
			E. faecalis, L. murinus (24 h)	1		
			E. faecalis, E. coli (24 h)	1		
			E. faecalis, B. licheniformis, S. xylosus (48 h)	1		
			S. xylosus, E. faecalis (48 h)	1		
			S. xylosus, S. aureus, E. faecalis, No ID (36 h)	1		

Table 5. Bacterial species identified in 328 samples analyzed in the CBA culture medium (continuation).

Organ	Monoculture	n	Polyculture	n	Non-growing culture	n
Brain	*S. xylosus* (2 h, 4 h, 12 h, 48)	4	*L. gasseri, L. murinus* (0 h)	1	0 h (3), 2 h (2), 4 h, 8 h (2), 10 h, 16 h, 24 h (2), 36 h	13
	L. gasseri (12 h)	1	*S. xylosus*, No ID [0 h (2), 8 h, 16 h, 36 h]	5		
	E. faecalis (10 h, 24 h)	2	*S. xylosus, M. lentus*, No ID (4 h)	1		
	L. murinus (10 h)	1	*S. xylosus, M. lentus* (12 h)	1		
			S. xylosus, L. murinus, L. gasseri (20 h)	1		
			E. faecalis, L. murinus (20 h)	1		
			E. coli, E. faecalis (48 h)	1		
			E. faecalis, S. xylosus (48 h)	1		
Heart	*B. licheniformis* (0 h, 2 h)	2	*S. xylosus, L. murinus* [0 h (2)]	2	0 h, 2 h, 4 h (2), 8 h (2), 10 h, 12 h, 20 h, 24 h	10
	L. murinus (2 h)	1	*B. licheniformis*, No ID (4 h)	1		
	S. xylosus (24 h, 48 h)	2	*S. xylosus*, No ID (16 h, 36 h)	2		
	E. faecalis (36 h)	1	*M. osloensis, S. epidermidis* (0 h)	1		
	No ID (48 h)	1	*S. xylosus, S. newyorkensis, R. kristinae, S. epidermidis* (8 h)	1		
			S. xylosus, E. faecalis (10 h, 48 h)	2		
			L. murinus, No ID (0 h, 12 h, 20 h)	3		
			L. murinus, L. gasseri (12 h, 16 h)	2		
			E. faecalis, L. murinus (10 h)	1		
			E. faecalis, E. coli (24 h)	1		

The timepoints when each bacterial species or combination of bacterial species were identified are indicated in brackets. Non-growing cultures do not necessarily mean total sterility but less than the limit of detection. Abbreviations: No ID, no identification was achieved by the MALDITOF-MS database.

Table 6. Bacterial species identified in 329 samples analyzed in the MAC culture medium.

Organ	Monoculture	n	Polyculture	n	Non-growing culture	n
Skeletal Muscle	*E. coli* (0 h, 2 h, 8 h, 10 h, 48 h)	5			0 h (5), 2 h (2), 4 h (3), 8 h (2), 10 h (2), 12h (3), 16 h (2), 20 h (2), 24 h (3), 36 h (2), 48 h (2)	28
Intestine	*E. coli* [0 h (3), 2 h, 4 h, 8 h (3), 10 h, 12 h (3), 16 h (2), 20 h, 24 h (2), 48 h (3)]	20			0 h (3), 2 h (2), 4 h (2), 10 h (2), 20 h, 24 h, 36 h (2)	13
Stomach	*E. coli* [0 h (2), 2 h, 4 h (2), 10 h, 12 h, 20 h (2), 24 h, 36 h, 48 h (2)]	13	*E. coli, P. monteilii* (8 h)	1	0 h (4), 2 h (2), 4 h, 8 h (2), 10 h (2), 12 h (2), 16 h (2), 24 h (2), 36 h	18
			E. coli, P. putida (48 h)	1		
Bladder	*E. coli* (48 h)	1			0 h (5), 2 h (3), 4 h (3), 8 h (3), 10 h (3), 12 h (3), 16 h (2), 20 h (2), 24 h (3), 36 h (2), 48 h (2)	31
Kidney	*E. coli* (24 h)	1			0 h (6), 2 h (3), 4 h (3), 8 h (3), 10 h (3), 12 h (3), 16 h (2), 20 h (2), 24 h (2), 36 h (2), 48 h (3)]	32
Liver	*E. coli* [0 h, 24 h (2), 48 h]	4			0 h (5), 2 h (3), 4 h (3), 8 h (3), 10 h, 12 h (3), 16 h (2), 20 h (2), 24 h, 36 h (2), 48 h (2)	29
Spleen	*E. coli* (24 h, 48 h)	2			0 h (6), 2 h (3), 4 h (3), 8 h (3), 10 h (3), 12 h (3), 16 h (2), 20 h (2), 24 h (2), 36 h (2), 48 h (2)	31
Lungs	*E. coli* (20 h, 24 h, 48 h)	3			0 h (6), 2 h (3), 4 h (3), 8 h (3), 10 h (3), 12 h (3), 16 h (2), 20 h, 24 h (2), 36 h (2), 48 h (2)	30
Brain	*E. coli* (20 h, 24 h, 48 h)	3			0 h (6), 2h (3), 4 h (3), 8 h (3), 10 h (3), 12 h (3), 16 h (2), 20 h, 24 h (2), 36 h (2), 48 h (2)	30
Heart	*E. coli* (48 h)	1			0 h (6), 2 h (3), 4 h (3), 8 h (3), 10 h (3), 12 h (3), 16 h (2), 20 h (2), 24 h (3), 36 h (2), 48 h (2)	32

The timepoints when each bacterial species or combination of bacterial species were identified are indicated in brackets. Non-growing cultures do not necessarily mean total sterility but less than the limit of detection. Abbreviations: No ID, no identification was achieved by the MALDITOF-MS database.

Table 7. Bacterial species identified in 327 samples analyzed in the SLB culture medium.

Organ	Monoculture	n	Non-growing culture	n
Skeletal Muscle	*E. faecalis* [0 h (3), 2 h, 4 h, 8 h, 10 h (2), 24 h (3), 36 h, 48 h]	13	0 h (3), 2 h (2), 4 h (2), 8 h (2), 10 h, 12 h (3), 16 h (2), 20 h (2), 36 h, 48 h (2)	20
Intestine	*E. faecalis* [0 h (4), 2 h (2), 4 h (3), 8 h (3), 10 h (3), 12 h (3), 16 h (2), 20 h (2), 24 h (3), 36 h (2), 48 h (3)]	30	0 h (2), 2 h	3
Stomach	*E. faecalis* [0 h (4), 2 h (2), 4 h (2), 8 h (2), 10 h (3), 12 h (2), 16 h (2), 20 h (2), 24 h (2), 36 h (2), 48 h (3)]	26	0 h (2), 2 h, 4 h, 8 h, 12 h, 24 h	7
Bladder	*E. faecalis* (20 h, 36 h)	2	0 h (5), 2 h (3), 4 h (3), 8 h (3), 10 h (3), 12 h (3), 16 h (2), 20 h, 24 h (3), 36 h, 48 h (3)	30
Kidney	*E. faecalis* [16 h (2), 24 h (2), 36 h, 48 h (3)]	8	0 h (6), 2 h (3), 4 h (3), 8 h (3), 10 h (3), 12 h (3), 20 h (2), 24 h, 36 h	25
Liver	*E. faecalis* [0 h, 10 h, 12 h, 20 h, 24 h (2), 36 h, 48 h (3)]	10	0 h (5), 2 h (3), 4 h (3), 8 h (3), 10 h (2), 12 h (2), 16 h (2), 20 h, 24 h, 36 h	23
Spleen	*E. faecalis* [0 h, 2 h, 10 h, 24 h (2), 48 h (2)]	7	0 h (5), 2 h (2), 4 h (3), 8 h (3), 10 h (2), 12 h (3), 16 h (2), 20 h (2), 36 h, 48 h	24
Lungs	*E. faecalis* [10 h, 12 h, 16 h (2), 20 h, 24 h (3), 36 h (2), 48 h (3)]	13	0 h (6), 2 h (3), 4 h (3), 8 h (3), 10 h (2), 12 h (2), 20 h	20
Brain	*E. faecalis* [20 h, 24 h, 48 h (2)]	4	0 h (6), 2 h (3), 4 h (3), 8 h (3), 10 h (3), 12 h (3), 16 h (2), 20 h, 24 h (2), 36 h (2), 48 h	29
Heart	*E. faecalis* [10 h (2), 24 h (2), 36 h, 48 h]	6	0 h (6), 2 h (3), 4 h (3), 8 h (3), 10 h, 12 h (3), 16 h (2), 20 h (2), 24 h, 36 h, 48 h (2)	27

The timepoints when each bacterial species or combination of bacterial species were identified are indicated in brackets. Non-growing cultures do not necessarily mean total sterility but less than the limit of detection. Abbreviations: No ID, no identification was achieved by the MALDITOF-MS database.

In the cases we observed bacterial growth on MSA medium at the starting point (0 h), it corresponded to monocultures of staphylococci (most cases: brain, heart, lungs) or on CBA monocultures of *B. licheniformis* (heart) or mixed cultures of lactobacillus, *Moraxella osloensis* and staphylococci in heart (Table 3), which are part of mice microbiota. Intestinal bacteria like *E. faecalis* or *E. coli* were only detected at 0 h *postmortem* in the case of liver, spleen, stomach, gut, and muscle. Although we cannot discard the possibility of sample contamination, this is less probable since we employed strict conditions and precautions during sampling and in handling animals to prevent it. As we maintained the mice at 21 ºC (and not at 4 ºC), *postmortem* translocation could probably start taking place more quickly.

Possible sources of *postmortem* bacterial migration include skin, respiratory tract, oral cavity and other mucosa. Overall, our study revealed the clear presence of intestinal

(e.g., *E. coli* and *E. faecalis*) as well as skin (e.g., *S. xylosus*) bacteria in all organs at some timepoints. Indeed, a mixed profile, as it was obtained from most blood agar samples, points to a *postmortem* invasion as a consequence of a contamination from skin or intestine. The first two seem to have a particular potential for gut translocation (Mesli et al., 2017), while staphylococci from skin/mucosa microbiota showed prominent growth in several organs and timepoints, often since 0 h *postmortem*.

4.4. Total aerobic bacterial loads and fluctuations of target bacterial species during decomposition across different organs.

The analysis of the total bacterial load (CFU/g) in the different organs across time was performed by a kinetic survey of *postmortem* changes in main bacterial species that can grow aerobically by routine culture media (Figures 15-24). In general, the results revealed instances where significant growth of bacteria was already detected at 0 h (2) in one animal model, but not in another at 0 h (1) (e.g., *E. faecalis* and *E. coli* in muscle and liver; *E. faecalis* in spleen) or vice versa, that is, contaminated at 0 h (1) and not at 0 h (2) (e.g., *E. coli* in lungs) (numbers 1 and 2 represent 2 independent animals used at 0 h *postmortem*). This denotes the potential of variability between different animals and assays, and the relevance of biological and technical replicas. We could not identify statistically significant differences of bacterial counts between the different timepoints for each organ analysed probably due to the significant variability in results across the three assays. This underscores the necessity for additional assays and the inherent variability in the methodology employed together with the hundreds of bacterial cells competing for growth and survival *postmortem*.

4.4.1. The skeletal muscle.

Culture analysis of skeletal muscle samples showed a mean total load varying between a minimum of 0.5×10^1 CFU/g at 16 h and a maximum of 2.6×10^3 CFU/g at 48 h. Fluctuating increases and decreases were observed throughout decomposition with an increasing trend being notorious after 16 h and until 48 h (Figure 15.A). The particular analysis of *E. faecalis* (Figure 15.C) and *E. coli* (Figure 15.D), which have grown in selective culture media for these species, revealed a notably fluctuating bacterial load during decomposition. This fluctuation can be attributed to the intense competition with other commensal bacteria that invade the muscle from the initial, 0 h stage. Overall, and

despite the great fluctuations observed between different assays, consistent results could be obtained for SBA and MacConkey culture media in all three experiments at different timepoints showing the absence of *E. faecalis* (Figure 15.C) or *E. coli* (Figure 15.D), respectively.
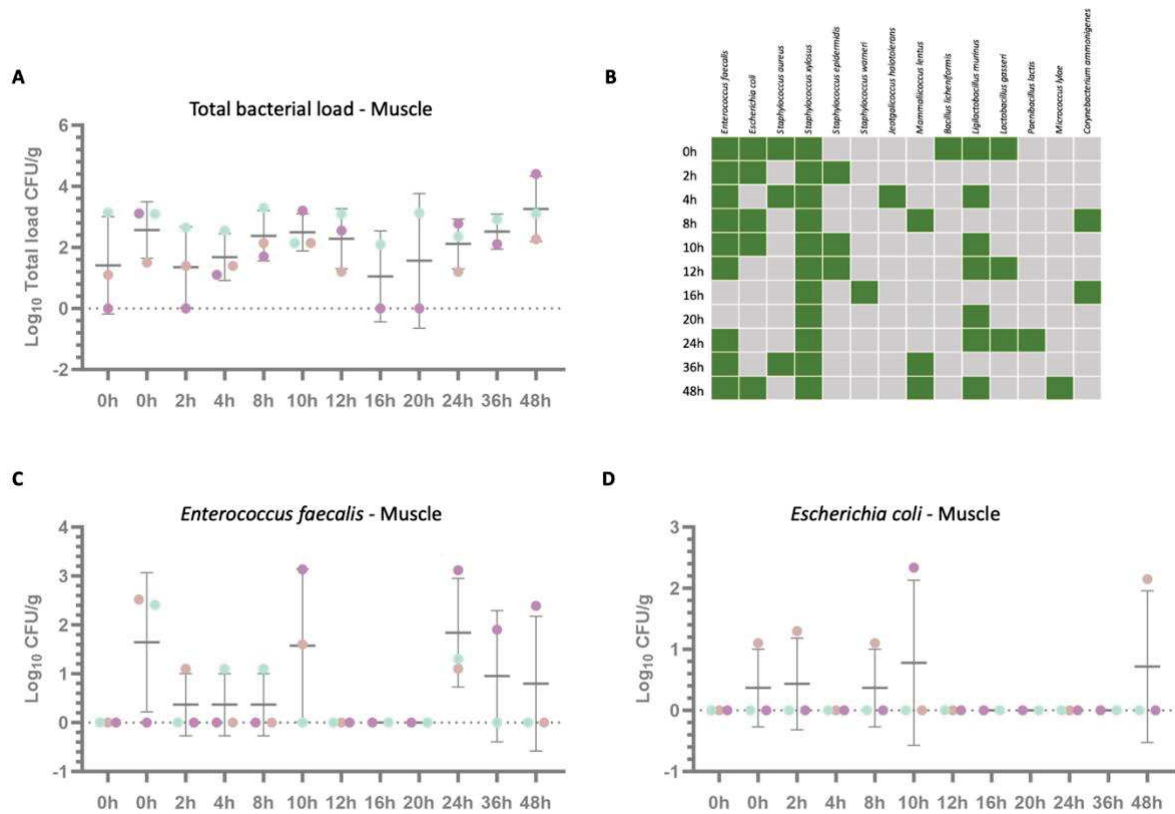

Figure 15. Kinetic cultural analysis of the skeletal muscle microbiota changes *postmortem*. (A) Total bacterial counts as well as numbers of **(C)** Enterococci and **(D)** *E. coli* were determined by detection of colony forming units (CFU) per gram of tissue on appropriate culture media (total, enterococci and *E. coli* loads were quantified in sheep blood agar, Slanetz & Bartley agar and MacConkey, respectively). Data are shown as mean ± standard deviation. The P-values obtained through the Kruskal-Wallis test and Dunn's test demonstrated no significant differences between conditions. Data came from the three independent experiments (the pilot assay in pink, experiment 1 in green and experiment 2 in purple). **B** represents the occurrence (presence in green, absence in grey) of all bacterial species identified in any of the culture media used (including mannitol salt agar) at different timepoints. Bacterial species are organized by the families they belong to.

Across a total of 132 analyses (33 per the 4 culture media) performed on skeletal muscle in various media and time points, we observed 10 monocultures on mannitol agar and 5 on blood agar. In the specific media used to detect *E. coli* and *E. faecalis*, whenever bacterial growth occurred in these analyses, we consistently obtained monocultures (see Table 3 for details). Taking in consideration all culture media used, we observed that

skeletal muscle was already positive, at 0 h *postmortem*. for intestinal (*E. faecalis* and *E. coli*) and skin (*S. xylosus, S. aureus, S. epidermidis, S. warneri*) bacteria, suggesting that this organ is not sterile together with its close interaction with other organs such as the skin and different mucosa. Other species that could be identified only once (*J. halotolerans, Micrococcus lylae, B. licheniformis, Paenibacillus lactis*), twice (*M. lentus, C. ammonigenes*) or in most timepoints (*L. murinus*) are typical of mice microbiota.

To the best of our knowledge, this is the first study assessing the *postmortem* variation of main bacterial species within mouse muscle tissue. Muscle tissue is a very rich source of minerals, such as phosphorus, potassium, magnesium, iron, copper, zinc, and selenium and the last tissue to get degraded (Javan et al., 2019). Consequently, post-rigor muscle tissue provides a rich medium for the support of bacterial growth, as evidenced by the increasing total bacterial loads over time (>16 h). Nonetheless, the early and substantial contamination observed in this organ renders it unsuitable for inclusion in *postmortem* calculations. Additionally, *E. faecalis* and *E. coli* do not emerge as reliable *postmortem* markers for this particular tissue.

4.4.2. Intestine.

Culture analysis of intestinal samples showed a mean total load varying between a minimum of 9.2×10^3 CFU/g at 10 h and a maximum of 4.6×10^7 CFU/g at 36 h (Figure 16.A). As expected, and in line with prior descriptions, the total bacterial load progressively increased over time, ultimately reaching its mean maximum level at 48 h hours *postmortem* (Hauther et al., 2015). In agreement with our results showing a decrease of the microaerophilic lactobacilli during the first hours (Figure 10), Heimesaat *et al*. (Heimesaat et al., 2012) reported a decrease of the total bacterial load between 3 h (we observed a mean of 8.1×10^4 at 2 h) and 6 h (we observed a mean of 4.0×10^4 at 8 h and 9.20×10^3 at 10 h).These authors, who used a multi-media cultural approach similar to ours, also described a duplication of enterococci levels between 6 h and 12 h, while *E. coli* numbers were relatively stable. In our study *E. faecalis* counts (Figure 16.C) fluctuated until 12 h and gradually increased until the end, whereas *E. coli* counts (Figure 16.D) remained more stable until 36 h with a maximum peak at 48 h. Molecular analyses by Heimesaat *et al*. (Heimesaat et al., 2012) also confirmed this trend in which the enterobacteria and enterococci population significantly increased at 12 h and 24 h *postmortem*, respectively, to maximum loads at 72 h *postmortem*. Overall, fluctuating

increases and decreases were observed throughout decomposition for both species along decomposition, but an increasing trend was detectable in both species, especially after 12 h for *E. faecalis* and at 48 h for *E. coli*.

Across a total of 132 analyses (33 for each culture media – 4 in total) performed on intestinal samples in various media and timepoints, we only observed polycultures in CBA and MSA media. In the specific media used to detect *E. coli* and *E. faecalis*, whenever bacterial growth occurred in these analyses, we consistently obtained monocultures in all cases (see Table 3 for details). Taking in consideration all culture media used, we were able to identify 21 different bacterial species with our approach. At 0 h *postmortem*, the intestine was already positive for a number of bacterial species naturally occurring in the gut, such as *E. faecalis, E. coli* and lactobacilli. Most species (12 out of 21) were only identified at 0 h *postmortem* or until 12 h given that the overgrowth and dominance of *E. faecalis* and *E. coli* (besides *S. xylosus* or *L. murinus* for example) after this timepoint prevents the growth of other less frequent intestinal bacteria. It is noteworthy that *S. aureus*, a human/animal pathogen, was detected in one of the assays right from the beginning (0 h) (Table 3) and remained detectable until the 48-hour timepoint, despite our initial fecal screening failing to identify the presence of *S. aureus* (Table 3).

A limited number of studies assessed *S. aureus postmortem* counts in the gut (Burcham et al., 2016; Burcham, Pechal, et al., 2019) and when this was done, it was only after nasal inoculation of *S. aureus* strains, not naturally followed. These studies revealed the ability to trace an individual *S. aureus* bacterial strain as it migrates across different organs with a consistent behavior in terms of when it reaches its peak abundance and subsequently starts to decline, regardless of the specific organ it colonizes. As we investigated the natural *postmortem* evolution of the microbiota in C57BL/6J mice, we encountered challenges in drawing robust conclusions due to the limited number of samples that tested positive for *S. aureus* (n=8, Table 3).
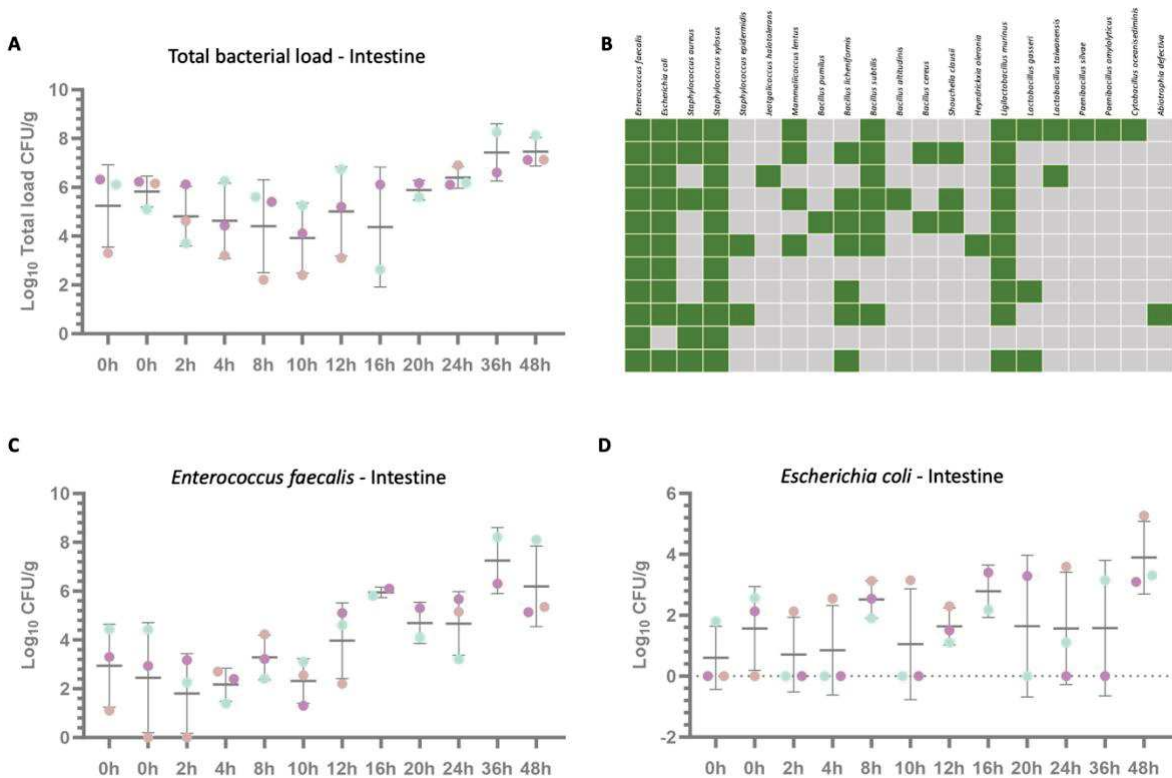
Figure 16. Kinetic cultural analysis of the intestine microbiota changes *postmortem*. (A) Total bacterial counts as well as numbers of **(C)** Enterococci and **(D)** *E. coli* were determined by detection of colony forming units (CFU) per gram/organ on appropriate culture media (total, enterococci and *E. coli* loads were quantified in sheep blood agar, Slanetz-Bartley agar and MacConkey, respectively). Data are shown as mean ± standard deviation. The P-values obtained through the Kruskal-Wallis test and Dunn's test that demonstrated no significant between conditions. The data presented came from three independent experiments (the pilot assay in pink, experiment 1 in green and experiment 2 in purple). **B** represents the occurrence (presence in green, absence in grey) of all bacterial species identified in any of the culture media used (including mannitol salt agar) at the different timepoints. Bacterial species are organized by the families they belong to.

Overall, our results corroborate previous studies showing a bacterial load increase over time and with the more resistant species (detected at 48 h) belonging to the Bacillota phylum (enterococci, *E. coli*, lactobacilli, staphylococci).

4.4.3. Stomach.

Culture analysis of stomach samples showed a mean total load varying between a minimum of 8.7×10^2 CFU/g at 0 h and a maximum of 6.4×10^5 CFU/g at 20 h. As expected, and described, the basal total load (at 0 h) was lower than that of the intestine

since the stomach contains fewer microbial densities and less bacterial diversity due to the gastric pH, mucosal thickness and peristalsis that limit microbial growth (Hyde, 2017; Martinez-Guryn et al., 2019). Indeed, stomach microbiota is dominated by acid-tolerant bacteria belonging to Pseudomonadota and this was the only organ where we could detect *Pseudomonas* species (one of them only at 48 h timepoint; Figure 17.B). Fluctuating increases and decreases were observed throughout decomposition without a prominent increasing trend as observed for the intestine (Figure 17.A). In the specific analysis of *E. faecalis* (Figure 17.C) and *E. coli* (Figure 17.D), a common and relatively consistent mean bacterial load was observed for both species throughout the study period. Interestingly, both also exhibited an interim peak at 20 h before ultimately reaching their maximum loads at 48 h.

Across a total of 132 analyses (33 per for each culture medium – 4 media in total) performed on stomach samples in various media and timepoints, we mostly observed polycultures in CBA and MSA. In the specific media used to detect *E. coli* and *E. faecalis*, whenever bacterial growth occurred in these analyses, we consistently obtained monocultures in most cases (see Table 3 for details). Considering all the culture media utilized, we successfully identified a total of 16 distinct bacterial species, primarily comprised of intestinal bacteria. Remarkably, a significant proportion (9 out of 16) of these species persisted until the 48-hour timepoint. Furthermore, mirroring the gut environment, *S. aureus* was also detected in the stomach, maintaining its presence from the initial 0 h timepoint all the way through to 48 h.

We could not find comparable studies exploring the *postmortem* variation of main bacterial species in the stomach, but the literature states that it is one of the first organs to degrade (Eden et al., 2022; Javan et al., 2019). Similar to the skeletal muscle, the baseline contamination of this organ poses challenges in its utilization for *postmortem* calculations.
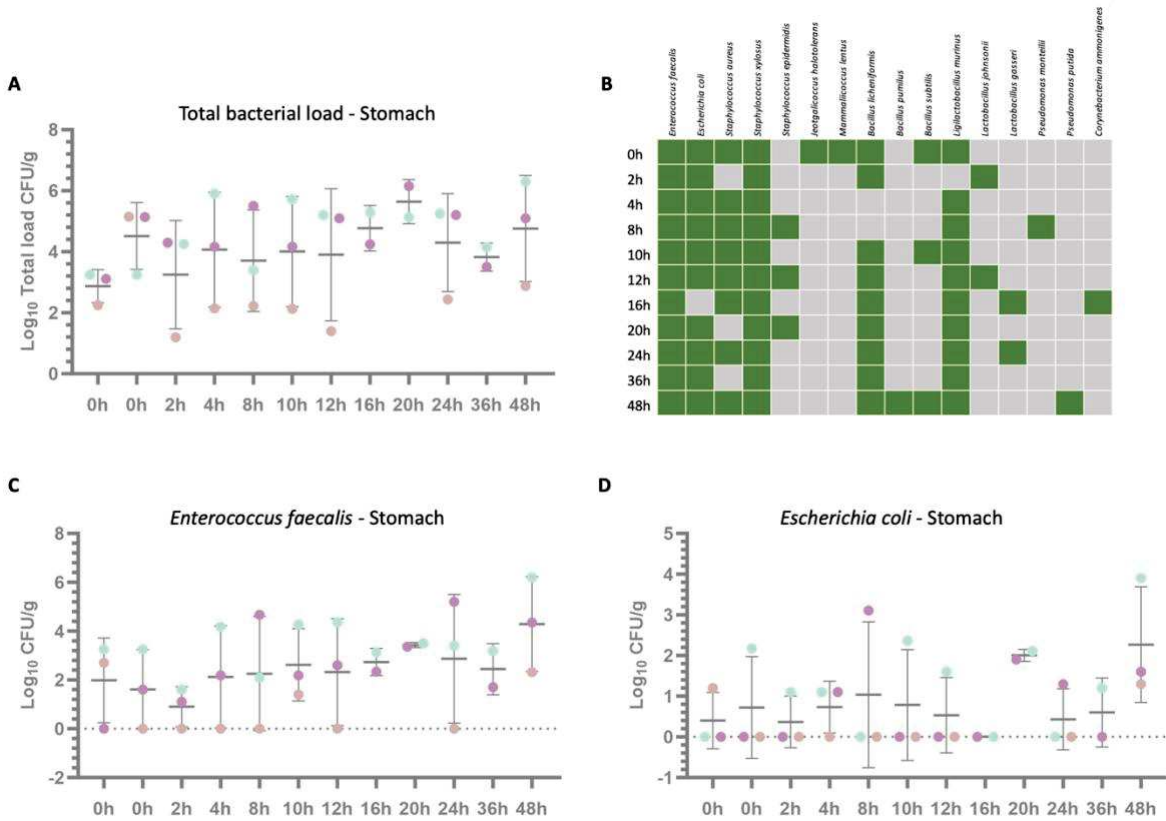
Figure 17. Kinetic cultural analysis of the stomach microbiota changes *postmortem*. (A) Total bacterial counts as well as numbers of **(C)** Enterococci and **(D)** *E. coli* were determined by detection of colony forming units (CFU) per gram/organ on appropriate culture media (total, enterococci and *E. coli* loads were quantified in sheep blood agar, Slanetz & Bartley agar and MacConkey, respectively). Data are shown as mean ± standard deviation. The P-values obtained through the Kruskal-Wallis test and Dunn's test demonstrated no significant differences between conditions. The data presented came from three independent experiments (the pilot assay in pink, experiment 1 in green and experiment 2 in purple). **B** represents the occurrence (presence in green, absence in grey) of all bacterial species identified in any of the culture media used (including mannitol salt agar) at the different timepoints. Bacterial species are organized by the families they belong to.

4.4.4. Bladder/Urine.

We analyzed bladder samples containing urine since this organ was collected by removing the entire sample from the abdominal cavity, avoiding bladder rupture. Culture analysis of bladder samples showed a mean total load varying between a minimum of 0.7×10^1 CFU/g at 8 h and a maximum of 1.8×10^3 CFU/g at 0 h, which is much lower than in the intestine. Interestingly, the maximum total load was detected at the beginning (0 h) followed by a similar peak at 36 h (mean 8.6×10^2). We noted a decline in the overall

bacterial load between the 4 h and 10 h timepoints, followed by a subsequent increase at the 12 h timepoint (Figure 18.A).
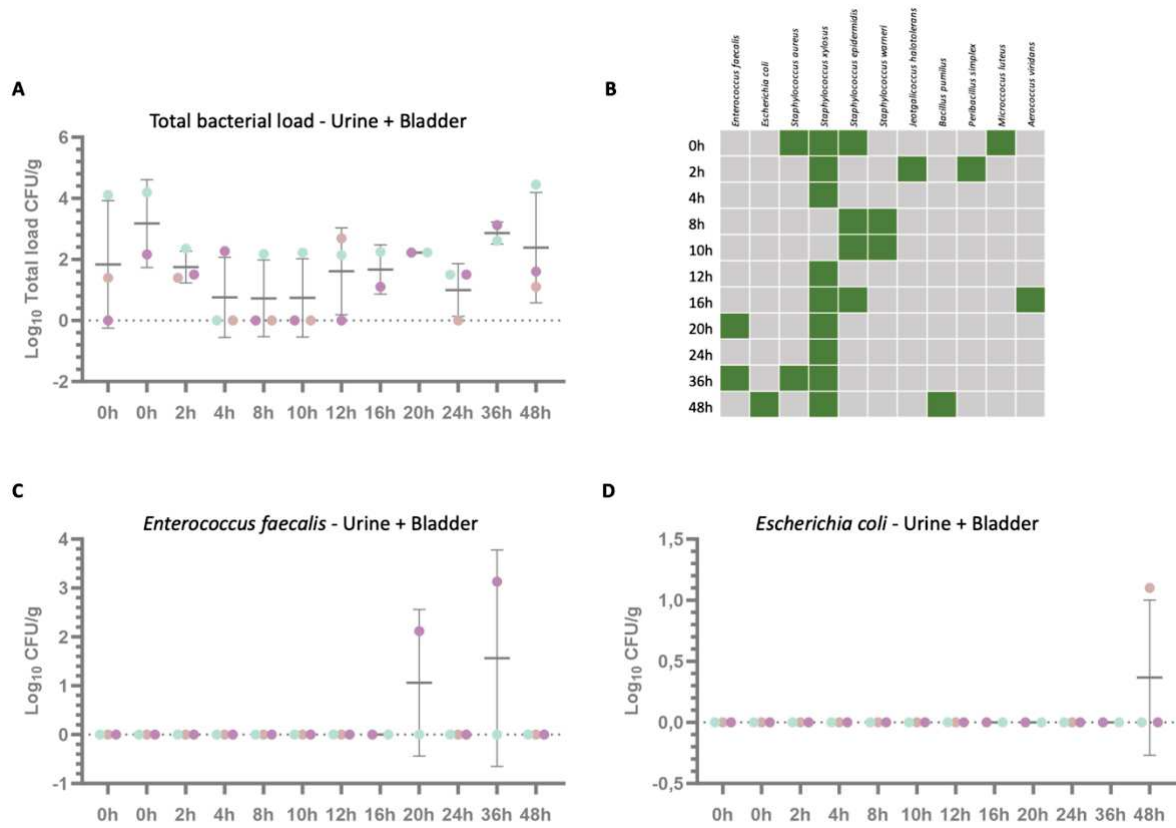

Figure 18. Kinetic cultural analysis of the urine and bladder microbiota changes *postmortem*. (A) Total bacterial counts as well as numbers of **(C)** Enterococci and **(D)** *E. coli* were determined by detection of colony forming units (CFU) per gram/organ on appropriate culture media (total, enterococci and *E. coli* loads were quantified in sheep blood agar, Slanetz & Bartley agar and MacConkey, respectively). Data are shown as mean ± standard deviation. The P-values obtained through the Kruskal-Wallis test and Dunn's test demonstrated no significant differences between conditions. The data presented came from the three independent experiments (the pilot assay in pink, experiment 1 in green and experiment 2 in purple). **B** represents the occurrence (presence in green, absence in grey) of all bacterial species identified in any of the culture media used (including mannitol salt agar) at the different timepoints. Bacterial species are organized by the families they belong to.

When analyzing *E. faecalis* and *E. coli* species in particular, it is noteworthy that all three assays consistently yielded negative results in detecting them across the culture media used: *E. faecalis* was detected at 20 h and 36 h (but only in one of two assays) (Figure 18.C) and *E. coli* was only detected at 48 h (in one of three assays) (Figure 18.D). Consequently, additional experiments are warranted to affirm the sterility of urine with respect to these species within the initial 20 h, as they may be constituents of the mouse microbiota at low levels that fall below the detection limit of this routine methodology.

Although it is currently accepted that women urinary bladder is not sterile and contains a specific microbiota (Ksiezarek et al., 2021), which can include *E. faecalis* and *E. coli*, much less is known about the mouse C57BL/6J used in this study.

Across a total of 126 analyses (30 in MSA, 32 in each of the CBA, MAC, and SLB culture medium) performed on bladder samples in various media and timepoints, we mostly observed polycultures. In the specific media used to detect *E. coli* and *E. faecalis*, whenever bacterial growth occurred in these analyses, we consistently obtained monocultures in the few positive cases (see Table 3 for details). Considering all the culture media utilized, we successfully identified a total of 11 distinct bacterial species, of which nine belonged to Bacillota and greatly comprised of staphylococcaceae (5/11) since the beginning. In addition to *B. pumillus* and *S. xylosus*, *E. faecalis* and *E. coli* emerged as the most resilient species during the latter stages of our *postmortem* study. More studies are needed to better explore if these species can be used as markers of bladder invasion after the 20 h mark.

4.4.5. Kidney.

The analysis of kidney sample cultures showed a mean total load ranging from a minimum of 5.0×10^1 CFU/g at 36 h to a maximum of 6.7×10^2 CFU/g at 48 h. We observed undulating positivity over time as previously reported (Burcham et al., 2016), with a notable maximum peak at 48 h being reached after a previous decrease trend between 20 h and 36 h (Figure 19.A). In common to Heimesaat *et al*. (Heimesaat et al., 2012), we observed an increase of the total load >2 h with fluctuating levels until the maximum peak at 48 h.

The specific analysis of *E. faecalis* (Figure 19.C) showed colonization of this species at 16 h, consistent in the 2 experiments conducted. From 24 h, it exhibited qualitative fluctuations until the maximum load at 48 h. The presence of *E. coli* (Figure 19.D) was only detected at 24 h and in only one of the three experiments conducted at that timepoint. These results were somehow congruent with that from the bladder urine, where *E. faecalis* and *E. coli* were only detected only after 20 h. his is consistent with available research suggesting that the microbiota of the bladder can affect the microbiota of the kidneys. Moreover, it is known that the kidneys may sense changes in the levels of metabolites derived from the gastrointestinal microbiome (Jansen et al., 2019).
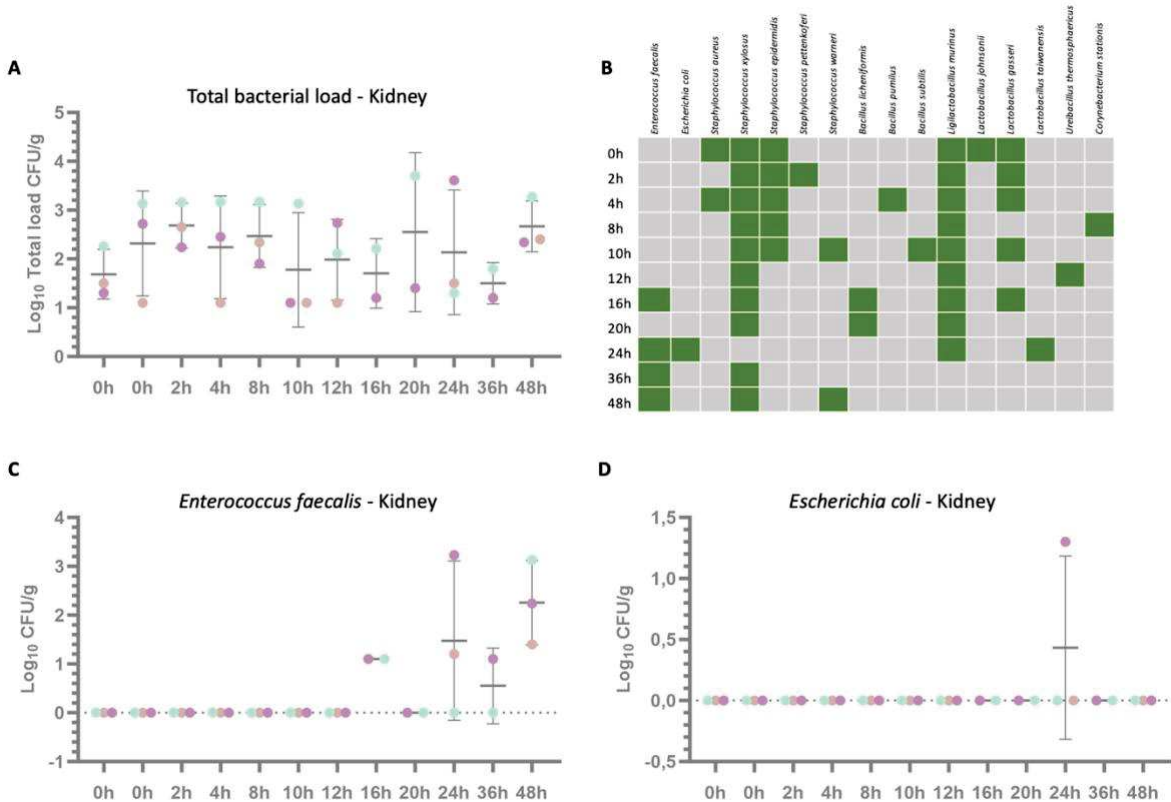
Figure 19. Kinetic cultural analysis of the kidney microbiota changes *postmortem*. (A) Total bacterial counts as well as numbers of **(C)** Enterococci and **(D)** *E. coli* were determined by detection of colony forming units (CFU) per gram/organ on appropriate culture media (total, enterococci and *E. coli* loads were quantified in sheep blood agar, Slanetz & Bartley agar and MacConkey, respectively). Data are shown as mean ± standard deviation. The P-values obtained through the Kruskal-Wallis test and Dunn's test demonstrated no significant differences between conditions. The data came from the three independent experiments (the pilot assay in pink, experiment 1 in green and experiment 2 in purple). **B** represents the occurrence (presence in green, absence in grey) of all bacterial species identified in any of the culture media used (including mannitol salt agar) at the different timepoints. Bacterial species are organized by the families they belong to.

Coincidentally the greatest shift towards maximum loads in the intestine were at 20 h for *E. faecalis* and at 48 h for *E. coli*. Finally, Liu *et al*. (Liu et al., 2023) described that after 12 h of decomposition, the pyruvate metabolism pathway is enriched in the kidney compared to other organs, which may serve as a trigger for bacterial growth within this organ from this timepoint onwards. These authors also described a significant proportion of Enterobacteriaceae at 0.5 h *postmortem* by sequencing analyses, but our culturomics approach did not confirm the presence of *E. coli* in early timepoints, probably due to the detection limit constraint. Notably, there was consistency among the different

experiments in the absence of the target bacterial species at various timepoints (Figure 19.C and Figure 19.D).

In the kidney, 132 analyses were performed, considering the different culture media (33 analysis for each culture medium – 4 culture media in total) and timepoints. On CBA media, we mostly observe polycultures. In the specific media used to detect *E. coli* and *E. faecalis*, whenever bacterial growth occurred in these analyses, we consistently obtained monocultures in the few positive cases (see Table 3 for details). Considering all the culture media utilized, we successfully identified a total of 16 distinct bacterial species (all Bacillota), most of them (14/16) being sporadically detected at 1-4 timepoints. In contrast, *S. xylosus* (until 48 h) and *L. murinus* (until 24 h) were detected in most timepoints. In addition, species such as *U. thermosphaericus* from the Caryophanaceae family, *S. pettenkoferi* from the Staphylococcaceae family, and *C. stationis* from the Corynebacteriaceae family and Actinomycetota phylum were uniquely identified in this organ. (see Table 3 for details). In common to the bladder organ*, E. faecalis* and *E. coli* emerged as the most resilient species invading the kidney at the latter timepoints studied, but the results of *E. coli* were not so consistent as those of *E. faecalis*. As so, *E. faecalis* species needs to be further explored as a potential biomarker of kidney invasion after the 16 h mark.

4.4.6. Liver and Spleen.

The analysis of liver and spleen samples showed a mean total load varying between a minimum of 5.4×10^1 CFU/g (liver, at 10 h) and 0.4×10^1 CFU/g (spleen, at 12 h) and a maximum of 2.5×10^4 CFU/g (liver) and 8.3×10^2 CFU/g (spleen), both at 48 h (Figure 20.A and 21.A). The mean starting total load in both organs (7.3×10^2 CFU/g in liver and 0.8×10^1 CFU/g in spleen) was already considerable. Nevertheless. It becomes difficult to establish a comparison with the few available similar studies performed with mice models because the timepoint zero was not described in any of them and they did not quantify bacteria by culturing (Burcham et al., 2016; Heimesaat et al., 2012; Liu et al., 2023). The lowest timepoint assessed in these studies described bacterial growth in these organs at intervals <5 min (Heimesaat et al., 2012).
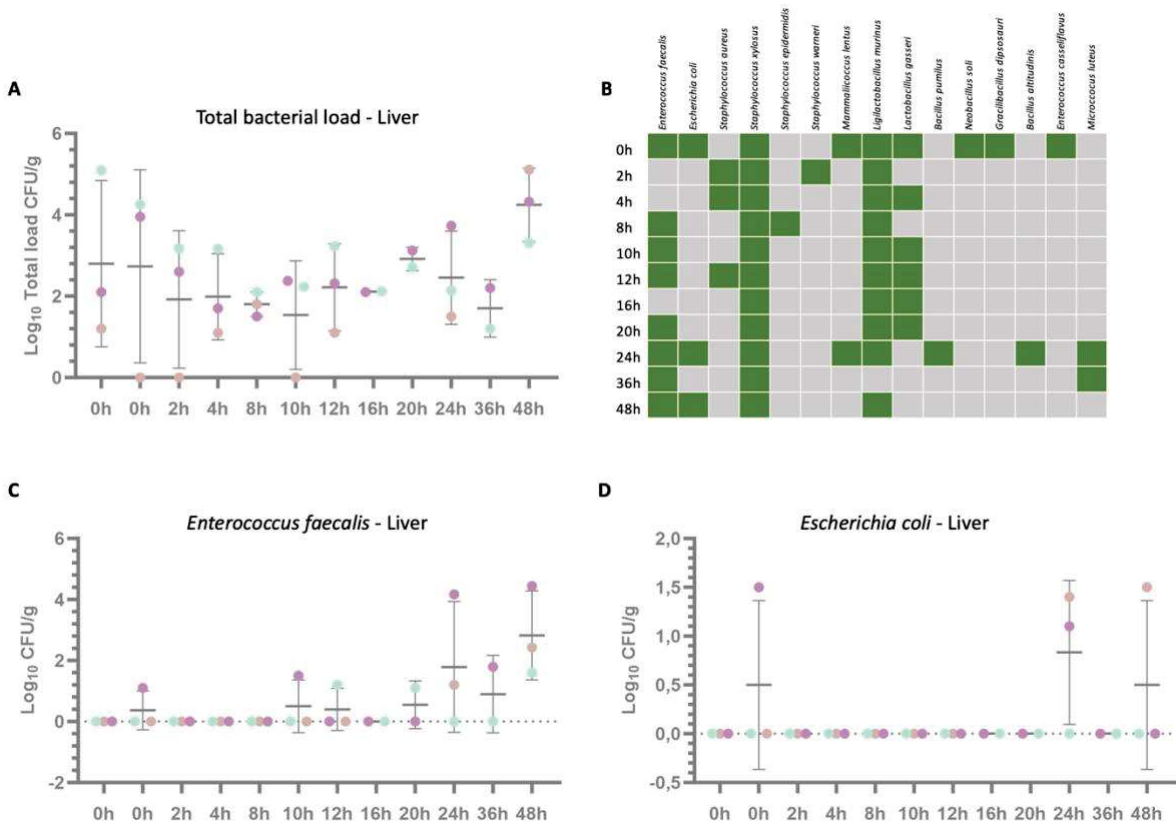
Figure 20. Kinetic cultural analysis of the liver microbiota changes *postmortem*. (A) Total bacterial counts as well as numbers of **(C)** Enterococci and **(D)** *E. coli* were determined by detection of colony forming units (CFU) per gram/organ on appropriate culture media (total, enterococci and *E. coli* loads were quantified in sheep blood agar, Slanetz & Bartley agar and MacConkey, respectively). Data are shown as mean ± standard deviation. The P-values obtained through the Kruskal-Wallis test and Dunn's test demonstrated no significant different between conditions. The data presented came from the three independent experiments (the pilot assay in pink, experiment 1 in green and experiment 2 in purple). **B** represents the occurrence (presence in green, absence in grey) of all bacterial species identified in any of the culture media used (including mannitol salt agar) at the different timepoints. Bacterial species are organized by the families they belong to.
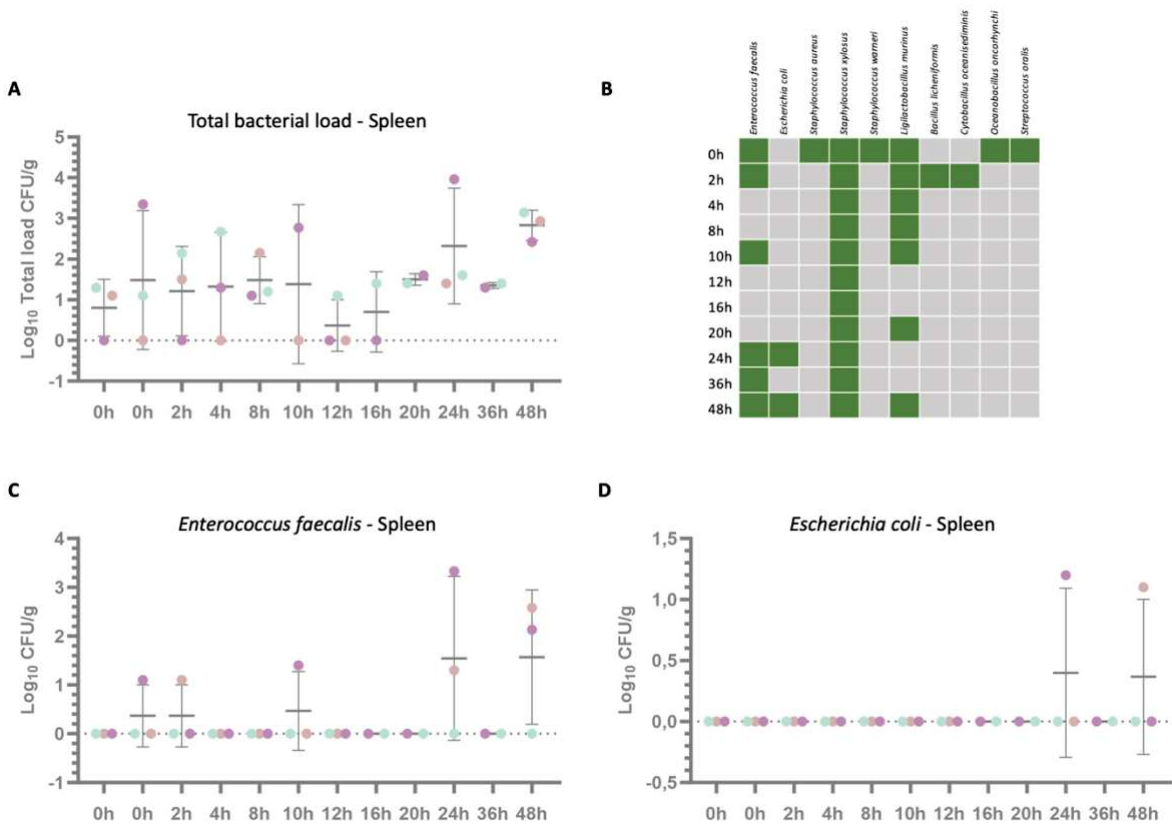
Figure 21. Kinetic cultural analysis of the spleen microbiota changes *postmortem*. (A) Total bacterial counts as well as numbers of **(C)** Enterococci and **(D)** *E. coli* were determined by detection of colony forming units (CFU) per gram/organ on appropriate culture media (total, enterococci and *E. coli* loads were quantified in sheep blood agar, Slanetz & Bartley agar and MacConkey, respectively). Data are shown as mean ± standard deviation. The P-values obtained through the Kruskal-Wallis test and Dunn's test demonstrated no significant differences between conditions. The data presented came from three independent experiments (the pilot assay in pink, experiment 1 in green and experiment 2 in purple). **B** represents the occurrence (presence in green, absence in grey) of all bacterial species identified in any of the culture media used (including mannitol salt agar) at the different timepoints. Bacterial species are organized by the families they belong to.

In our study, an undulating but quite stable mean total load was observed in liver and spleen samples until 36 h, with a marked increase registered at 48 h. Interestingly the lowest total load detected in liver paralleled that observed in the intestine at 10 h (mean of 9.2×10^3 CFU/g), the called nadir phenomenon of translocation rates described by Heimesaat *et al*. (Heimesaat et al., 2012) that in this study occurred at 1 h. Although the detection of bacteria in organs, such as the liver, that are theoretically sterile unless there is a true infection, is an indicator of bacterial migration (Speruda et al., 2021), bacteria may pass through the gut epithelium and migrate to the liver in portal vein blood during life. Due to the anatomically-close location and the connection through the vascular

91

system, the liver is continuously exposed to microbial products from the gut. Indeed, and as described by Tuomisto *et al*. (Tuomisto et al., 2013), the relative number of intestinal bacteria also increased in liver with time *postmortem*. Our results corroborate this based on the specific analysis of *E. faecalis* progression over time since this species reached maximum amounts also at 48 h (Figure 20.C and Figure 21.C).

In the liver and spleen, 132 and 122 analyses were performed respectively for each organ, considering the different culture media (33 per medium for the liver and in case of spleen 22 in MSA, 32 in CBA, 31 in SLB and 33 in MAC) and timepoints. In the specific media used to detect *E. coli* and *E. faecalis*, whenever bacterial growth occurred in these analyses, we consistently obtained monocultures in both organs in the few positive cases (see Table 3 for details). Considering all the culture media utilized, we successfully identified a total of 15 distinct bacterial species in the liver and 10 species in the spleen (all Bacillota), with several of them (8/15 in liver and 6/10 in spleen) being only detected once. In contrast, *S. xylosus* and *L. murinus* (until 48 h) in both organs, and *L. gasseri* (until 20 h) only in the liver, were detected in most timepoints. In this study, we enlarged the list of bacterial species found in these organs in comparison to previous studies with the identification of *Enterococcus* spp, *Escherichia* spp, *and Staphylococcus* spp being common to that observed in human cadavers (Campobasso et al., 2022; Tuomisto et al., 2013).

The specific analysis of *E. faecalis* (Figure 20.C) and *E. coli* (Figure 20.D) in the liver showed colonization of these bacteria in the same experiment at 0 h-timepoint. Liu *et al.* (Liu et al., 2023) also detected *Enterococcus* spp in liver at 0.5 h by 16S rDNA sequencing analyses using C57BL/6 J mice, and they explained that the nutrition in liver was already sufficient at this timepoint. *E. faecalis* was particularly detected at residual levels between 10 h and 20 h with a marked increase at 48 h observed in all the three assays, coincident with that observed for the total bacterial load. *E. coli* numbers were more unpredictable without any consistent results across the 3 assays. Also, Campobasso *et al.* (Campobasso et al., 2022) have described *Enterococcus* spp. as the dominant genera in liver samples of human cadavers since the first samples (only collected after ~72 h *postmortem*) and it resisted at least until 168 h *postmortem*.

Analysis of *E. faecalis* (Figure 21.C) in the spleen showed a residual positivity since time 0 h with the two highest peaks coinciding with that of the total load at 24 h and 48 h, whereas *E. coli* (Figure 21.D) was only detected in these two peaks in one of the

experiments. In a study conducted with murine models similar to ours (bacterial culturing), Annuziata *et al*. (Dell'Annunziata et al., 2022) reported that the liver and spleen were sterile at 0 h *postmortem*. They only detected the presence of *Enterococcus* spp after 3 days, which for the whole monitored period dominated liver and spleen colonization, preventing the proliferation of other bacterial contaminants. While these authors swabbed internal organs for a few seconds, our approach involved utilizing the entire organs. We meticulously fragmented them and suspended the fragments, thereby optimizing the chances of bacterial detection in culture media. This could, at least in part, explain the different results obtained.

Based on human cadavers, Tuomisto *et al.* (Tuomisto et al., 2013) have previously suggested that liver is rarely contaminated, that the bacterial findings before being invaded are quite stable over time and mostly mono-isolates (<5 days *postmortem* in human cadavers), and should correspond to true findings. Taking all the aforementioned statements in consideration, and according to our approach, we hypothesize that in our study a true invasion of liver occurred around 48 h when the mean total load almost doubled in comparison to the 0 h timepoint, in parallel with the prominent increase of *E. faecalis* counts. This species is well known for being particularly resistant to the bile salts present in the liver and enterococcal translocation from the gut to the liver has already been proved in live rodent models (Nunez et al., 2022). Therefore, *E. faecalis* should be explored as a biomarker of liver invasion. Regarding the spleen, it has been suggested that it corresponds to one of the first organs starting decomposition after the stomach and intestine, with the liver following in sequence (Eden et al., 2022; Javan et al., 2019). Following the same rationale as in the liver, our results suggest that spleen started being invaded at 24 h *postmortem* coinciding with the invasion of intestinal bacteria at this timepoint.

4.4.7. Lungs.

The analysis of lung sample cultures showed a mean total load varying between a minimum of 6.5×10^1 CFU/g at 4 h and a maximum of 9.0×10^3 CFU/g at 48 h, with colonization being noted at the control timepoints (0 h) (Figure 22.A). An undulating positivity was observed throughout decomposition with two maximum mean peaks registered at 20 h and 48 h. In one of the scarce studies evaluating microbial growth *postmortem* in lungs (Burcham et al., 2016), authors documented bacterial growth at the

earliest timepoint, which was 1 h *postmortem*. The concept of complete organ sterility, such as in the case of lungs, is not accurate. Indeed, Dickson *et al.* (Dickson et al., 2018) described that the lung microbiota of healthy C57BL/6 mice is highly variable and is strongly affected by the environment (with variations depending on cage, shipment, and vendor) and correlate with concentrations of key inflammatory cytokines in the lung. They also suggest that, although transient and dynamic, variation in lung microbiota should be considered as a source of experimental variability. Our data suggest a basal total load of 2.7×10^2 CFU/g composed of common mice microbiota (*E. faecalis, E. coli, S. xylosus, S. epidermidis, L. murinus*) according to our approach.

The specific analysis of *E. faecalis* (Figure 22.C) indicated a growing trend of this bacterium starting from 10 h (0.4×10^1 CFU/g) with a marked increase after 16 h when the mean load of this species more than doubled (4.9×10^2 CFU/g). *E. coli* (Figure 22.D) counts were more inconsistent, being detected at 0 h, 20 h, 24 h and 48 h only in one of the three experiments, precluding reliable conclusions. However, there is consistency among the different experiments in the absence of the target bacterial species at various timepoints (Figure 22.C and Figure 22.D).
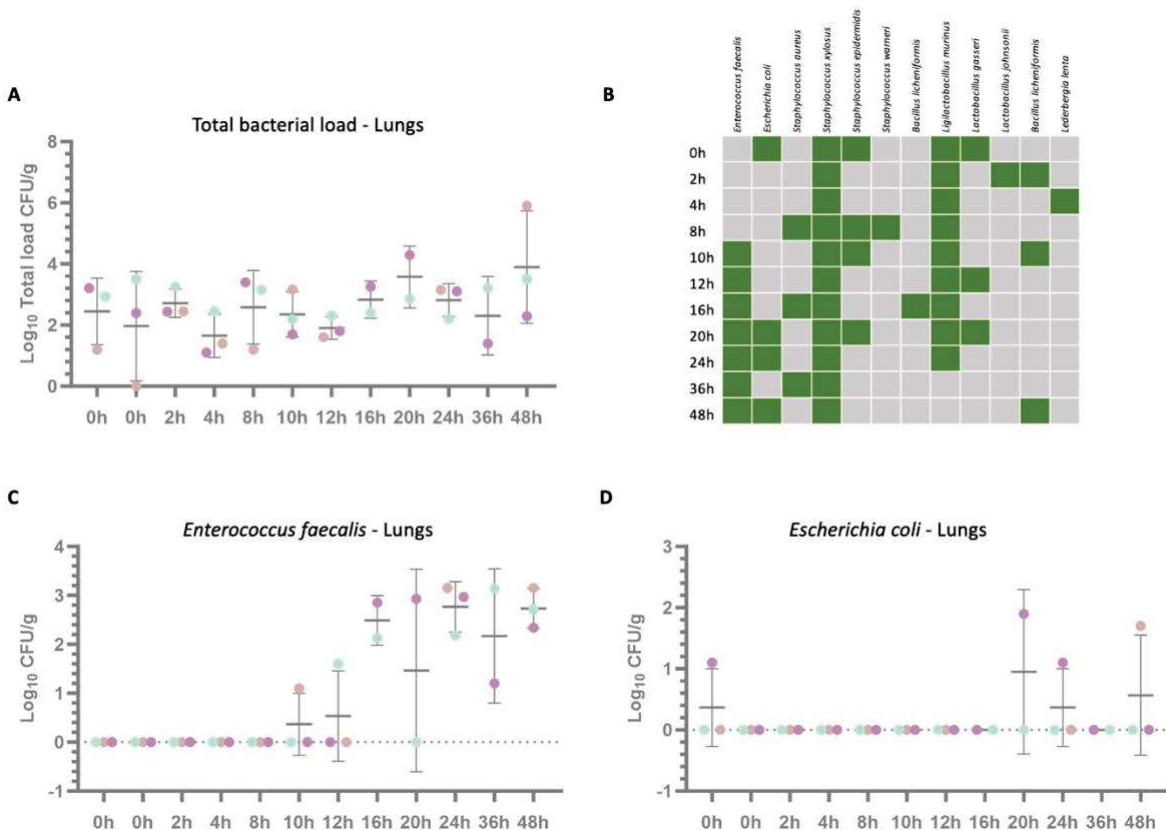

Figure 22. Kinetic cultural analysis of the lungs microbiota changes *postmortem*. (A) Total bacterial counts as well as numbers of **(C)** Enterococci and **(D)** *E. coli* were determined by detection of colony

forming units (CFU) per gram/organ on appropriate culture media (total, enterococci and *E. coli* loads were quantified in sheep blood agar, Slanetz & Bartley agar and MacConkey, respectively). Data are shown as mean ± standard deviation. The P-values obtained through the Kruskal-Wallis test and Dunn's test demonstrated no significant differences between conditions. The data presented came from the three independent experiments (the pilot assay in pink, experiment 1 in green and experiment 2 in purple). **B** represents the occurrence (presence in green, absence in grey) of all bacterial species identified in any of the culture media used (including mannitol salt agar) at the different timepoints. Bacterial species are organized by the families they belong to.

In the specific media used to detect *E. coli* and *E. faecalis*, whenever bacterial growth occurred in these analyses, we consistently obtained monocultures in both organs (see Table 3 for details). Considering all the 132 analyses performed for each organ and the different culture media (33 per medium) and timepoints, we successfully identified a total of 12 distinct bacterial species (all Bacillota) including *S. aureus* at 8 h and 16 h (Figure 22.B). Burcham *et al.* (Burcham et al., 2016) suggested that *S. aureus* in lungs is occasional before 5 days *postmortem*. Further studies are essential to unveil if our results are reproducible and the precise timepoints of lung bacterial invasion.

4.4.8. Brain and Heart.

Mean total loads varying between a common minimum of 0.4×10^1 CFU/g at 2 h for the brain and at 4 h for heart, and a maximum of 7.0×10^2 CFU/g for brain and 7.0×10^1 CFU/g for heart, both at 48 h, were observed. In common to lungs, these organs were not sterile at the 0 h timepoint. A very unstable undulating load was observed across time for the brain samples, with the maximum peak differing substantially from the initial load (Figure 23.A) By contrast, in heart samples bacterial counts fluctuated more stably reaching a final load very similar to the initial timepoint (Figure 24.A). Liu *et al.* (Liu et al., 2023) reported bacterial growth in brain and heart samples at 0.5 h *postmortem* by sequencing. Other study analyzing murine swabs of these organs describe that bacteria growth remained undetactable for 7 days (Dell'Annunziata et al., 2022) and other reported that the thanatomicrobiota was detectable in the brain and heart only in human bodies with a PMI > 168 h (Campobasso et al., 2022). It becomes evident that more studies on these organs are needed, but our methodological approach in murine models generated results closer to that of DNA sequencing.
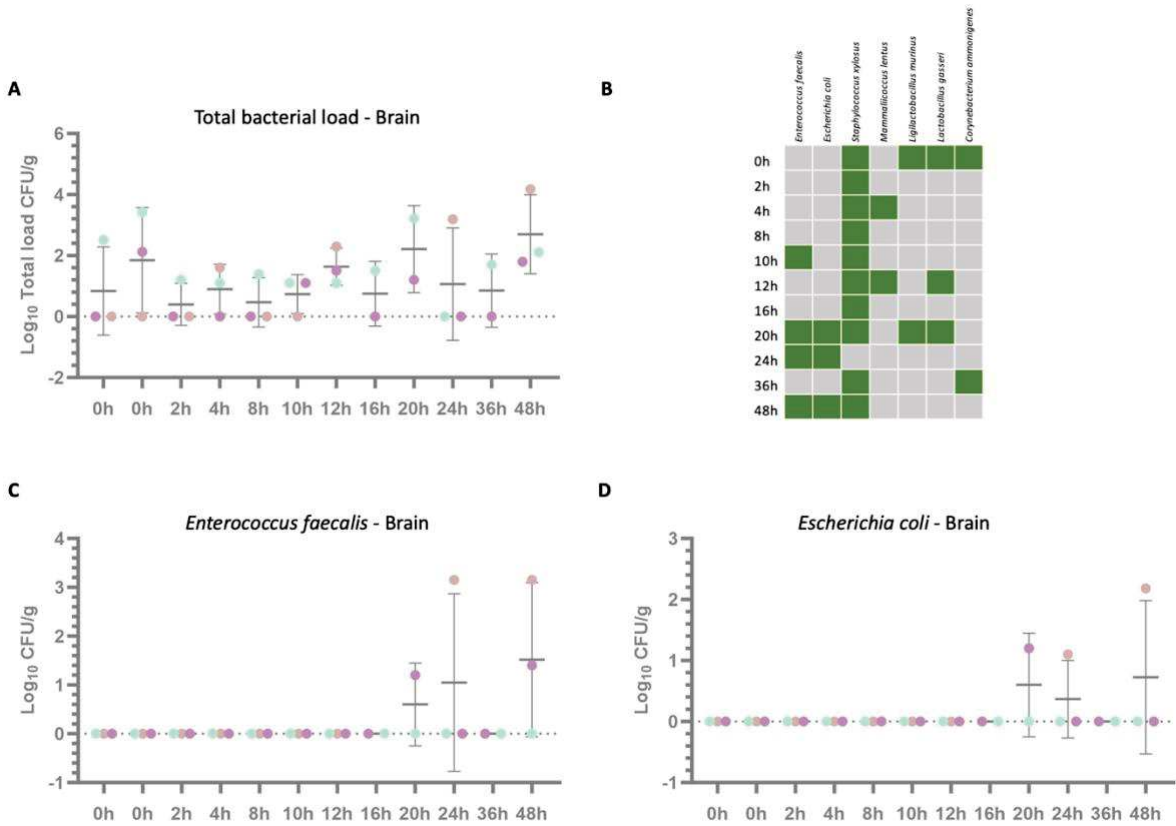
Figure 23. Kinetic cultural analysis of the brain microbiota changes *postmortem.* **(A)** Total bacterial counts as well as numbers of **(C)** Enterococci and **(D)** *E. coli* were determined by detection of colony forming units (CFU) per gram/organ on appropriate culture media (total, enterococci and *E. coli* loads were quantified in sheep blood agar, Slanetz & Bartley agar and MacConkey, respectively). Data are shown as mean ± standard deviation. The P-values obtained through the Kruskal-Wallis test and Dunn's test demonstrated no significant differences between conditions. The data presented came from the three independent experiments (the pilot assay in pink, experiment 1 in green and experiment 2 in purple). **B** represents the occurrence (presence in green, absence in grey) of all bacterial species identified in any of the culture media used (including mannitol salt agar) at the different timepoints. Bacterial species are organized by the families they belong to.

Figure 24. Kinetic cultural analysis of the heart microbiota changes *postmortem.* **(A)** Total bacterial counts as well as numbers of **(C)** Enterococci and **(D)** *E. coli* were determined by detection of colony forming units (CFU) per gram/organ on appropriate culture media (total, enterococci and *E. coli* loads were quantified in sheep blood agar, Slanetz & Bartley agar and MacConkey, respectively). Data are shown as mean ± standard deviation. The P-values obtained through the Kruskal-Wallis test and Dunn's test demonstrated no significant differences between conditions. The data presented came from the three independent experiments (the pilot assay in pink, experiment 1 in green and experiment 2 in purple). **B** represents the occurrence (presence in green, absence in grey) of all bacterial species identified in any of the culture media used (including mannitol salt agar) at the different timepoints. Bacterial species are organized by the families they belong to.
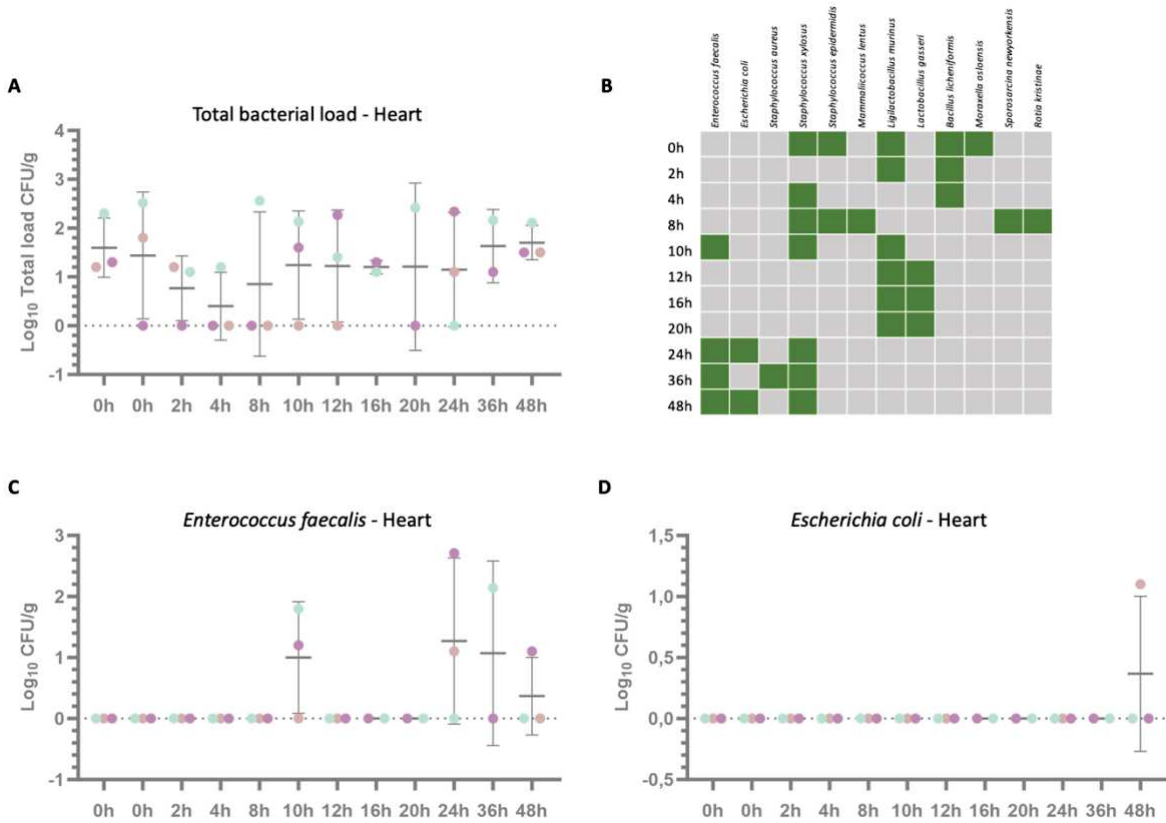
The detection of *E. faecalis* (as shown in Figure 23.C and 24.C) and *E. coli* (Figure 23.D and 24.D) in their respective selective culture media, designed to select these organisms, displayed inconsistency. At no timepoint did all three assays yield positive results for both organs, but both species started being detected after 20 h in the brain, whereas in the heart, *E. faecalis* was detected at 10 h, and *E. coli* only at 48 h.

In the specific media used to detect *E. coli* and *E. faecalis*, whenever bacterial growth occurred in these analyses, we consistently obtained monocultures in both organs (see Table 3 for details). Considering all the 132 analyses performed for each organ and the different culture media (33 analyses per medium) and timepoints, we successfully

97

identified a total of 6 and 12 bacterial species (mostly Bacillota) in brain (Figure 23.B) and heart (Figure 24.B) samples, respectively. Brain was the less diverse organ among all sampled in our study. Liu *et al*. (Liu et al., 2023) reported that the most striking differences occurring in the brain occurred after 8 h *postmortem* and corresponded to the increase of *Acinetobacter*, which we could not detect, in abundance. They also stated that after 8 h of decomposition, several metabolic pathways (e.g., the biotin, lipoic acid metabolism) are depleted in brain samples compared to those in other organs (heart, liver, kidney). These authors further suggested that the proportion of species detected decreased with brain decomposition and this occurred more slowly than in other organs, suggesting that *postmortem* microbial diversity depends on the distance between the organ and the gut. Remarkably, recent evidence showed that gut commensal bacteria can translocate directly to the brain when mice are fed with an altered diet that causes dysbiosis and intestinal permeability, without entering systemic sites or the blood (Thapa et al., 2023). We can hypothesize that this may also occur after death given the potential increase in the permeability of the intestine wall after death. In this case, *E. faecalis* could act as a biomarker of brain invasion after 20 h, but more assays are needed to confirm the reproducibility of our results since they were not detected at 36 h. In contrast, *E. faecalis* does not emerge as an evident biomarker of heart invasion, while more studies are needed to follow the evolution of *E. coli* and *S. aureus* at longer intervals since these species has been described as the most significantly linked to heart blood of *postmortem* cases (Morris et al., 2006).

Once is established that Bacillota and Pseudomonadota are the most important phyla in *postmortem* microbiota (Liu et al., 2020), our study brings relevant insights into the bacterial cargo and evolution of key bacterial species belonging to these phyla (*E. faecalis*-Bacillota and *E. coli*-Pseudomonadota) that have the potential to be used as stable and reliable biomarkers. Even though classic culturing methods have known limitations (e.g., prolonged cultivation periods required by some bacterial species, unculturable and unknown bacteria as reflected by the several "No ID" obtained by MALDITOF-MS), our study focused on key bacterial species that not only make part of human/intestinal microbiota, but easily and rapidly grow under routine culture media and laboratory conditions. It is of note that we could have false negatives even with these bacterial species if they were present under the limit of detection (theoretically one organism per

25 g or 0.04 CFU/g; Sage, 2007). Indeed, Tuomisto *et al*. (Tuomisto et al., 2013) compared culturing and RT-PCR and, as expected, sterility obtained using the latter was considerably less compared with culturing. Nonetheless, culturing methods, akin to ours, can serve as a valuable means to explore the same bacterial species through sequencing. In fact, our culturing approach provides a means to characterize bacterial with a high degree of accuracy and taxonomic resolution (until the species level), which contrast with most studies employing DNA sequencing that can accurately identify bacteria until the family or, at most, the genus level. Finally, overall, our results greatly align with previous studies suggesting enterococci and *E. faecalis,* in particular, as one of the most informative bacteria in the decomposition process (Heimesaat et al., 2012; Li et al., 2021; Liu et al., 2020).

5. Conclusions

- Our study is unique for proactively confirming the presence of common commensal species in mice fecal samples prior to conducting experimental assays, emphasizing the need to consider the microbiota of experimental mice, which can have implications for biomedical research.

- The culturomic analysis of *postmortem* changes in various mouse organs (1304 analyses) allowed us to detect a total of 44 different bacterial species from 13 families and 3 phyla, with notable consistency in the presence of species such as *S. xylosus, E. faecalis,* and *E. coli* across multiple organs. Most species belong to the Bacillota phylum, while the remaining species were categorized under the Pseudomonadota and Actinomycetota phyla, aligning with previous studies that highlighted these as predominant phyla across various timepoints.

- Key microbial shifts during *postmortem* progression included the diminishing dominance of Staphylococcaceae, the rise of Enterococcaceae and Enterobacteriaceae, the stability of the resilient Bacillaceae, and an initial increase, followed by a decline, in Lactobacillaceae, confirming the ordered and dynamic nature of *postmortem* microbial communities.

- The extensive culturomics analysis conducted clearly showed a predominance of monocultures at early timepoints, associated with species typical of skin/mucosa. Beyond 24 h, the overgrowth and invasion of specific species inhibited the growth of less dominant bacteria, particularly in the gut microbiota. Mixed cultures, on the other hand, were consistently associated with the presence of commensal mice microbiota across all organs and timepoints, with *E. faecalis* and/or *E. coli* combinations predominantly emerging in the later *postmortem* intervals.

- The kinetic survey of *postmortem* changes in bacterial species using routine culture media revealed variability in contamination at the initial time point between different assays, emphasizing the importance of replicates. The early and substantial

contamination observed in several organs in addition to the intestine (muscle, stomach) renders them as less reliable for inclusion in *postmortem* calculations.

• Intestinal samples displayed a progressive increase in bacterial load, while stomach samples had fluctuating counts and persistent S. aureus. Kidney samples showed fluctuating loads, suggesting *E. faecalis* as a potential kidney invasion marker. Liver and spleen displayed ongoing fluctuations, especially for *E. faecalis*, hinting at its role as a liver invasion marker. The lung was non-sterile, with variable *E. faecalis* growth, warranting more research. Brain and heart samples were not sterile, and further investigations are needed to understand *postmortem* microbial dynamics in these organs.

• None of the internal organs could be considered initially sterile. Even though no significant differences in bacterial counts between timepoints for each organ were observed (due to considerable variability between the three assays), *E. faecalis* emerged as a potential biomarker of kidney and liver invasion, which are located close to the gut and decompose at the early stages. While the brain is not anatomically close to the gut, the potential as a biomarker for brain invasion is noteworthy, especially considering established gut-brain bacterial translocation. Additionally, *E. faecalis* and *E. coli* in the bladder, as well as *E. coli* in the spleen and heart, exhibit promising evidence for further exploration as potential biomarkers.

• This is one of the first quantitative cultural studies assessing how time elapsing *postmortem* affects the growth and evolution of key bacterial species that can be easily monitored on a routine-basis wet lab experiment. While further comprehensive research is warranted to delve into organ-specific bacterial shifts, our pilot study aligns with previous molecular findings and offers a baseline for future human-oriented investigations.

6. References

Adams RI, Bateman AC, Bik HM, Meadow JF. Microbiota of the indoor environment: a meta-analysis. *Microbiome*, *3*, 49, 2015.

Adserias-Garriga J, Hernández M, Quijada NM, Rodríguez Lázaro D, Steadman D, Garcia-Gil J. Daily thanatomicrobiome changes in soil as an approach of postmortem interval estimation: An ecological perspective. *Forensic Sci Int*, *278*, 388-395, 2017.

Adserias-Garriga J, Quijada NM, Hernandez M, Rodríguez Lázaro D, Steadman D, Garcia-Gil LJ. Dynamics of the oral microbiota as a tool to estimate time since death. *Mol Oral Microbiol*, *32*(6), 511-516, 2017.

Ahannach S, Spacova I, Decorte R, Jehaes E, Lebeer S. At the Interface of Life and Death: Post-mortem and Other Applications of Vaginal, Skin, and Salivary Microbiome Analysis in Forensics. *Front Microbiol*, *12*, 694447, 2021.

Amadasi A, Cappella A, Cattaneo C, Cofrancesco P, Cucca L, Merli D, Sguazza E. Determination of the post mortem interval in skeletal remains by the comparative use of different physico-chemical methods: Are they reliable as an alternative to. *Homo*, *68*(3), 213-221, 2017.

Amendt J, Krettek R, Zehner R. Forensic entomology. *Naturwissenschaften*, *91*(2), 51-65, 2004.

American Society for Microbiology, FAQ: Human Microbiome. Washington (DC), 2013.

Azparren JE, F-RA, Vallejo G. Diagnosing death by drowning in fresh water using blood strontium as an indicator. In (Vol. 137, pp. 55-59). Forensic Science International, 2003.

Balzan S, de Almeida Quadros C, de Cleva R, Zilberstein B, Cecconello I. Bacterial translocation: overview of mechanisms and clinical impact. *J Gastroenterol Hepatol*, *22*(4), 464-471, 2007.

Battaglia M, Garrett-Sinha LA. Staphylococcus xylosus and Staphylococcus aureus as commensals and pathogens on murine skin. *Lab Anim Res*, *39*(1), 18, 2023.

Baud D, Pattaroni C, Vulliemoz N, Castella V, Marsland BJ, Stojanov M. Sperm Microbiota and Its Impact on Semen Parameters. *Front Microbiol*, *10*, 234, 2019.

Belheouane M, Vallier M, Čepić A, Chung CJ, Ibrahim S, Baines JF. Assessing similarities and disparities in the skin microbiota between wild and laboratory populations of house mice. *ISME J*, *14*(10), 2367-2380, 2020.

Bell CR, Wilkinson JE, Robertson BK, Javan GT. Sex-related differences in the thanatomicrobiome in postmortem heart samples using bacterial gene regions V1-2 and V4. *Lett Appl Microbiol*, *67*(2), 144-153, 2018.

Benbow ME, Pechal JL. Approaches and considerations for forensic microbiology decomposition research, *Chapter 3* (Wiley ed.). Forensic Microbiology, 2017

Benbow ME, Barton PS, Ulyshen MD, Beasley JC, DeVault TL, Strickland MS, Tomberlin JK, Jordan HR, Pechal JL. Necrobiome framework for bridging decomposition ecology of autotrophically and heterotrophically derived organic matter. Ecological Monographs 89(1):e01331, 2019.

Berg G, Rybakova D, Fischer D, Cernava T, Vergès MC, Charles T, Schloter M. Microbiome definition re-visited: old concepts and new challenges. *Microbiome*, *8*(1), 103, 2020.

Blondeau LD, Rubin JE, Deneer H, Kanthan R, Sanche S, Hamula C, Blondeau JM. Forensic, investigative and diagnostic microbiology: similar technologies but different priorities. *Future Microbiol*, *14*, 553-558, 2019.

Brinkac L, Clarke TH, Singh H, Greco C, Gomez A, Torralba MG, Nelson KE. Spatial and Environmental Variation of the Human Hair Microbiota. *Sci Rep*, *8*(1), 9017, 2018.

Brooks JW. Postmortem Changes in Animal Carcasses and Estimation of the Postmortem Interval. *Vet Pathol*, *53*(5), 929-940, 2016.

Burcham Z, Jordan H. History, current, and future use of microorganisms as physical evidence. (pp. 25-55). Forensic microbiology, 2017.

Burcham ZM, Cowick CA, Baugher CN, Pechal JL, Schmidt CJ, Rosch JW, Jordan HR. Total RNA Analysis of Bacterial Community Structural and Functional Shifts Throughout Vertebrate Decomposition. *J Forensic Sci*, *64*(6), 1707-1719, 2019.

Burcham ZM, Hood JA, Pechal JL, Krausz KL, Bose JL, Schmidt CJ, Jordan HR.Fluorescently labeled bacteria provide insight on post-mortem microbial transmigration. *Forensic Sci Int*, *264*, 63-69, 2016.

Burcham ZM, Pechal JL, Schmidt CJ, Bose JL, Rosch JW, Benbow ME, Jordan HR. Bacterial Community Succession, Transmigration, and Differential Gene Transcription in a Controlled Vertebrate Decomposition Model. *Front Microbiol*, *10*, 745, 2019.

Campobasso CP, Mastroianni G, Feola A, Mascolo P, Carfora A, Liguori B, Galdiero M. MALDI-TOF Mass Spectrometry Analysis and Human Post-Mortem Microbial Community: A Pilot Study. *Int J Environ Res Public Health*, *19*(7), 2022.

Can I, Javan GT, Pozhitkov AE, Noble PA. Distinctive thanatomicrobiome signatures found in the blood and internal organs of humans. *J Microbiol Methods*, *106*, 1-7, 2014.

Carter DO, Yellowlees D, Tibbett M. Temperature affects microbial decomposition of cadavers (Rattus rattus) in contrasting soils. Applied Soil Ecology, Volume 40, Issue 1, 129-137, 2008.

Carter DO, Tomberlin JK, Benbow ME, Metcalf JL, ProQuest. *Forensic microbiology* (1st ed.). Wiley, 2017.

Carter DO, Yellowlees D, Tibbett M. Cadaver decomposition in terrestrial ecosystems. *Naturwissenschaften*, *94*(1), 12-24, 2007.

Castle JW, Butzbach D, Walker S, Lenehan C, Reith F, Kirkbride P. Microbial impacts in postmortem toxicology. *Forensic Microbiology   Chapter 9* (D.O. Carter, J.K. Tomberlin, M.E. Benbow and J.L. Metcalf ed.). In Forensic Microbiology, 2017

Clarke TH, Gomez A, Singh H, Nelson KE, Brinkac LM. Integrating the microbiome as a resource in the forensics toolkit. *Forensic Sci Int Genet*, *30*, 141-147, 2017.

Clavel T, Lagkouvardos I, Blaut M, Stecher B. The mouse gut microbiome revisited: From complex diversity to model ecosystems. *Int J Med Microbiol*, *306*(5), 316-327, 2016.

Convenor MM, Berard M, Feinstein R, Gallagher, Illgen-Wilcke B, Pritchett-Corning K, rabbits F. FELASA recommendations for the health monitoring of mouse, rat, hamster, guinea pig and rabbit colonies in breeding and experimental units. *Lab Anim*, *48*(3), 178-192, 2014.

Cordeiro C, Ordóñez-Mayán L, Lendoiro E, Febrero-Bande M, Vieira DN, Muñoz-Barús JI. A reliable method for estimating the postmortem interval from the biochemistry of the vitreous humor, temperature and body weight. *Forensic Sci Int*, *295*, 157-168, 2019.

Costa I, Carvalho F, Magalhães T, Pinho PG, Silvestre R, Dinis-Oliveira RJ. Promising blood-derived biomarkers for estimation of the *postmortem*interval. In: *Toxicology Rechearch, Issue* 6, 2015.

Costello EK, Lauber CL, Hamady M, Fierer N, Gordon JI, Knight R. Bacterial community variation in human body habitats across space and time. *Science*, *326*(5960), 1694-1697, 2009.

Coyle HM, Lee C, Lin W, Lee HC, Palmbach TM. Forensic botany: using plant evidence to aid in forensic death investigation. In (pp. 606). *Croatian medical journal*, 2005.

Croxatto A, Prod'hom G, Greub G. Applications of MALDI-TOF mass spectrometry in clinical diagnostic microbiology. *FEMS Microbiol Rev*, *36*(2), 380-407, 2012.

D'Argenio V, Torino M, Precone V, Casaburi G, Esposito MV, Iaffaldano L, Sacchetti L. The Cause of Death of a Child in the 18th Century Solved by Bone Microbiome Typing Using Laser Microdissection and Next Generation Sequencing. *Int J Mol Sci*, *18*(1), 2017.

Darnaud M, De Vadder F, Bogeat P, Boucinha L, Bulteau AL, Bunescu A, Tamellini A. A standardized gnotobiotic mouse model harboring a minimal 15-member mouse gut microbiota recapitulates SOPF/SPF phenotypes. *Nat Commun*, *12*(1), 6686, 2021.

Dash HR, Das S. Thanatomicrobiome and epinecrotic community signatures for estimation of post-mortem time interval in human cadaver. *Appl Microbiol Biotechnol*, *104*(22), 9497-9512, 2020.

DeBruyn JM, Hauther KA. Postmortem succession of gut microbial communities in deceased human subjects. *PeerJ*, *5*, e3437, 2017.

Dekaboruah E, Suryavanshi MV, Chettri D, Verma AK. Human microbiome: an academic update on human body site specific surveillance and its possible role. *Arch Microbiol*, *202*(8), 2147-2167, 2020.

Dell'Annunziata F, Martora F, Pepa MED, Folliero V, Luongo L, Bocelli S, Galdiero M. Postmortem interval assessment by MALDI-TOF mass spectrometry analysis in murine cadavers. *J Appl Microbiol*, *132*(1), 707-714, 2022.

Deo PN, Deshmukh R. Oral microbiome: Unveiling the fundamentals. *J Oral Maxillofac Pathol*, *23*(1), 122-128, 2019.

Dewhirst FE, Chen T, Izard J, Paster BJ, Tanner AC, Yu WH, Wade WG. The human oral microbiome. *J Bacteriol*, *192*(19), 5002-5017, 2010.

Dickson RP, Erb-Downward JR, Falkowski NR, Hunter EM, Ashley SL, Huffnagle GB. The Lung Microbiota of Healthy Mice Are Highly Variable, Cluster by Environment, and Reflect Variation in Baseline Lung Innate Immunity. *Am J Respir Crit Care Med*, *198*(4), 497-508, 2018.

Dinis-Oliveira RJ. The Auto-Brewery Syndrome: A Perfect Metabolic "Storm" with Clinical and Forensic Implications. *J Clin Med*, *10*(20), 2021.

Dinis-Oliveira RJ, Carvalho F, Duarte JA, Remião F, Marques A, Santos A, Magalhães T. Collection of biological samples in forensic toxicology. *Toxicol Mech Methods*, *20*(7), 363-414, 2010.

Dinis-Oliveira RJ, Magalhães T. Forensic toxicology in drug-facilitated sexual assault. *Toxicol Mech Methods*, *23*(7), 471-478, 2013.

Dinis-Oliveira, RJ, Vieira DN, Magalhães T. Guidelines for Collection of Biological Samples for Clinical and Forensic Toxicological Analysis. *Forensic Sci Res*, *1*(1), 42-51, 2016.

Dixon R, Egan S, Hughes S, Chapman B. The Sexome - A proof of concept study into microbial transfer between heterosexual couples after sexual intercourse. *Forensic Sci Int*, *348*, 111711, 2023.

Donaldson AE, Lamont IL. Biochemistry changes that occur after death: potential markers for determining post-mortem interval. *PLoS One*, *8*(11), e82011, 2013.

Dong K, Xin Y, Cao F, Huang Z, Sun J, Peng M, Shi P. Succession of oral microbiota community as a tool to estimate postmortem interval. *Sci Rep*, *9*(1), 13063, 2019.

Duong V-A, Park J-M, Lim H-J, Lee H. Proteomics in Forensic Analysis: Applications for Human Samples. *Appl. Sci*, *11*, 3393, 2021.

Eden, RE, Thomas B. StatPearls. In *Algor Mortis*, 2022.

Emmons AL, Mundorff AZ, Hoeland KM, Davoren J, Keenan SW, Carter DO, DeBruyn JM. Postmortem Skeletal Microbial Community Composition and Function in Buried Human Remains. *mSystems*, *7*(2), e0004122, 2022.

Escobar JS, Klotz B, Valdes BE, Agudelo GM. The gut microbiota of Colombians differs from that of Americans, Europeans and Asians. *BMC Microbiol*, *14*, 311, 2014.

Flores GE, Caporaso JG, Henley JB, Rideout JR, Domogala D, Chase J, Fierer N. Temporal variability is a personalized feature of the human microbiome. *Genome Biol*, *15*(12), 531, 2014.

Fouts DE, Torralba M, Nelson KE, Brenner DA, Schnabl B. Bacterial translocation and changes in the intestinal microbiome in mouse models of liver disease. *J Hepatol*, *56*(6), 1283-1292, 2012.

Franceschetti L, Amadasi A, Bugelli V, Bolsi G, Tsokos M. Estimation of Late Postmortem Interval: Where Do We Stand? A Literature Review. *Biology (Basel)*, *12*(6), 2023.

Francés-Cuesta C, de la Caba I, Idigoras P, Fernández-Rodríguez A, Del Valle Pérez D, Marimón JM, González-Candelas F. Whole-genome sequencing of Neisseria gonorrhoeae in a forensic transmission case. *Forensic Sci Int Genet*, *42*, 141-146, 2019.

Gao W, Li B, Ling L, Zhang L, Yu S. MALDI-TOF MS method for differentiation of methicillin-sensitive and methicillin-resistant Staphylococcus aureus using (E)-Propyl α-cyano-4-Hydroxyl cinnamylate. *Talanta*, *244*, 123405, 2022.

García MG, Pérez-Cárceles MD, Osuna E, Legaz I. Impact of the Human Microbiome in Forensic Sciences: a Systematic Review. *Appl Environ Microbiol*, *86*(22), 2020.

Gevers W. Biochemical aspects of cell death. 2004.

Gilbert JA, Blaser MJ, Caporaso JG, Jansson JK, Lynch SV, Knight R. Current understanding of the human microbiome. *Nat Med*, *24*(4), 392-400, 2018.

Gimblet C, Meisel JS, Loesche MA, Cole SD, Horwinski J, Novais FO, Grice EA. Cutaneous Leishmaniasis Induces a Transmissible Dysbiotic Skin Microbiota that Promotes Skin Inflammation. *Cell Host Microbe*, *22*(1), 13-24.e14, 2017.

Goldwater PN. Gut Microbiota and Immunity: Possible Role in Sudden Infant Death Syndrome. *Front Immunol*, *6*, 269, 2015.

Gopalakrishna KP, Hand TW. Influence of Maternal Milk on the Neonatal Intestinal Microbiome. *Nutrients*, *12*(3), 2020.

Gouello A, Dunyach-Remy C, Siatka C, Lavigne JP. Analysis of Microbial Communities: An Emerging Tool in Forensic Sciences. *Diagnostics (Basel)*, *12*(1), 2021.

Grice EA, Kong HH, Conlan S, Deming CB, Davis J, Young AC, Program NCS. Topographical and temporal diversity of the human skin microbiome. *Science*, *324*(5931), 1190-1192, 2009.

Grice EA, Segre JA. The skin microbiome. *Nat Rev Microbiol*, *9*(4), 244-253, 2011.

Guo J, Fu X, Liao H, Hu Z, Long L, Yan W, Cai J. Potential use of bacterial community succession for estimating post-mortem interval as revealed by high-throughput sequencing. *Sci Rep*, *6*, 24197, 2016.

Guo J, Song C, Liu Y, Wu X, Dong W, Zhu H, Qin C. Characteristics of gut microbiota in representative mice strains: Implications for biological research. *Animal Model Exp Med*, *5*(4), 337-349, 2022.

Haarkötter C, Saiz M, Gálvez X, Medina-Lozano MI, Álvarez JC, Lorente JA. Usefulness of Microbiome for Forensic Geolocation: A Review. *Life (Basel)*, *11*(12), 2021.

Hauther KA, Cobaugh KL, Jantz LM, Sparer TE, DeBruyn JM. Estimating Time Since Death from Postmortem Human Gut Microbial Communities. *J Forensic Sci*, *60*(5), 1234-1240, 2015.

Heimesaat MM, Bereswill S, Fischer A, Fuchs D, Struck D, Niebergall J, Liesenfeld O. Gram-negative bacteria aggravate murine small intestinal Th1-type immunopathology following oral infection with Toxoplasma gondii. *J Immunol*, *177*(12), 8785-8795, 2006.

Heimesaat MM, Boelke S, Fischer A, Haag LM, Loddenkemper C, Kühl AA, Bereswill S. Comprehensive postmortem analyses of intestinal microbiota changes and bacterial translocation in human flora associated mice. *PLoS One*, *7*(7), e40758, 2012.

Highet AR, Berry AM, Bettelheim KA, Goldwater PN. Gut microbiome in sudden infant death syndrome (SIDS) differs from that in healthy comparison babies and offers an explanation for the risk factor of prone position. *Int J Med Microbiol*, *304*(5-6), 735-741, 2014.

Huang S, Haiminen N, Carrieri AP, Hu R, Jiang L, Parida L, Xu ZZ. Human Skin, Oral, and Gut Microbiomes Predict Chronological Age. *mSystems*, *5*(1), 2020.

Hyde ER, Metcalf JL, Bucheli SR, Lynne AM, Knight R. Microbial communities associated with decomposing corpses. In Forensic Microbiology (eds D.O. Carter, J.K. Tomberlin, M.E. Benbow and J.L. Metcalf), 2017.

Hyde ER, Haarmann DP, Lynne AM, Bucheli SR, Petrosino JF. The living dead: bacterial community structure of a cadaver at the onset and end of the bloat stage of decomposition. *PLoS One*, *8*(10), e77733, 2013.

Hyde ER, Haarmann DP, Petrosino JF, Lynne AM, Bucheli SR. Initial insights into bacterial succession during human decomposition. *Int J Legal Med*, *129*(3), 661-671, 2015.

Janaway RC, Steven ASW, Percival L. Decomposition of Human Remains. Microbiology and Aging, pp. 313-334, 2017.

Jansen J, Jansen K, Neven E, Poesen R, Othman A, van Mil A, Masereeuw R. Remote sensing and signaling in kidney proximal tubules stimulates gut microbiome-derived organic anion secretion. *Proc Natl Acad Sci U S A*, *116*(32), 16105-16110, 2019.

Jauréguy F, Chariot P, Vessières A, Picard B. Prevalence of Chlamydia trachomatis and Neisseria gonorrhoeae infections detected by real-time PCR among individuals reporting sexual assaults in the Paris, France area. *Forensic Sci Int*, *266*, 130-133, 2016.

Javan GT, Finley SJ, Abidin Z, Mulle JG. The Thanatomicrobiome: A Missing Piece of the Microbial Puzzle of Death. *Front Microbiol*, *7*, 225, 2016.

Javan GT, Finley SJ, Can I, Wilkinson JE, Hanson JD, Tarone AM. Human Thanatomicrobiome Succession and Time Since Death. *Sci Rep*, *6*, 29598, 2016.

Javan GT, Finley SJ, Tuomisto S, Hall A, Benbow ME, Mills D. An interdisciplinary review of the thanatomicrobiome in human decomposition. *Forensic Sci Med Pathol*, *15*(1), 75-83, 2019.

Javan GT, Wells T, Allen J, Visona S, Moretti M, Tipton C, Finley SJ. Correlation between postmortem microbial signatures and substance abuse disorders. *PLoS One*, *17*(9), e0274401, 2022.

Jo J, Oh J, Park C. Microbial community analysis using high-throughput sequencing technology: a beginner's guide for microbiologists. *J Microbiol*, *58*(3), 176-192, 2020.

Johnson JS, Spakowicz DJ, Hong BY, Petersen LM, Demkowicz P, Chen L, Weinstock GM. Evaluation of 16S rRNA gene sequencing for species and strain-level microbiome analysis. *Nat Commun*, *10*(1), 5029, 2019.

Joo-Young Na JHP, Soo-Hyun Kim, Jong-Tae Park. Bacteria as Normal Flora in Postmortem Body Fluid Samples, 2017.

Jovel J, Patterson J, Wang W, Hotte N, O'Keefe S, Mitchel T, Wong GK. Characterization of the Gut Microbiome Using 16S or Shotgun Metagenomics. *Front Microbiol*, *7*, 459, 2016.

João P. Decay Process of a Cadaver. In *Chapter 5* (A. Schmitt, E. Cunha, and J. Pinheiro © Humana Press Inc., Totowa, NJ ed.). From Forensic Anthropology and Medicine:Complementary Sciences From Recovery to Cause of Death, 2016.

Jung B, Hoilat GJ. MacConkey Medium. In *StatPearls*. StatPearls Publishing Copyright ©, StatPearls Publishing LLC, 2023.

Jung JY, Yoon HK, An S, Lee JW, Ahn ER, Kim YJ, Lim, S. K. Rapid oral bacteria detection based on real-time PCR for the forensic identification of saliva. *Sci Rep*, *8*(1), 10852, 2018.

Kakizaki E, Kozawa S, Imamura N, Uchiyama T, Nishida S, Sakai M, Yukawa N. Detection of marine and freshwater bacterioplankton in immersed victims: Post-mortem bacterial invasion does not readily occur. *Forensic Sci Int*, *211*(1-3), 9-18, 2011.

Kakizaki E, Ogura Y, Kozawa S, Nishida S, Uchiyama T, Hayashi T, Yukawa N. Detection of diverse aquatic microbes in blood and organs of drowning victims: first metagenomic approach using high-throughput 454-pyrosequencing. *Forensic Sci Int*, *220*(1-3), 135-146, 2012.

Khoudia Diop, Jean-Charles Dufour, Anthony Levasseur, Florence Fenollar. Exhaustive repertoire of human vaginal microbiota. Human Microbiome Journal, Volume 11, 100051, 2019.

Kodama WA, Xu Z, Metcalf JL, Song SJ, Harrison N, Knight R, Happy CB. Trace Evidence Potential in Postmortem Skin Microbiomes: From Death Scene to Morgue. *J Forensic Sci*, *64*(3), 791-798, 2019.

Ksiezarek M, Perovic SU, Rocha J, Grosso F, Peixe L. Long-term stability of the urogenital microbiota of asymptomatic European women. *BMC Microbiol*, *21*(1), 64, 2021.

Kuiper I. Microbial forensics: next-generation sequencing as catalyst: The use of new sequencing technologies to analyze whole microbial communities could become a powerful tool for forensic and criminal investigations. *EMBO Rep*, *17*(8), 1085-1087, 2016.

Lauber CL, Metcalf JL, Keepers K, Ackermann G, Carter DO, Knight R. Vertebrate decomposition is accelerated by soil microbes. *Appl Environ Microbiol*, *80*(16), 4920-4929, 2014.

Lax S, Hampton-Marcell JT, Gibbons SM, Colares GB, Smith D, Eisen JA, Gilbert JA. Forensic analysis of the microbiome of phones and shoes. *Microbiome*, *3*, 21, 2015.

Leong LEX, Taylor SL, Shivasami A, Goldwater PN, Rogers GB. Intestinal Microbiota Composition in Sudden Infant Death Syndrome and Age-Matched Controls. *J Pediatr*, *191*, 63-68.e61, 2017.

Li C, Ma D, Deng K, Chen Y, Huang P, Wang Z. Application of MALDI-TOF MS for Estimating the Postmortem Interval in Rat Muscle Samples. *J Forensic Sci*, *62*(5), 1345-1350, 2017.

Li H, Zhang S, Liu R, Yuan L, Wu D, Yang E, Xu J. Potential use of molecular and structural characterization of the gut bacterial community for postmortem interval estimation in Sprague Dawley rats. *Sci Rep*, *11*(1), 225, 2021.

Liu R, Gu Y, Shen M, Li H, Zhang K, Wang Q, Wang Z. Predicting postmortem interval based on microbial community sequences and machine learning algorithms. *Environ Microbiol*, *22*(6), 2273-2291, 2020.

Liu R, Wang Q, Zhang K, Wu H, Wang G, Cai W, Wang Z. Analysis of Postmortem Intestinal Microbiota Successional Patterns with Application in Postmortem Interval Estimation. *Microb Ecol*, *84*(4), 1087-1102, 2022.

Liu R, Zhang K, Li H, Sun Q, Wei X, Zhang S, Wang Z. Dissecting the microbial community structure of internal organs during the early postmortem period in a murine corpse model. *BMC Microbiol*, *23*(1), 38, 2023.

López CD, Montiel González D, Haas C, Vidaki A, Kayser M. Microbiome-based body site of origin classification of forensically relevant blood traces. *Forensic Sci Int Genet*, *47*, 102280, 2020.

Lutz H, Vangelatos A, Gottel N, Osculati A, Visona S, Finley SJ, Javan GT. Effects of Extended Postmortem Interval on Microbial Communities in Organs of the Human Cadaver. *Front Microbiol*, *11*, 569630, 2020.

Maccallum WG, Hastings TW. A case of acute endocarditis caused by micrococcus zymogenes (nov. Spec.), with a description of the microorganism. *J Exp Med*, *4*(5-6), 521-534, 1899.

Mansour SR, Moustafa MAA, Saad BM, Hamed R, Moustafa AA. Impact of diet on human gut microbiome and disease risk. *New Microbes New Infect*, *41*, 100845, 2021.

Martinez-Guryn K, Leone V, Chang EB. Regional Diversity of the Gastrointestinal Microbiome. *Cell Host Microbe*, *26*(3), 314-324, 2019.

Matuszewski S, Konwerski S, Frątczak K, Szafałowicz M. Effect of body mass and clothing on decomposition of pig carcasses. *Int J Legal Med*, *128*(6), 1039-1048, 2014.

Mesli V, Neut C, Valery H. Postmortem bacterial translocation. Forensic Microbiology, Chapter 8, pp. 192-211, 2017.

Metcalf JL. Estimating the postmortem interval using microbes: Knowledge gaps and a path to technology adoption. *Forensic Sci Int Genet*, *38*, 211-218, 2019.

Metcalf JL, Carter DO, Knight R. Microbiology of death. *Curr Biol*, *26*(13), R561-R563, 2016.

Metcalf JL, Parfrey WL, Gonzalez A, Lauber CL, Knights D, Ackermann G, Knight R. A microbial clock provides an accurate estimate of the postmortem interval in a mouse model system. *Elife*, *2*, e01104, 2013.

Metcalf JL, Xu ZZ, Weiss S, Lax S, Van Treuren W, Hyde ER, Knight R. Microbial community assembly and metabolic function during mammalian corpse decomposition. *Science*, *351*(6269), 158-162, 2016.

Mohammed FFA, Fairozekhan AT, Bhat S, Menezes RG. Forensic Odontology. In. StatPearls, 2022.

Mondor E, Tremblay M, tomberlin J, Benbow M, Tarone A. The Ecology of Carrion Decomposition: Nature Education Knowledge, 3(10):21, 2012.

Morris J, Harrison L, Partridge S. Practical and theoretical aspects of postmortem bacteriology. Current Diagnostic Pathology. 13. 65-74, 2007.

Morris JA, Harrison LM, Partridge SM. Postmortem bacteriology: a re-evaluation. *J Clin Pathol*, *59*(1), 1-9, 2006.

Nearing JT, Comeau AM, Langille MGI. Identifying biases and their potential solutions in human microbiome studies. *Microbiome*, *9*(1), 113, 2021.

Neu AT, Allen EE, Roy K. Defining and quantifying the core microbiome: Challenges and prospects. *Proc Natl Acad Sci U S A*, *118*(51), 2021.

Nguyen TL, Vieira-Silva S, Liston A, Raes J. (2015). How informative is the mouse for human gut microbiota research? *Dis Model Mech*, *8*(1), 1-16, 2015.

Nunez N, Derré-Bobillot A, Trainel N, Lakisic G, Lecomte A, Mercier-Nomé F, Archambaud C. The unforeseen intracellular lifestyle of. *Gut Microbes*, *14*(1), 2058851, 2022.

O'Rourke J, Lee A, McNeill J. Differences in the gastrointestinal microbiota of specific pathogen free mice: an often unknown variable in biomedical research. *Lab Anim*, *22*(4), 297-303, 1988.

Ohta J, Sakurada K. Oral gram-positive bacterial DNA-based identification of saliva from highly degraded samples. *Forensic Sci Int Genet*, *42*, 103-112, 2019.

Oliveira M, Amorim A. Microbial forensics: new breakthroughs and future prospects. *Appl Microbiol Biotechnol*, *102*(24), 10377-10391, 2018.

Opal SM. A Brief History of Microbiology and Immunology. Vaccines: A Biography, *Chapter 3,* 10:31–56, 2009.

Ossowicki A, Raaijmakers JM, Garbeva P. Disentangling soil microbiome functions by perturbation. *Environ Microbiol Rep*, *13*(5), 582-590, 2021.

Park J, Kim S, Lee J-A, Kim J, Kim S. Microbial Forensic Analysis of Human-Associated Bacteria Inhabiting Hand Surface. Forensic Science International: Genetics Supplement Series 6, 2017.

Parkinson CM, O'Brien A, Albers TM, Simon MA, Clifford CB, Pritchett-Corning KR. Diagnostic necropsy and selected tissue and sample collection in rats and mice. *J Vis Exp*(54), 2011.

Pearson AL, Rzotkiewicz JLPA, Schmidt CJ, Jordan HR, Zwickle A, M. Eric Benbow Initial Evidence of the Relationships between the Human Postmortem Microbiome and Neighborhood Blight and Greening Efforts, pp. 958-978, Annals of the American Association of Geographers, 2019

Pechal JL, Crippen, TL, Benbow ME, Tarone AM, Dowd S, Tomberlin JK.The potential use of bacterial community succession in forensics as described by high throughput metagenomic sequencing. *Int J Legal Med*, *128*(1), 193-205, 2014.

Pechal JL, Schmidt CJ, Jordan HR, Benbow ME. A large-scale survey of the postmortem human microbiome, and its potential to provide insight into the living health condition. *Sci Rep*, *8*(1), 5724, 2018.

Percival SL. Microbiology and aging: clinical manifestations, 2009.

Perovic SU, Ksiezarek M, Rocha J, Cappelli EA, Sousa M, Ribeiro TG, Peixe L. Urinary Microbiome of Reproductive-Age Asymptomatic European Women. *Microbiol Spectr*, e0130822, 2022.

Phan K, Barash M, Spindler X, Gunn P, Roux C. Retrieving forensic information about the donor through bacterial profiling. *Int J Legal Med*, *134*(1), 21-29, 2020.

Piette MH, De Letter EA. Drowning: still a difficult autopsy diagnosis. *Forensic Sci Int*, *163*(1-2), 1-9, 2006.

Pittner S, Bugelli V, Weitgasser K, Zissler A, Sanit S, Lutz L, Amendt J. A field study to evaluate PMI estimation methods for advanced decomposition stages. *Int J Legal Med*, *134*(4), 1361-1373, 2020.

Praveen V, Prveen S. Microbiome-Gut-Brain Axis: A Pathway for Improving Brainstem Serotonin Homeostasis and Successful Autoresuscitation in SIDS-A Novel Hypothesis. *Front Pediatr*, *4*, 136, 2016.

Roy D, Tomo S, Purohit P, Setia P. Microbiome in Death and Beyond: Current Vistas and Future Trends [Review]. *Frontiers in Ecology and Evolution*, *9*, 2021.

Sage L. Detecting pathogens on produce. *Anal Chem*, *79*(1), 7-9, 2007

Sampaio-Silva F, Magalhães T, Carvalho F, Dinis-Oliveira RJ, Silvestre R. Profiling of RNA degradation for estimation of post mortem [corrected] interval. *PLoS One*, *8*(2), e56507, 2013

Schmedes SE, Sajantila A, Budowle B. Expansion of Microbial Forensics. *J Clin Microbiol*, *54*(8), 1964-1974, 2016.

Schmedes SE, Woerner AE, Novroski NMM, Wendt FR, King JL, Stephens KM, Budowle B. Targeted sequencing of clade-specific markers from skin microbiomes for forensic human identification. *Forensic Sci Int Genet*, *32*, 50-61, 2018.

Schulz D, Grumann D, Trübe P, Pritchett-Corning K, Johnson S, Reppschläger K, Holtfreter S. Laboratory Mice Are Frequently Colonized with. *Front Cell Infect Microbiol*, *7*, 152, 2017.

Sharon I, Quijada NM, Pasolli E, Fabbrini M, Vitali F, Agamennone V, Turroni S. The Core Human Microbiome: Does It Exist and How Can We Find It? A Critical Review of the Concept. *Nutrients*, *14*(14), 2022.

Shetty SA, Hugenholtz F, Lahti L, Smidt H, de Vos WM. Intestinal microbiome landscaping: insight in community assemblage and implications for microbial modulation strategies. *FEMS Microbiol Rev*, *41*(2), 182-199, 2017.

Speruda M, Piecuch A, Borzęcka J, Kadej M, Ogórek R. Microbial traces and their role in forensic science. *J Appl Microbiol*, 2021.

Swayambhu M, Kümmerli NAR. Microbiome-Based Stain Analyses in Crime Scenes. American Society for Microbiology, 2023.

Tan CCS, Ko KKK, Chen H, Liu J, Loh M, SG10K_Health Consortium, Chia M, Nagarajan N. No evidence for a common blood microbiome based on a population study of 9,770 healthy humans. Nature microbiology, 8(5), 973–985, 2023.

Tarone AM, Mann AE, Zhang Y, Zascavage RR, Mitchell EA, Morales E, Allen MS. The devil is in the details: Variable impacts of season, BMI, sampling site temperature, and presence of insects on the post-mortem microbiome. *Front Microbiol*, *13*, 1064904, 2022.

Tavakkol Z, Samuelson D, deLancey Pulcini E, Underwood RA, Usui ML, Costerton JW, James GA, Olerud JE, Fleckman P. Resident bacterial flora in the skin of C57BL/6 mice housed under SPF conditions. J Am Assoc Lab Anim Sci, 49(5):588-91, 2010.

The Human Microbiome Project Consortium. Structure, function and diversity of the healthy human microbiome. Nature, 486: p. 207–214, 2012.

Thapa M, Kumari A, Chin CY, Choby JE, Jin F, Bogati B, Grakoui A. Translocation of gut commensal bacteria to the brain. *bioRxiv*, 2023.

Thomas-White K, Brady M, Wolfe AJ, Mueller ER. The bladder is not sterile: History and current discoveries on the urinary microbiome. Curr Bladder Dysfunct Rep., 11(1):18-24, 2016.

Tomberlin JK, Benbow ME., Barnes KM, Jordan HR. Arthropod–microbe interactions on vertebrate remains. In Forensic Microbiology (eds D.O. Carter, J.K. Tomberlin, M.E. Benbow and J.L. Metcalf), chapter 11, 2017.

Tridico SR, Murray DC, Addison J, Kirkbride KP, Bunce M. Metagenomic analyses of bacteria on human hairs: a qualitative assessment for applications in forensic science. *Investig Genet*, *5*(1), 16, 2014.

Tu Q, He Z, Zhou J. Strain/species identification in metagenomes using genome-specific markers. *Nucleic Acids Res*, *42*(8), e67, 2014.

Tu Q, Li J, Shi Z, Chen Y, Lin L, Wang H, He Z. HuMiChip2 for strain level identification and functional profiling of human microbiomes. *Appl Microbiol Biotechnol*, *101*(1), 423-435, 2017.

Tuomisto S, Karhunen PJ, Pessi T. Time-dependent post mortem changes in the composition of intestinal bacteria using real-time quantitative PCR. *Gut Pathog*, *5*(1), 35, 2013.

Tuomisto S, Karhunen PJ, Vuento R, Aittoniemi J, Pessi T. Evaluation of postmortem bacterial migration using culturing and real-time quantitative PCR. *J Forensic Sci*, *58*(4), 910-916, 2013.

Turnbaugh PJ, Ley RE, Hamady M, Fraser-Liggett CM, Knight R & Gordon JI. The human microbiome project. *Nature*, *449*(7164), 804-810, 2007

Ubelaker DH & Wu Y. Fragment analysis in forensic anthropology. *Forensic Sci Res*, *5*(4), 260-265, 2020.

Uchiyama T, Kakizaki E, Kozawa S, Nishida S, Imamura N & Yukawa N. A new molecular approach to help conclude drowning as a cause of death: simultaneous detection of eight bacterioplankton species using real-time PCR assays with TaqMan probes. *Forensic Sci Int*, *222*(1-3), 11-26, 2012.

Vass AA. Beyond the Grave—Understanding Human Decomposition. In (pp. 190-192). Microbiology Today, 2001.

Walker AW & Hoyles L. Human microbiome myths and misconceptions. *Nat Microbiol*, *8*(8), 1392-1396, 2023.

Wang J, Lang T, Shen J, Dai J, Tian L & Wang X. Core Gut Bacteria Analysis of Healthy Mice. *Front Microbiol*, *10*, 887, 2019.

Weber MA, Hartley JC, Brooke I, Lock PE, Klein NJ, Malone M & Sebire NJ. Post-mortem interval and bacteriological culture yield in sudden unexpected death in infancy (SUDI). *Forensic Sci Int*, *198*(1-3), 121-125, 2010.

Wernroth ML, Peura S, Hedman AM, Hetty S, Vicenzi S, Kennedy B, Fall T. Development of gut microbiota during the first 2 years of life. *Sci Rep*, *12*(1), 9080, 2022.

Wilkins D, Leung MH & Lee PK. Microbiota fingerprints lose individually identifying features over time. *Microbiome*, *5*(1), 1, 2017.

Williams DW & Gibson G. Individualization of pubic hair bacterial communities and the effects of storage time and temperature. *Forensic Sci Int Genet*, *26*, 12-20, 2017.

Williams DW, & Gibson G. Classification of individuals and the potential to detect sexual contact using the microbiome of the pubic region. *Forensic Sci Int Genet*, *41*, 177-187, 2019.

Williams T, Soni S, White J, Can G & Javan GT. Evaluation of DNA degradation using flow cytometry: promising tool for postmortem interval determination. *Am J Forensic Med Pathol*, *36*(2), 104-110, 2015.

Xiao L, Feng Q, Liang S, Sonne SB, Xia Z, Qiu X, Kristiansen K. A catalog of the mouse gut metagenome. *Nat Biotechnol*, *33*(10), 1103-1108, 2015.

Zhang J, Liu W, Simayijiang H, Hu P, & Yan J. Application of Microbiome in Forensics. *Genomics Proteomics Bioinformatics*, 2022.

Zhang Y, Pechal JL, Schmidt CJ, Jordan HR, Wang WW, Benbow ME, Tarone AM. Machine learning performance in a microbial molecular autopsy context: A cross-sectional postmortem human population study. *PLoS One*, *14*(4), e0213829, 2019.

Zhou W, Bian Y. Thanatomicrobiome composition profiling as a tool for forensic investigation. *Forensic Sci Res*, *3*(2), 105-110, 2018.

Zolfo M, Asnicar PMF, Pasolli E, Tett A, Segata N. Profiling microbial strains in urban environments using metagenomic sequencing data. (Ed.). <i data-test="journal-title" style="box-sizing: inherit;">Biology Direct   volume, 2018.

7. Appendix

7.1. Microbiological characteristics of the C57BL/6J SPF mice.

Mouse Models - Health Profiles

Charles River is committed to providing you with high-quality genetically standardized models such as SPF (Specific Pathogen Free) and SOPF (Specific and Opportunistic Pathogen Free)*.

Immunocompetent Strains Available from Charles River with an SOPF Health Status:

From Europe

Crl:CD1 (ICR)   C3H/HeNCrl
Crl:NMRI(Han)   C57BL/6J
129S2/SvPasCrl   C57BL/6NCrl
BALB/cByJ

From North America*

BALB/cAnNCrl
SJL/JOrlcoCrl
Crl:SKH1-Hr*

	SPF – Immunocompetent mice	SOPF - Immunocompetent mice
Viruses		
Minute Virus of Mice (MVM)	•	•
Mouse Parvovirus (MPV)	•	•
Mouse Hepatitis Virus (MHV)	•	•
Mouse Norovirus (MNV)	•	•
Theiler's Murine Encephalomyelitis Virus (TMEV -GDVII)	•	•
Mouse Rotavirus (EDIM)	•	•
Sendai virus (SEND)	•	•
Reovirus 3 (REO3)	•	•
Pneumonia virus of Virus (PVM)	•	•
Mouse Thymic Virus (MTV)	•	•
Mouse Cytomegalovirus (MCMV)	•	•
Hantaan Virus (HANT)	•	•
Lymphocytic Choriomeningitis Virus (LCMV)	•	•
Mouse Adenovirus (MAV 1 & 2)	•	•
K Virus (K)	•	•
Ectromelia virus (ECTRO)	•	•
Polyoma Virus (POLY)	•	•
Lactate Dehydrogenase Virus (LDV)	•	•
Bacterias		
Tyzzer's Disease (CPIL)	•	•
Bordetella bronchiseptica	b	•
Citrobacter rodentium	•	•
Corynebacterium kutscheri	•	•
Mycoplasma pulmonis	•	•
Pasteurella pneumotropica	b	•
Pasteurella multocida	•	•
Salmonella spp	•	•
Streptobacillus moniliformis	•	•
Streptococcus pneumoniae	b	•
Helicobacter hepaticus	•	•
Helicobacter bilis	•	•
Helicobacter typhlonius	•	•
Helicobacter spp, other species	•	•
Cilia-Associated Respiratory Bacillus	•	•
Opportunistic Organisms		
Staphylococcus aureus	c	•
Pseudomonas aeruginosa	c	•
Klebsiella pneumoniae	c	•
Klebsiella oxytoca	c	•
Pneumocystis spp	c	•
Proteus mirabilis	c	•
Beta haemolytic Streptococcus – Grp A	c	•
Beta haemolytic Streptococcus - Grp B	c	•
Beta haemolytic Streptococcus - Grp C	c	•
Beta haemolytic Streptococcus - Grp G	c	•
Corynebacterium bovis	c	•
Parasites		
Ectoparasites	•	•
Helminths	•	•
Enteric Pathogenic Protozoa	•	•
Other protozoa	c	•
E. cuniculi	•	•

• = excluded agents - b = planned recycle - c = no action

* List of agents for North America may differ from table listed above

www.criver.com

7.2. First page of the self-authored review from which the introduction of this work was adapted.

Review

The Future Is Now: Unraveling the Expanding Potential of Human (Necro)Microbiome in Forensic Investigations

Ana Cláudia-Ferreira [1], Daniel José Barbosa [1,2,*], Veroniek Saegeman [3,†], Amparo Fernández-Rodríguez [4,†], Ricardo Jorge Dinis-Oliveira [1,5,6,7], Ana R. Freitas [1,7,8,*,†] and on behalf of the ESCMID Study Group of Forensic and Post-Mortem Microbiology (ESGFOR)

[1] 1H-TOXRUN, One Health Toxicology Research Unit, University Institute of Health Sciences (IUCS), CESPU, CRL, 4585-116 Gandra, Portugal; a32336@alunos.cespu.pt (A.C.-F.); ricardo.dinis@iucs.cespu.pt (R.J.D.-O.)
[2] Instituto de Investigação e Inovação em Saúde (i3S), Universidade do Porto, 4200-135 Porto, Portugal
[3] Department of Infection Control and Prevention, University Hospitals Leuven, 3000 Leuven, Belgium; veroniek.saegeman@uzleuven.be
[4] Microbiology Laboratory, Biology Service, Institute of Toxicology and Forensic Sciences, 28232 Madrid, Spain; amparo.fernandezrodriguez@justicia.es
[5] Department of Public Health and Forensic Sciences, and Medical Education, Faculty of Medicine, University of Porto, 4200-319 Porto, Portugal
[6] UCIBIO—Applied Molecular Biosciences Unit, Laboratory of Toxicology, Department of Biological Sciences, Faculty of Pharmacy, University of Porto, 4050-313 Porto, Portugal
[7] Associate Laboratory i4HB—Institute for Health and Bioeconomy, Faculty of Pharmacy, University of Porto, 4050-313 Porto, Portugal
[8] UCIBIO—Applied Molecular Biosciences Unit, Laboratory of Microbiology, Department of Biological Sciences, Faculty of Pharmacy, University of Porto, 4050-313 Porto, Portugal
[*] Correspondence: daniel.barbosa@iucs.cespu.pt (D.J.B.); ana.freitas@iucs.cespu.pt (A.R.F.)
[†] ESCMID (European Society of Clinical Microbiology and Infectious Diseases) Study Group of Forensic and Post-Mortem Microbiology (ESGFOR).

check for updates

Abstract: The relevance of *postmortem* microbiological examinations has been controversial for decades, but the boom in advanced sequencing techniques over the last decade is increasingly demonstrating their usefulness, namely for the estimation of the *postmortem* interval. This comprehensive review aims to present the current knowledge about the human *postmortem* microbiome (the necrobiome), highlighting the main factors influencing this complex process and discussing the principal applications in the field of forensic sciences. Several limitations still hindering the implementation of forensic microbiology, such as small-scale studies, the lack of a universal/harmonized workflow for DNA extraction and sequencing technology, variability in the human microbiome, and limited access to human cadavers, are discussed. Future research in the field should focus on identifying stable biomarkers within the dominant Bacillota and Pseudomonadota phyla, which are prevalent during *postmortem* periods and for which standardization, method consolidation, and establishment of a forensic microbial bank are crucial for consistency and comparability. Given the complexity of identifying unique *postmortem* microbial signatures for robust databases, a promising future approach may involve deepening our understanding of specific bacterial species/strains that can serve as reliable *postmortem* interval indicators during the process of body decomposition. Microorganisms might have the potential to complement routine forensic tests in judicial processes, requiring robust investigations and machine-learning models to bridge knowledge gaps and adhere to Locard's principle of trace evidence.

Keywords: microbiome; necrobiome; thanatomicrobiome; decomposition; bacteria; *postmortem*

1. Introduction

The beginning of microbiology occurred in the late 17th century when van Leeuwenhoek performed the first microscopic observations of bacteria ("little animals"). However, it

113

7.3. Publication of congress abstract in Revista Científica Internacional da Rede Académica das Ciências da Saúde da Lusofonia (RevSALUS).

POSTER 43

Current perspective on the relevance of bacterial communities to estimate post-mortem intervals – how far are we?

Ana Cláudia-Ferreira[1*], **Daniel Barbosa**[1,2], **Ricardo Jorge Dinis-Oliveira**[1,3,4], **Ana R. Freitas**[1,5,6]

[1]TOXRUN – Toxicology Research Unit, University Institute of Health Sciences, CESPU, CRL, 4585-116 Gandra, Portugal.

[2]Instituto de Investigação e Inovação em Saúde (i3S), Universidade do Porto, 4200-135 Porto, Portugal; IBMC - Instituto de Biologia Molecular e Celular, Universidade do Porto, 4200-135 Porto, Portugal.

[3]Department of Public Health and Forensic Sciences, and Medical Education, Faculty of Medicine, University of Porto, 4200-319 Porto, Portugal.

[4]UCIBIO - REQUIMTE, Department of Biological Sciences, Laboratory of Toxicology, Faculty of Pharmacy, University of Porto, 4050-313 Porto, Portugal.

[5]UCIBIO - Applied Molecular Biosciences Unit, REQUIMTE, Department of Biological Sciences, Laboratory of Microbiology, Faculty of Pharmacy, University of Porto, 4050-313 Porto, Portugal.

[6]Associate Laboratory i4HB - Institute for Health and Bioeconomy, Faculty of Pharmacy, University of Porto, 4050-313 Porto, Portugal.

* ✉ anacoelhoferreira@hotmail.com

Resumo

Introduction: The relevance of postmortem microbiological examinations is controversial for decades, but the boom in advanced sequencing techniques over the last decade is increasingly demonstrating their usefulness, including for determination of the postmortem interval (PMI; time since death). This is an emerging field with a growing number of studies unveiling the feasibility of using microbial community changes to track the progression of decomposition if reliably quantified by high-throughput DNA sequencing [1]. **Objective:** We aimed to provide an overview of current knowledge about the role and utility of bacterial populational shifts in PMI calculations. **Methods:** A bibliographic research was conducted in PubMed database using the keywords forensic research, post mortem interval, bacteria and microbiology. We selected five recent articles (2020-2021) offering novel/broad overviews of the topic. **Results:** Most microbial forensic studies focus on gut samples, whereas microbial communities from the skin, mouth and intimate areas are underexplored, with the recent ones applying advance sequencing tools reaching different taxonomic levels until genus [2,3]. An approach to estimate PMI is the study of microbes colonizing internal organs/orifices after death, the thanatomicrobiome. Studies analyzing the sequences of bacterial 16S rRNA genes on model animals and humans, respectively, indicated a high accuracy (>94%) and that class or phylum taxonomic levels models provided the most accurate PMI predictions [1]. Different studies in internal organs reported a shift in microbial communities from dominant aerobic (e.g., *Staphylococcus/Enterobacterales*) to more facultative/obligate anaerobic bacteria (e.g., *Enterococcus/Clostridium*) [1,2]. However, thanatomicrobiome composition may be affected by other factors, including post-mortem translocation or sample contamination [4]. Recent studies applying machine learning models have identified particular bacterial species (e.g.*Enterococcus faecalis*) as the most informative in the decomposition process [3,5]. **Conclusions:** Several limitations preclude the current use of bacteria in PMI estimations. Even when applied to healthy humans, the lack of uniformization in methods/databases makes the interpretation of microbiome studies debatable. Given the complexity in identifying unique post-mortem microbial signatures to generate robust databases, a deeper knowledge on individual bacterial species/strains that can act as PMI indicators during body decomposition is warranted – ideally, they could be included in routine analysis for PMI estimation.

Keywords: rorensic research; decomposition; bacteria; microbiology; thanatomicrobiome.

References:

[1] Robinson, J.M., et al., *Forensic Applications of Microbiomics: A Review.* Front Microbiol, 2020. 11: p. 608101.

[2] Ahannach, S., et al., *At the Interface of Life and Death: Post-mortem and Other Applications of Vaginal, Skin, and Salivary Microbiome Analysis in Forensics.* Front Microbiol, 2021. 12: p. 694447.

[3] Roy, D., et al., *Microbiome in Death and Beyond: Current Vistas and Future Trends.* Frontiers in Ecology and Evolution, 2021. 9.

[4] Speruda, M., et al., *Microbial traces and their role in forensic science.* J Appl Microbiol, 2021.

[5] Liu, R., et al., *Predicting postmortem interval based on microbial community sequences and machine learning algorithms.* Environ Microbiol, 2020. 22(6): p. 2273-2291.

CURRENT PERSPECTIVE ON THE RELEVANCE OF BACTERIAL COMMUNITIES TO ESTIMATE POST-MORTEM INTERVALS – HOW FAR ARE WE?

Ana Cláudia-Ferreira[1*], Daniel Barbosa[1,2], Ricardo J. Dinis-Oliveira[1,3,4], Ana R. Freitas[1,5,6]

[1] TOXRUN—Toxicology Research Unit, University Institute of Health Sciences, Advanced Polytechnic and University Cooperative (CESPU), CRL, 4585-116 Gandra, Portugal.
[2] Instituto de Investigação e Inovação em Saúde (i3S), Universidade do Porto, 4200-135 Porto, Portugal; IBMC - Instituto de Biologia Molecular e Celular, Universidade do Porto, 4200-135 Porto, Portugal.
[3] Department of Public Health and Forensic Sciences, and Medical Education, Faculty of Medicine, University of Porto, 4200-319 Porto, Portugal.
[4] UCIBIO - REQUIMTE, Department of Biological Sciences, Laboratory of Toxicology, Faculty of Pharmacy, University of Porto, 4050-313 Porto, Portugal.
[5] UCIBIO - Applied Molecular Biosciences Unit, REQUIMTE, Department of Biological Sciences, Laboratory of Microbiology, Faculty of Pharmacy, University of Porto, 4050-313 Porto, Portugal.
[6] Associate Laboratory i4HB - Institute for Health and Bioeconomy, Faculty of Pharmacy, University of Porto, 4050-313 Porto, Portugal.

Introduction

The relevance of postmortem microbiological examinations is controversial for decades, but the boom in advanced sequencing techniques over the last decade is increasingly demonstrating their usefulness (Figure 1), including for determination of the *postmortem* interval (PMI – time since death). This is an emerging field with a growing number of studies unveiling the feasibility of using microbial community changes to track the progression of decomposition if reliably quantified by high-throughput DNA sequencing [1,2].
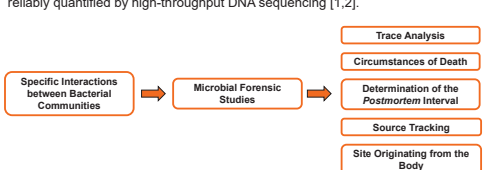

Figure 1: Representative scheme of the usefulness of specific interactions between bacterial communities in forensic studies.

The study of thanatomicrobiome, the communities of microorganisms that are found in different parts of the body, in organs and fluids after death, may be useful in PMI calculations, allowing to establish a relationship between microbial succession after death and stages of decomposition (Figure 2) [3].
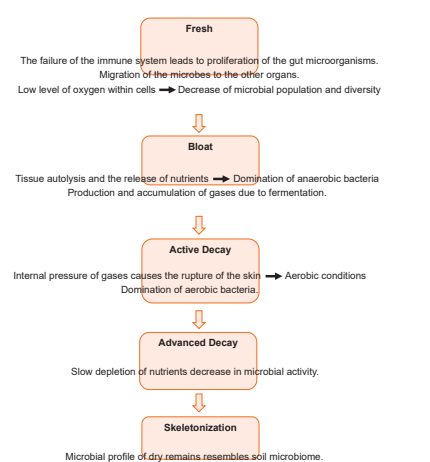

Figure 2: The various stages of decomposition of the human body and the corresponding characteristic microbiological processes. Adapted by Speruda, M., et al., *Microbial traces and their role in forensic science*. J Appl Microbiol, 2021.

Objective

In this context, we aimed to provide an overview of current knowledge about the role and utility of bacterial counts and populational shifts in PMI calculations.

Methods

A bibliographic research was conducted in PubMed database using the keywords forensic research, *postmortem* interval, bacteria and microbiology. We selected seven recent articles offering novel/broad overviews on the topic.

Results

Microbial forensic samples (Figure 3) are studied through varied methodologies, including DNA/RNA extraction kits, group-specific PCR primers, metagenomics, transcriptomics and whole-genome sequencing tools reaching different taxonomic levels until genus [2,4].
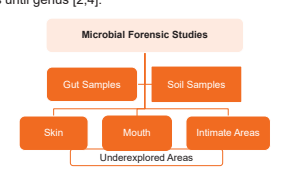

Figure 3: Representative schematic of the main samples used in microbial forensic studies; skin, mouth and intimate zones are much more underexplored than gut samples.

An approach to estimate PMI is the study of microbes colonizing internal organs/orifices after death, the thanatomicrobiome. Studies analyzing the sequences of bacterial 16S rRNA genes on model animals and humans respectively indicated a high accuracy (>94%) and that class or phylum taxonomic levels models provided the most accurate PMI predictions [1].

Different studies in internal organs showed a shift in microbial communities from dominant aerobic to more facultative/obligate anaerobic bacteria (Figure 4). Particular bacteria species (e.g., *Enterococcus faecalis*) have been identified as the most informative in the decomposition process according recent reports [3,5].
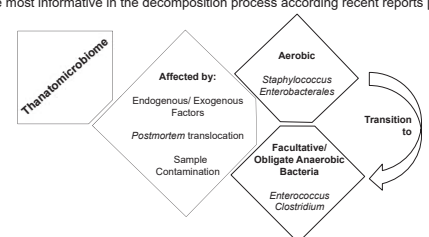

Figure 4: Representative scheme of factors that influence the thanatomicrobiome and examples of putrefaction indicator species.

Putting aside exogenous factors that can contaminate microbiological analysis of forensic samples, the microbial clock is more accurate in the first 48 hours after discovery, when the cadaver is fresh and not yet contaminated by soil microorganisms, because most of bacteria found in the soil are not cultivable due to inhibition of PCR by humic acids [6,7].

Conclusions

Several limitations preclude the current use of bacteria in PMI estimations. Even when applied to healthy humans, the lack of uniformization in methods/databases makes the interpretation of microbiome studies debatable. Given the complexity in identifying unique post-mortem microbial signatures to generate robust databases, a deeper knowledge on individual bacterial species/strains that can act as PMI indicators during body decomposition is warranted – ideally, they could be included in routine analysis for PMI estimation.

References

1. Robinson, J.M., et al., *Forensic Applications of Microbiomics: A Review*. Front Microbiol, 2020. **11**.
2. Ahannach, S., et al., *At the Interface of Life and Death: Post-mortem and Other Applications of Vaginal, Skin, and Salivary Microbiome Analysis in Forensics*. Front Microbiol, 2021. **12**.
3. Speruda, M., et al., *Microbial traces and their role in forensic science*. J Appl Microbiol, 2021. **132**(4): p. 2547-57
4. Roy, D., et al., *Microbiome in Death and Beyond: Current Vistas and Future Trends*. Frontiers in Ecology and Evolution, 2021. **9**.
5. Liu, R., et al., *Predicting postmortem interval based on microbial community sequences and machine learning algorithms*. Environ Microbiol, 2020. **22**(6): p. 2273-91.
6. Finley, S.J., M.E. Benbow, and G.T. Javan, *Microbial communities associated with human decomposition and their potential use as postmortem clocks*. Int J Legal Med, 2015. **129**(3): p. 623-32.
7. Gouello, A., et al., *Analysis of Microbial Communities: An Emerging Tool in Forensic Sciences*. Diagnostics (Basel), 2021. **12**(1).

7.5. Abstract under revision submitted on 3rd november 2023 to the European Congress of Clinical Microbiology and Infectious Diseases (ECCMID 2024).

00320
***In vivo* mapping of key bacterial species reveals *Enterococcus faecali*s and *Escherichia coli* as promising biomarkers of *postmortem* interval estimation**

09. Experimental microbiology, microbial pathogenesis & biofilms

09b. Host-pathogen interaction (incl basic microbiome studies, animal models)

Cláudia Cláudia-Ferreira [1], Daniel J. Barbosa [1, 2], Carla Campos [3, 4], Ricardo J. Dinis-Oliveira [1, 5, 6], Ana R. Freitas [1, 7]

[1]*1H-TOXRUN, University Institute of Health Sciences, CESPU - Gandra (Portugal),* [2]*Instituto de Investigação e Inovação em Saúde (i3S), Universidade do Porto - Porto (Portugal),* [3]*Instituto Português de Oncologia do Porto - Porto (Portugal),* [4]*Escola Superior de Saúde, Instituto Politécnico do Porto - Porto (Portugal),* [5]*UCIBIO, Toxicology, Faculty of Pharmacy of Porto - Porto (Portugal),* [6]*Department of Public Health and Forensic Sciences, and Medical Education, Faculty of Medicine, University of Porto - Porto (Portugal),* [7]*UCIBIO, Microbiology, Faculty of Pharmacy of Porto - Porto (Portugal)*

Background

Estimation of the *postmortem* Interval (PMI), the time elapsed since death, is one of the most challenging issues in forensic sciences. Most studies focus on extensive bacterial sequencing of postmortem samples, but culture-based experiments for higher taxonomic resolution remain scarce. We aimed to analyze total bacterial counts and map three key bacterial species (*Enterococcus faecalis, Staphylococcus aureus, Escherichia coli*) in different organs and timepoints.

Methods

Male C57BL/6J SPF mice underwent three independent assays during 11 postmortem timepoints, adhering to European/Portuguese regulations for animal sacrifice at controlled temperatures. Feces and organs (n=10: intestine/stomach/skeletical-muscle/liver/spleen/kidney/bladder/lungs/brain/heart) were collected, weighed and thoroughly resuspended in buffered peptone water, then plated onto enriched nonselective/selective culture media (n=4). Following routine aerobic incubation, Colony Forming Units (CFU) per gram of tissue or per mL of sample were quantified for total/individual bacterial loads. Bacterial species were identified by MALDI-TOF mass spectrometry, and statistical analysis performed in GraphPad-Prism/10.0.1.

Results

Thirty-eight bacterial species from 11 families and 3 phyla were identified (Figure1), with notable consistency in the presence of *Staphylococcus xylosus, E. faecalis,* and *E. coli* across all experiments. Particular families were consistently identified across all organs, including Enterococcaceae and Enterobacteriaceae mostly in the later stages of decomposition, and